FUNCTIONAL CONNECTIVITY ANALYSIS UNDER VIGILANCE

DECREMENT AND ENHANCED MENTAL STATES

by

Omnia Hassanin

A Thesis Presented to the Faculty of the
American University of Sharjah
College of Engineering
in Partial Fulfillment
of the Requirements
for the Degree of

Master of Science in
Biomedical Engineering

Sharjah, United Arab Emirates
June 2020

Declaration of Authorship

I declare that this thesis is my own work and, to the best of my knowledge and belief, it does not contain material published or written by a third party, except where permission has been obtained and/or appropriately cited through full and accurate referencing.

Signature …………………….Omnia Mohammed Hassanin………………………….

Date……………….………… May 11, 2020……………………………………

Approval Signatures

We, the undersigned, approve the Master's Thesis of

Thesis Title:

Date of Defense:

Name, Title and Affiliation	Signature
Dr. Lotfi Romdhane Associate Dean for Graduate Studies and Research College of Engineering	
Dr. Sirin Tekinay Dean College of Engineering	
Dr. Mohamed El-Tarhuni Vice Provost for Graduate Studies Office of Graduate Studies	

Acknowledgements

First and foremost, I would like to express my sincere gratitude to my supervisors Prof. Hasan Al Nashash and Dr. Usman Tariq for providing me with this valuable research opportunity and for guiding me throughout different research stages. Their immense knowledge and expertise were my inspiration to work harder and explore new ideas. I extend my gratitude to Dr. Fares Al Shargie for being a supportive research mentor and for spending hours to answer all my questions without hesitation. His efforts were pivotal to establishing the research protocol, and his suggestions were integral to shaping and improving this thesis. I am deeply indebted to the Biomedical Engineering Graduate Program for providing me with a graduate assistantship to pursue my master's studies. Special thanks to the Biosciences and Bioengineering Research Institute for funding this research work. I also thank all the volunteers for sparing some of their time to take part in our research experiment. Finally, I would like to express my appreciation to all researchers in the field who paved the way for this work. Their contributions were an essential guide and a great source of inspiration.

Dedication

I dedicate my effort to my beloved family, whose affection, encouragement, and prayers of day and night made me reach where I am. Thank you for always believing in me ...

Abstract

This thesis proposes electroencephalogram (EEG) functional connectivity and graph theory analysis (GTA) to quantify brain activity under alertness, vigilance decrement, and enhanced mental states in four frequency bands. The vigilance decrement state was induced by performing a 30 min computerized incongruent Stroop color-word test (I-SCWT). Meanwhile, the enhancement states were provoked by integrating a 250Hz pure sinusoidal tone (PST) or 16Hz beta binaural beats (BB) with the I-SCWT. We estimated functional connectivity using the phase-locking value (PLV) statistic and characterized the topological structure of the network based on concepts of node strength, clustering coefficient, and efficiency. We then evaluated the proposed methods using statistical analysis and a support vector machine classifier. The experimental results showed that the 30 min I-SCWT significantly elicited alteration in cortical connectivity ($p < 0.05$). PLV between brain regions significantly decreased with vigilance decrement ($p < 0.05$), resulting in a less optimal network structure. Investigation of the intra-regional PLV networks suggested that changes in connectivity under vigilance decrement are specific to cortical areas and EEG frequency bands. Our Assessment results confirm that PLV+GTA provides a reliable index to quantify different aspects of cortical functional connectivity under different vigilance levels. Subject independent classification analysis based on GTA features corresponding to a single cortical region showed an average accuracy of 84.27% to discriminate vigilance decrement from alertness state. Under enhanced mental states, cortical connectivity remained high until the end of the total task duration. Also, significant improvements in the participants' performance were observed in comparison to the no-audio condition. On average, PST stimulation showed a 25.84% improvement in the participants' detection accuracy towards the end of the task. Similarly, BB stimulation showed a 26.01% improvement.

Search Terms: *Vigilance decrement, Stroop color-word task, electroencephalogram, cortical functional connectivity, graph theory analysis, pure sinusoidal tone, and auditory binaural beats.*

Table of Contents

List of Figures

List of Tables

List of Abbreviations and Symbols

NS_g Global Node Strength

CC_g Global Clustering Coefficient

E_g Global Efficiency

ANOVA   Analysis of Variance

BBS   Binaural Beats Stimulation

BRUMS   Brunel Mood Scale

CG   Chewing Gum

CWM   Cognitive Workload Modulation

ECG   Electrocardiogram

EEG   Electroencephalogram

EI   Engagement Index

EOG   Electrooculogram

ERP   Event Related-Potential

fMRI   Functional Magnetic Resonance Imaging

GTA   Graph Theory Analysis

HPS   Haptic Stimulation

HRV   Heart Rate Variability

I-SCWT   Incongruent Stroop Color-Word Task

LI   Laterality Index

LOSO   Leave One Subject Out

MATLAB   Matrix Laboratory

MVARM   Multivariate Auto-Regressive Model

PC   Personal Computer

PDC   Partial Directed Coherence

PLV   Phase-Locking Value

POMSO   Profile of Mood States Questionnaire

PSTS   Pure Sinusoidal Tone Stimulation

ROI   Region of Interest

SSSQ   Short Stress State Questionnaire

SVM   Support Vector Machine

tACS   Transcranial Alternating Current Stimulation

tDCS   Transcranial Direct Current Stimulation

TLS   NASA Task Load Index

TOT   Time on Task

VG   Video Games

Chapter 1. Introduction

This chapter provides a short introduction to the topic of vigilance assessment and enhancement. Following that, the problem investigated in this thesis is presented, followed by a summary of major research contributions. Finally, the general outline of this thesis is provided.

1.1. Overview

Vigilance, also known as sustained attention, refers to the cognitive ability to maintain attentiveness to a specific stimulus or task over prolonged periods [1]. With increased time on task (TOT), the ability to maintain sustained vigilance levels tends to drop, leading to undesirable performance declines. This phenomenon is known as vigilance decrement. The cause of Vigilance decrement has been regarded as either reduced arousal or depleted cognitive resources, as suggested by the under-load (mind-wandering) and cognitive resource theories [2–4]. The under-load theory suggests that monotony or lack of stimulation in vigilance tasks may lead to habituation, withdrawal, or disengagement, which in return, may lead to vigilance decrement. In contrast, the cognitive resource theory explains the attributes of vigilance decrement in workload, fatigue, or stress scenarios. The theory views the human cognitive capacity as resources that get allocated based on task requirements. It thus suggests that extensive workload ultimately deteriorate vigilance performance as a result of depleted cognitive resources.

The phenomenon of vigilance decrement is usually investigated during long-term attentional or cognitive tasks. Typically, vigilance tasks require operators to respond to rare or critical visual signals and withhold responses to other neutral stimuli. More complex tasks may involve other cognitive aspects, such as the use of declarative or working memory [5]. Under these settings, vigilance decrement is usually inferred from the decreased detection rate or increased reaction time. Previous studies have reported several factors affecting the magnitude and rate of vigilance decrement. These factors are generally related to the nature of the performed task and the associated cognitive load. Examples may include stimulus duration, event rate, source complexity, and the use of multiple cognitive resources [6, 7]. Under most conditions, vigilance decrement becomes evident within the first 20-35 min of attentional effort, with 50% of

the decrement observed during the first 15 min [8]. However, the decline in detection performance can occur more quickly if the task demand conditions are high [7]. These observations are evident for both experienced and novice performers.

1.2. Thesis Objectives

Vigilance decrement is a fundamental cognitive component in a variety of operational settings including education, screening and monitoring, road and air traffic control, long-distance driving, and targeted security monitoring [9–14]. Workers in these settings are usually involved in long-term monotonous or mentally demanding tasks. Vigilance decrement in such sensitive settings can lead to unpredicted performance declines, which in return, may lead to serious consequences. In this regard, objective, quantitative, and continuous vigilance assessment methods that can be integrated within the previously mentioned settings are of great importance. These methods should ensure simplicity and non-intrusiveness for user convenience, and at the same time should be sensitive, effective and accurate enough to detect and quantify vigilance level decrements. In addition, the integration of cognitive enhancement interventions within these settings can improve productivity and reduce risks. Despite the assortment of factors that influence the vigilance decrement, theoretical debates about the underlying mechanisms have not been resolved. In the light of previous observations, the objective of this thesis is twofold. Firstly, we investigate cortical functional connectivity as an objective biomarker to quantify different vigilance levels. Secondly, we propose auditory stimulation as a non-invasive solution to mitigate vigilance decrement.

1.3. Research Contribution

This thesis investigates changes in electroencephalograph (EEG) functional connectivity as a result of long term attentional performance. In specific, we hypothesize that connectivity between cortical regions decreases under vigilance decrement and can be enhanced using auditory stimulation. We further hypothesize that decrements in cortical connectivity are region and band-specific. To address our hypotheses, we propose a novel protocol to induce semantic vigilance using a computerized version of the incongruent Stroop color-word task (I-SCWT). We believe that the I-SCWT is unique in comparison to traditional vigilance tasks since it does not fall neatly under the sensory

17

vigilance classification. Based on nature and the design of the test, the I-SCWT can involve both sensory and cognitive processes and is thus more suitable to mimic real-life tasks. Besides, we present a method to quantify the functional coupling between brain regions under alertness, vigilance decrement, and enhanced mental states by utilizing phase-locking value (PLV) and graph theory analysis (GTA). The experimental results showed that the proposed protocol successfully induced behavioral and cortical connectivity changes with increased TOT. The PLV was sensitive to vigilance decrement, and the overall phase synchronization between cortical regions significantly decreased after 30 min of TOT. Cortical phase synchrony networks showed full-scale and regional differences between alertness and vigilance decrement states. In Addition, regional hemispheric asymmetries were observed and quantified using a novel laterality index. Our results also confirmed cortical entrainment and enhanced connectivity effects as a result of pure tone and binaural beat auditory stimulation. Enhancement effects were further supported by the participants' enhanced vigilance performance.

1.4.   Thesis Organization

The rest of this thesis is organized as follows:

Chapter 2 provides an overview of vigilance assessment literature with emphasis on objectives tools and procedures. Different behavioral and physiological assessment approaches are presented, and their results are discussed and compared.

Chapter 3 provides an overview of existing vigilance enhancement interventions in literature. The overview compares different types of enhancement techniques taking into consideration the context in which studies were conducted and the associated effects on vigilance performance and/or brain activity.

Chapter 4 discusses the methodology of this thesis, namely the adopted experimental protocol to induce and enhance vigilance decrement, the process of selecting and recruiting participants, the experimental setup to acquire and record the EEG and behavioral data, and the methods of data analysis.

Chapter 5 explores changes in cortical functional connectivity as a result of increased TOT. GTA was employed at the sensor level to quantify and compare the full-

scale, intra-regional, and hemispheric asymmetry characteristics of the functional connectivity networks under cognitive alertness state vigilance decrement states.

Chapter 6 investigates the effect of auditory stimulation on the participants' behavioral performance and cortical connectivity while performing the I-SCWT. To explore potential enhancement effects, full-scale GTA at the global level is carried out at different auditory conditions. Indications of vigilance enhancement were further supported by analysis of behavioral data with increased TOT

Chapter 7 concludes this thesis by providing a summary of major research findings and recommendations for future research directions.

Chapter 2. Vigilance Assessment Techniques

This chapter provides a summary of vigilance assessment literature with emphasis on objectives tools and procedures. First, a short overview of different vigilance tasks and the associated subjective and behavioral assessment criteria is provided. Following that, the physiological correlates of alertness, mental fatigue, and vigilant decrement are investigated. In specific changes in EEG, eye tracking, skin resistance are heart rate measurements are compared for different vigilance levels. Finally, an extensive methodological overview is provided for EEG analysis.

2.1. Subjective and Behavioral Assessment

Sustained attention tests can take a variety of forms, depending on the purpose of the study. However, the traditional assessment of vigilance relies on prototypic psychomotor responding tasks. These tasks require the direction of attention to specific events, known as signals or target stimuli, for long and continuous periods [15–18]. In sensory vigilance tasks, the target stimulus may or may not change in shape, color, size, and/or position. The appearance of the target stimulus could be completely randomized or based on a fixed probability [19]. The literature also reported other types of naturalistic vigilance tasks or tasks involving one or more cognitive aspects. Examples may include simulated driving [20–22], N-Back [23], and mental rotation tasks [24–27].

Changes in vigilance and sustained attention levels can be inferred thought subjective and/or behavioral measures. Subjective assessment approaches mainly rely on psychometric self-report questionnaires for the evaluation of arousal, mindfulness, mood, stress, workload, or fatigue. Examples of popular self-report questionnaires employed in vigilance studies include the Brunel Mood Scale (BRUMS) [28, 29], the Profile of Mood States Questionnaire (POMSQ) [30, 31], the Short Stress State Questionnaire (SSSQ) [32, 33], and the NASA Task Load Index (TLX) [34]. As the name implies, subjective assessment tools mainly rely on the performers' judgments and feelings, without providing clear boundaries on how to differentiate between different responses, and thus obtained results might be biased [35].

Using behavioral assessment approaches, changes in sustained attention levels are usually inferred from fluctuations and deteriorations in performance as a function

of time [36]. Most vigilance tests are performed continuously for around 30 min [19]. The most popular performance measures are the reaction time and the target detection rate. The reaction time refers to the duration taken to respond to a particular stimulus or event. The target detection rate refers to the proportion of targets to which the performer correctly responds. Based on the test context, response slowing and decreased detection rates provide evidence for attentional shifts, fatigue, and vigilance decrement [37–39]. Several other performance measures such as the commission and omission errors have been recently employed in the literature [40, 41]. A commission error occurs when a performer incorrectly responds to a non-target event, whereas an omission error occurs if the target event is missed.

2.2. Physiological Assessment

Studies have shown that alterations in attentional levels are accompanied by physiological changes, mainly regulated by the brain and nervous system. To this end, many physiological measurements were employed to understand the bodily mechanisms of alertness and vigilance decrement. The studies in [42–44] used cerebral oximetry measurements to investigate changes in blood oxygen saturation as a result of vigilance decrement. Mostly, studies have reported increased oxygenation in the right hemisphere in comparison to the left hemisphere in correlation with declined performance. Other studies found that oxygen saturation varies with task difficulty and workload levels [45, 46]. For example, bilateral hemispheric increases in oxygenation were reported for complex vigilance tasks [46]. Another class of studies in literature utilized eye-tracking measurements to better understand human behavior under attentional tasks. In specific, pupillometry parameters such as fixations, saccades, blinks, and scan paths were monitored to understand the implications of enhanced and deteriorated attentional levels [47–52]. For example, the study in [51] reported increments in saccades velocity under higher workload levels. On the other hand, the study in [49] reported negative correlations between reactions times and fixation scores during a naturalistic driving task with complex workload levels. Moreover, studies have employed eye tracking as an objective tool to measure different subjective events such as mind-wandering, task engagement, and drowsiness [53, 54]. Similarly, changes in the electrical properties of the

skin, also known as the electrodermal activity, have been repeatedly related to changes in attentional motivation and task engagement [55–57]. Another important physiological parameter directly regulated by the activity of the autonomous nervous system is heart rate variability (HRV). HRV refers to variations in the lengths of complete cardiac cycles. Generally, studies have shown that heart rate varibaility decreases with increased TOT [58, 59].

Build upon the previous findings, several studies in the literature demonstrated that physiological markers such as heart rate, blood flow velocity, eye blink rate, pupil dilation, and facial expressions can be effectively used as vigilance decrement signatures [36, 60, 61]. The authors in [60] proposed a fuzzy logic-based system for providing hypo-vigilance alarm signals. The proposed system was based on Electrooculogram (EOG) features describing different eyelid movements. Another vigilance decrement detection system based on eye activity features extracted from facial images was reported in [61]. Extracted features captured differences in eye closure rate, blinking frequency, and eyelid distance changes between different vigilance levels. Following a similar approach, the authors in [36] developed a system to detect vigilance decrement in real-time driving settings.

Despite the evident importance of vigilance decrement detection in a variety of operation and industrial settings, the incomprehensive understanding of the underlying neural mechanisms limits reliable applications. Recently, EEG became the most popular neuroimaging modality employed in vigilance studies. In comparison to other neuroimaging techniques, EEG provides a high temporal resolution with low constraints on participants' behavioral performance. Discussed below are the different EEG quantitative approaches within the context of vigilance assessment.

2.3. Quantitative Electroencephalographic Analysis

2.3.1. Event related potentials analysis. Several studies have shown that increased time on cognitive and attentional tasks leads to observable stimuli-locked changes in both ongoing EEG activity and event-related potentials (ERP). Experimental studies have reported changes in the amplitudes of ERP components as a result of mental

fatigue [62–64]. For example, consistent findings showed that the amplitude of the P300 component decreased under vigilance decrement. The study in [65] used a single-trial event-related potential (ERP) approach to investigate the effect of multisensory haptic stimulation on vigilance performance. The experimental results showed a significant correlation between the increased reaction times (an indication of vigilance decrement) and the increased sensory perception and the motor response of ERP latencies. Considering the relationship between ERP amplitudes and vigilance performance, the study in [66] demonstrated that decreased vigilance performance of mild cognitive impairment patients was associated with significant suppression in late positive potentials in comparison to healthy subjects.

2.3.2. Spectral and time-frequency analysis. Several recent studies have reported high correlations between univariate EEG spectral dynamics and changes in vigilance levels. Generally, experimental results supporting evidence of high alertness have shown decreases in the power of low frequencies. Also, increased concentration levels were associated with higher power spectral densities within faster frequency ranges [67,68]. Other studies investigating the spectral correlates of vigilance decrement have reported changes specific to the delta, theta, alpha, and beta bands. The studies in [69, 70] power changes within the delta band as an attempt to indicate mental fatigue during long term driving. In both studies, power increases were evident during the transition from alertness to drowsiness then to sleep. Chuang et al. [69] further reported that delta activity was the lowest during the peak performance states. Compared to other EEG bands, increments in theta band activity has been repeatedly associated with time induced mental fatigue [71] and driving vigilance decrement [69], specially frontal areas. The study in [72] reported progressive activation within the theta range during periods of attentional challenge. Another study reported correlations between increased theta activity and decreased arousal or alertness [73]. Studies have also shown that the activity of alpha rhythms increased with increasing TOT [71, 74]. Following these findings, Martel and his colleagues observed increased activity in the alpha frequency range (8–14 Hz) for vigilance decrement [75]. They proposed predicting attention lapses in a convert setting up to 10s in advance.

23

Based on the previous findings, several studies attempted to classify different vigilance levels based on spectral features [76–78]. In specific, different variables corresponding to power changes in specific bands served as markers to detect vigilance decrements during sustained attention tasks. Other neurofeedback studies employed the ratio between different band powers as indices to timely detect decrements in arousal. For example, one of the popular power ratio indices is the engagement index (EI). The EI refers to the ratio between beta and the sum of alpha and theta powers. In [79,80], the EI, along with several machine learning classifiers, was employed to classify alertness, drowsy, and asleep states. Another popular index is the ratio between the frontal theta and parietal alpha powers [77].

2.3.3. Cortical connectivity analysis. The human brain is a highly complex structure that consists of functionally specialized areas of neuronal ensembles. To engage in a particular cognitive task, different patterns of dynamic coupling between these spatially-distributed neuronal ensembles take place [81]. Such coupled interactions have been modeled in literature based on the concepts of functional and effective connectivity. Functional connectivity refers to the statistical analysis of the dependence between the activity of two brain regions without inference to any causal interactions. In contrast, effective connectivity investigates the direct effect that one signal exerts on the other. Functional connectivity approached can be either directed or non-directed. Directionality is usually inferred as time delays or phase lag relations [82]. EEG connectivity analysis can be performed at the electrode or source level. Bivariate modeling approaches consider the interactions between two source or electrode signals, while multivariate approaches consider the coupling of three or more signals.

In EEG connectivity analysis, brain activity can be modeled as a network consisting of vertices (nodes) that are interconnected using links (edges) [83]. If an electrode-wise analysis is performed, the nodes represent to the electrodes, and the links correspond to the computed connectivities between pairs of electrode signals. The edges can be directed or undirected, depending on the employed connectivity statistic. As shown in Figure 1, functional networks can be visualized as graphs or adjacency matrices. The appropriateness of each of these visualization methods depends on the purpose of the

analysis. Graphical methods preserve information about the relative spatial locations of the nodes and thus can be used to visualize topological relationships. In contrast, adjacency matrices are more appropriate for large-scale networks; however, they discard any spatial properties [83]. When obtained from EEG data at the electrode level, the X and Y axes of the adjacency matrix will correspond to the electrode order, and the grey level will correspond to the connectivity status or weight between electrode pairs. It is worth mentioning that networks with undirected edges have symmetric adjacency matrices. After constructing the connectivity network (either directed or undirected), thresholding can be applied to retain only significant edges. Following that, the topological characteristics of the network can be characterized using different graph-theoretic metrics.
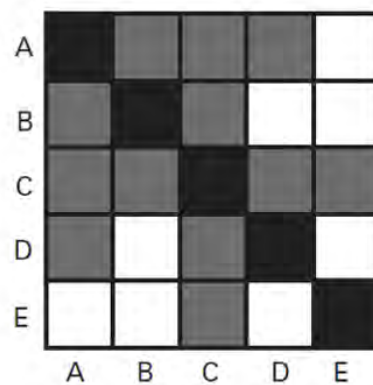
(a)
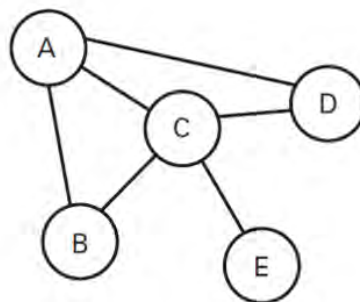
(b)

Figure 1: Visualization techniques of connectivity networks [84]. (a) Adjacency matrix representation, and (b) graphical network representation.

The literature reports various methods for assessing EEG connectivity. These methods vary depending on the purpose of the study and the investigated aspects of brain activity and EEG signal. Discussed below are some of the widely used connectivity and graph-theoretic approaches in the context of vigilance assessment.

The *Pearson correlation coefficient* is the simplest linear measure that provides a bivariate estimate of the statistical correlation between two variables. For two simultaneously recorded time series y_n and x_n $(n = 1, 2, ..., N)$, the Pearson correlation coefficient (r_{xy}) is calculated as the covariance between the two series normalized by their individual variances. This relation can be mathematically expressed as [85]:

$$r_{xy} = \frac{\sum_{n=1}^{N}(x_n - \bar{x})(y_n - \bar{y})}{(N-1)\sqrt{\sum_{n=1}^{N}(x_n - \bar{x})^2 \sum_{n=1}^{N}(y_n - \bar{y})^2}}, \tag{1}$$

where $\bar{x}$ and $\bar{y}$ denote the mean of x_n and y_n respectively. The values of the Pearson correlation coefficient are bounded between -1 and 1. The 0 value corresponds to no correlation, while the -1 and 1 values correspond to total positive and negative correlations respectively. By assuming the time series as realizations of random variables and by discarding any temporal associations, the Pearson correlation coefficient fails to convey directed relations within the data. This implies that the estimated connectivity will be the same even if the time series elements are randomly shuffled in time [86].

The cross-correlation function C_{XY} is another commonly used measure of correlation. It is obtained by computing the correlation coefficient as a function of the lag of one time series with respect to the other. Mathematically this relation can be expressed as [87]:

$$C_{XY}(\tau) = \frac{\sum_{n=1}^{N-\tau}(x_n - \bar{x})(y_{n+\tau} - \bar{y})}{(N-\tau)\sqrt{\sum_{n=1}^{N}(x_n - \bar{x})^2 \sum_{n=1}^{N}(y_n - \bar{y})^2}}, \tag{2}$$

where τ is the time lag between the signals x and y. In contrast to the Person correlation coefficient, cross correlation accounts for the temporal relations between the signals. In some well behaved scenarios, cross correlation can be used to infer directionality [88]. *The magnitude coherence coefficient* is an undirected measure that estimates the spectral correlation between two signals and is considered as the frequency domain equivalent of the cross-correlation function. For two signals X(t) and Y(t), the coherence function can

26

be computed as the cross-spectral density of the two signals scaled by their auto-spectral densities. This relation can be defined mathematically as [86]:

$$coh_{xy}(f) = \frac{|S_{xy}(f)|}{\sqrt{S_{xx}(f)S_{yy}(f)}}, \tag{3}$$

where S_{xy} represents the average cross spectral density between signals X and Y and S_{xx}, S_{yy} are the auto spectral densities of X and Y. A directed version of the magnitude coherence coefficient is the *partial directed coherence* (PDC) [89]. This measure is based on fitting the EEG time series to a multivariate auto-regressive model (MVARM), and then computing the magnitude coherence from the estimated model coefficients. Let $X(t) = [x_1(t),....,x_N(t)]^T$ be a zero mean EEG time series recorded from N channels. A MVAR model fitting the time series can be defined as [90]:

$$X(t) = -\sum_{\tau=1}^{P} A(\tau)X(t-\tau) + E(t), \tag{4}$$

where P is the model order, $E(n)$ is a noise vector, and A is the model coefficient matrix $(N \times N)$. Accordingly, the partial directed coherence from channel j to channel i can be defined as [90]:

$$PDC_{i,j}(f) = \frac{|A_{i,j}(f)|}{\sqrt{\sum_{k=1}^{N} A_{k,j}^{\star}(f)A_{k,j}(f)}}, \tag{5}$$

where $A_{i,j}$ is an element of $A(f)$, the Fourier transform of the MVAR coefficients matrix $A(t)$, and the asterisk denotes the complex conjugate operation. By fitting the data into an MVARM, the current value of the signal is estimated considering the previous values of the signal itself and the previous values of another related signal. Thus the model coefficient can be considered as weights to the causal relationships between the signals. It is worth mentioning that both the amplitude coherence and the partial directed coherence measures discard phase information and only look at the amplitude interactions of the signals.

The *phase locking value* (PLV) is one of the most commonly used measures to evaluate the consistency of phase differences between electrode signals over time windows or epochs. For two simultaneously recorded electrode signals y_n and x_n, the

PLV is calculated as the average phase differences between these two signals over time. This relation can be mathematically expressed as [91]:

$$PLV = n^{-1} \sum_{n=1}^{N} e^{i(\theta_x(n) - \theta_y(n))},$$
(6)

where N is the total number of sampled time points and θ_x and θ_y are the instantaneous phase values of x and y respectively at time points n. PLV is a non-directed connectivity measure with values bounded within the interval $[0, 1]$.

2.3.4. Network and graph theoretical approaches.   Based on accumulating research evidence, system neuroscientists believe that cortical networks show two contradicting topological attributes to maintain optimal cognitive processing and information transfer [92, 93]. The first attribute is functional segregation, which is the tendency to exhibit locally specialized information processing patterns. In contrast, the second attribute is functional integration, and it refers to the efficiency of information transfer between distributed brain regions [94]. The characterization of information transfer patterns in the context of these two concepts is fundamental to understand brain function. Graph theory provides adequate tools to investigate and quantify the topological characteristics of cortical connectivity dynamics under different cognitive states.

Many studies in the literature have adopted approaches from graph theory to investigate the altered topological structures of functional connectivity networks as induced by long-term attentional performance, fatigue, and vigilance decrement. The studies in [95–97] reported decreased functional integration of EEG and fMRI networks with increased TOT. In accordance with this observation, fatigue-related studies reported decreased integration in different connectivity networks after the elapse of less than 30 min task duration [33]. Moreover, repeated reports have shown that the increase in network functional segregation is associated with improved performance in long-term working memory tasks [98]. The findings of previous studies suggest that the study of brain connectivity through graph theory provides a descriptive tool in cognitive brain functions and biomarkers to distinguish different attentional and cognitive states.

Chapter 3. Vigilance Enhancement Interventions

This chapter provides an overview of existing vigilance enhancement interventions in literature. The overview highlights different types of enhancement techniques taking into consideration the context in which studies were conducted and the associated effects on vigilance performance and/or brain activity.

Vigilance enhancement refers to the deliberate use of technological, medical, or therapeutic interventions to improve cognitive processing and attentional performance [99]. Enhancement interventions can be employed in two contexts. The first is rehabilitative or therapeutic to restore a fundamental capability after disability of disfunction. On the other hand, enhancement interventions can be employed to augment the cognitive capacities for healthy humans. This thesis focuses on the second context, which is improving the performance of healthy individuals in work settings. The literature contains many studies that investigated the effect of different cognitive enhancers on vigilance decrement. Some of these interventions are generally mundane and often integrated with daily routines. Examples may include, but not limited to, meditation [100], sports [101, 102], yoga [103, 104], herbal extracts and diet [105], caffeine [106], chewing gum [107], and odor exposure [108, 109]. It is worth mentioning that conventional interventions have been examined in the literature for decades. Experimental studies have shown enhancement effects related to precipitation, attention, memory, and understanding. However, it is consensus among the research community that effective enhancements of cognition, mood, or behavior are highly subjective and short-lived. Another class of studies investigated the use of unconventional technological, neuroelectrical, or neurochemical interventions to enhance vigilance decrement. Different unconventional methods can be classified under haptics [65, 110–112], cognitive workload modulation (integration of challenge elements into the primary task) [113], auditory stimulation [114, 115], transcranial current stimulation [116–118], pharmaceuticals [119], and video games [120, 121].

A survey recently conducted by Al-Shargie et al. [122] extensively summarized the literature related to vigilance enhancement interventions. In this review, vigilance tasks were categorized under either monotonous or complex tasks. Monotonous tasks

include psychomotor paradigms that require sustained attention and targeted detection. On the other hand, complex tasks refer to those involving cognitive or cognitive-sensory aspects. Figures 2 and 3 summarizes the reaction time results reported in studies employing different interventions for monotonous and complex tasks, respectively. Positive values on the plots indicate increased reaction times and vise versa. The error bars on the plots represent the standard deviation of enhancement results extracted from different studies. As shown in Figure 2, all the interaction techniques significantly enhanced performance in the case of monotonous tasks. The highest effects were reported for video games, transcranial direct current stimulation, and haptic stimulation (more than 15%). Fragrance showed the lowest improvement of 8%. Video games showed the largest increase of 18%. This significant improvement can be explained according to previous studies investigating the impact of video games on the neuroplasticity of afferent neural networks [123, 124]. Studies have shown that playing video games correlates with stimulations in locomotor afferent nerves and adrenergic receptors, which in return improves responsiveness and motor behavior [124]. Also, behavioral and cognitive studies suggest that video games can enhance perceptual, visuospatial, and perceptuomotor skills [125, 126]. Improvements in these skills support cognitive control and flexibility [127, 128].

As shown in Figure 3, small average improvements with high standard deviations were observed in the case of complex vigilance tasks. Reported effects varied between -2% and 7%. Modafinil and transcranial direct and alternating current stimulation interventions showed the highest improvement (more than 6%). Interestingly, the alternating current stimulation techniques showed consistent effects among studies, as indicated by the relatively small standard error. On the other hand, the fragrance and cognitive workload modulation interventions did not affect performance. Integrating music with complex vigilance tasks resulted in a deteriorated performance. Modafinil is the standard medication used to treat sleepiness for narcolepsy patients. Studies have shown that small dosages of Modafinil can enhance sustained attention, learning, and memory for healthy individuals. These studies suggested that Modafinil improves adaptive response inhibition resulting in overall improved reaction times and detection accuracies. However, the effects were extremely inconsistent across the subjects [129].

Moreover, experiments involving Modafinil should be conducted under the supervision of medical experts, making it an impractical solution for consistent usage.

It is worth noting that binaural beats showed reasonable enhancement effects for both monotonous and complex tasks. Relatively small improvements in comparison to the other interventions could be due to the limited number of available studies. Generally, studies have shown that binaural beats stimulation increases connectivity and phase synchronization in the auditory cortex resulting in enhanced cortical communication and neural plasticity [130]. Several other studies have shown that binaural beats can improve emotions [131], stimulate arousal [132], and reduce anxiety [133, 134]. Moreover, binaural beat stimulation has the advantage of being a simple, pleasant, and non-invasive intervention.
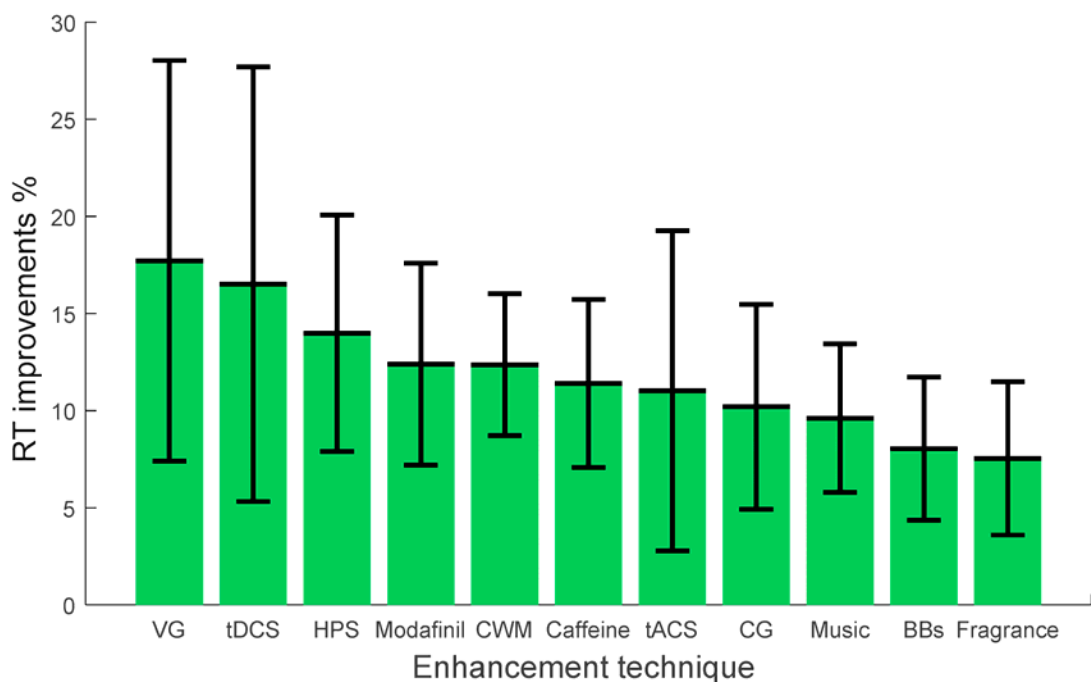
Figure 2: Percentage of reaction time improvements for different vigilance interventions when a monotonous task is considered [122]. The error bars represent the standard deviation of improvements across studies. X-axis abbreviations: VG: video games, tDCS: transcranial direct current stimulation, HPS: haptic stimulation, CWM: cognitive workload modulation, tACS: transcranial alternating current stimulation, CG: chewing gum, and BB: binaural beats
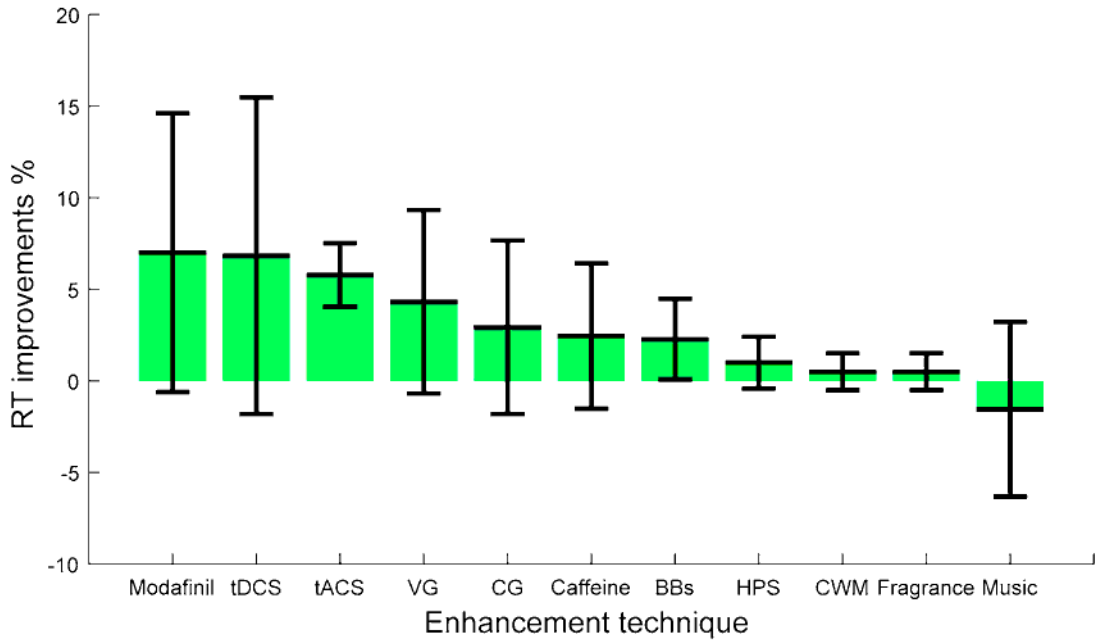
Figure 3: Percentage of reaction time improvements for different vigilance interventions when a complex task is considered [122]. The error bars represent the standard deviation of improvements across studies. X-axis abbreviations: tDCS: transcranial direct current stimulation, tACS: transcranial alternating current stimulation, VG: video games, CG: chewing gum, BB: binaural beats, HPS: haptic stimulation, and CWM: cognitive workload modulation

3.1 Auditory Binaural Beat Stimulation

Binaural beats (BB) refer to the subjective beat sensations perceived by the brain when two sinusoidal sound waves of equal intensities but slightly different frequencies are presented to each ear separately [135]. The beats are typically perceived as variations in loudness occurring at a rate equal to the difference between the forming carrier frequencies [136]. For instance, presenting a $240Hz$ tone to the right ear and a $250Hz$ tone to the left ear will yield a perceptual illusion of a $10Hz$ beat. Typically, BB are presented using stereophonic earphones to ensure full isolation between left and right channels. Experimental studies showed that binaural beats are ideally perceived if the carrier frequencies are around $200Hz$, and if the differences between the carrier frequencies are no more than $30Hz$ [135, 137]. Other studies suggested that the lower and higher limits for perceivable stimulating frequencies are $90Hz$ and $1000Hz$ respectively [135, 136]. Theories and experimental studies investigating the phenomenon of binaural beat precept suggest that the application of auditory beats binaural beats with

32

specific frequency characteristics to tune the frequency of neuronal oscillations within the brain. This process is known as brain wave entrainment [135].

The phenomenon of brain wave entrainment was first observed as frequency following responses in EEG signals [138]. Initial observations suggested that brain wave entrainment can tune cortical EEG potentials to oscillate at frequencies similar to those of the stimulating binaural beats. This observation was supported by later studies that showed entrainment effects in almost all EEG frequency bands [139, 140]. Following these findings, the frequency ranges of binaural beats are conventionally named in literature following the division of EEG bands as delta ($< 4Hz$), theta ($4 - 7Hz$), alpha ($7 - 13Hz$), beta ($13 - 30Hz$), gamma ($30 - 50Hz$). Modern research suggests that the synchronization of binaural beats and brainwaves at specific frequencies can lead to changes in mood and cognition. These studies investigated the effect of binaural beats on different aspects including working memory, visuospatial memory, cognitive flexibility, anxiety, and emotions [141–145]. In addition, several other studies in literature specifically investigated the use of different binaural beat frequencies for cognitive vigilance enhancement.

The study in [31] compared the effects of delta ($1.5Hz$), theta ($4Hz$), and beta ($24Hz$) binaural beats on vigilance performance. During the experimental studies, participants performed a 1-back vigilance test while listening to a single binaural beat frequency at a time. Different visual objects were presented in a random sequence, and the task was to detect successive repetitions of a specific target object. The assessment criterion in this study was merely based on the statistical comparison of the recorded correct target detection rates across different conditions. The results suggested that continuous presentation of beta binaural beats for 30 min yielded positive behavioral results in comparison to the control (no audio tone) and other binaural beat conditions.

The authors in [146] adopted a behavioural assessment approach to investigate the effect of high-frequency binaural beats on long-term attentional focusing. Specifically, the performance during a local-global vigilance task was compared between two audio conditions: continuous $340Hz$ pure tone (control) and continuous gamma ($40Hz$) binaural beat. The local-global test is typically used in psychology to assess selective attention based on the ability to focus on a specific local or global feature of a target

stimulus without being distracted by other features [147]. The four target stimuli conditions considered in this study consisted of either a large rectangle or square (global feature) composed of smaller rectangles or squares (local feature). Participants had to alternate between responding to a single local or global feature every 4 consecutive trials. A complete task session consisted of a total of 80 global trials and 80 local trials and lasted for 7 min on average. Statistical comparison of the error rates of the two audio conditions showed no significant differences suggesting that binaural beats did not impact the participants' ability to suppress irrelevant feature information. However, the analysis revealed significant improvement in the reaction time of correct detection in the presence of binaural beats indicating an overall improvement in attentional focusing.

The study in [148] failed to report positive enhancement effect using short-time binaural beats. In particular, the effects of theta ($7Hz$) and beta ($16Hz$) binaural beats, presented as 2 min pulses, were investigated during a 13 min zero-back target detection task. For a single experimental session, the complete 13 min task duration was divided into eight epochs. Each epoch consisted of a 2 min binaural beat period preceded and followed by a 2 min and 30 sec resting periods of white noise respectively. The order of binaural beat presentation was fixed for all subjects. In contrast to the two previous studies, the adopted assessment approach was mainly based on EEG spectral analysis. Reaction time data was also investigated. The experimental results showed that vigilance performance, as measured by the reaction time, was not altered by different binaural beat conditions. In addition, no significant differences in cortical frequency power during the enhancement periods compared to the white noise periods. These results suggest that short-time and pulsed binaural beat stimulation is ineffective to induce vigilance enhancement or cortical entrainment effects.

The contradictory results in the previous studies suggest that enhancement effects are highly sensitive to variability in the design of experimental paradigms. Several variables related to the binaural beat stimulus might include the beating and carrier frequencies, task duration vs. stimuli duration, and stimulus representation sequence. Other relevant variables might include the number and age of subjects, the type of vigilance task, and the day time of the experiment. It is worth mentioning that the existing literature specific to the effects on binaural beats on vigilance is insufficient, and that the

effects of the previously mentioned variable are still unclear. However, studies investigating the the effect of binaural beats on different cognitive aspects showed positive enhancement results as indicated by the improvements in the subjects' performance and the entrained EEG activity patterns.

Chapter 4. Methodology

This chapter details the methodology of this thesis. In specific, discussed below is the adopted experimental protocol to induce and enhance vigilance decrement, the process of selecting and recruiting participants, the experimental setup to acquire and record the EEG and behavioral data, and the methods of data analysis.

4.1. Experimental Protocol

4.1.1. Participants. Twenty-seven healthy student volunteers from the American University of Sharjah participated in this study (12 females and 15 males; aged 21 ± 4 years old). The inclusion criteria included having normal hearing, normal or corrected-to-normal vision, no history of psychiatric or cognitive disorders, no symptoms of drug addiction, and no intake of long-term medications. All participants voluntarily gave written consent after knowing about the nature of the study, the procedure to be followed, and the possibility of withdrawing a running session at their wish. The volunteers did not receive any reimbursement for their participation. The time of the experiment was restricted between 2 p.m. and 7 p.m. to eliminate the potential effect of circadian misalignment on cognitive performance [149]. The study protocol was designed following the declaration of Helsinki and was approved by the Institutional Review Board at the American University of Sharjah.

4.1.2. Auditory stimulus. Three auditory conditions were considered during the course of the experimental sessions: 1) no audio, 2) pure sinusoidal tone (R: 250 Hz, L: 250 Hz), and 3) 16 Hz beta binaural beats (R: 250 Hz, L: 266 Hz). The frequency of the sinusoidal tones presented to the left and right ears is indicated by L and R respectively. Figure 4 illustrates the presentation of the pure tone and binaural beats stimulus. The audio files were created via Matlab software (R2013a, Natick, MA, USA) and were introduced to the participants through a set of stereo earphones (MD827ZM Earpods, Apple, Sharjah, United Arab Emirates). At the commencement of the experiment, the desired sound volume was set by the participants. The tones were produced with a minimum intensity of 50 dB and were presented continuously with no pulsation to avoid the impact of the short auditory rests on both the participants' performance and brain

activity [122]. Besides, tones were generated at a sampling rate of 48 kHz and were saved as 32-bit integers to avoid the risk of aliasing or quantization distortion. A 250 Hz base frequency was chosen since it provides a compromise between being audibly pleasant and perceivable.

(a)
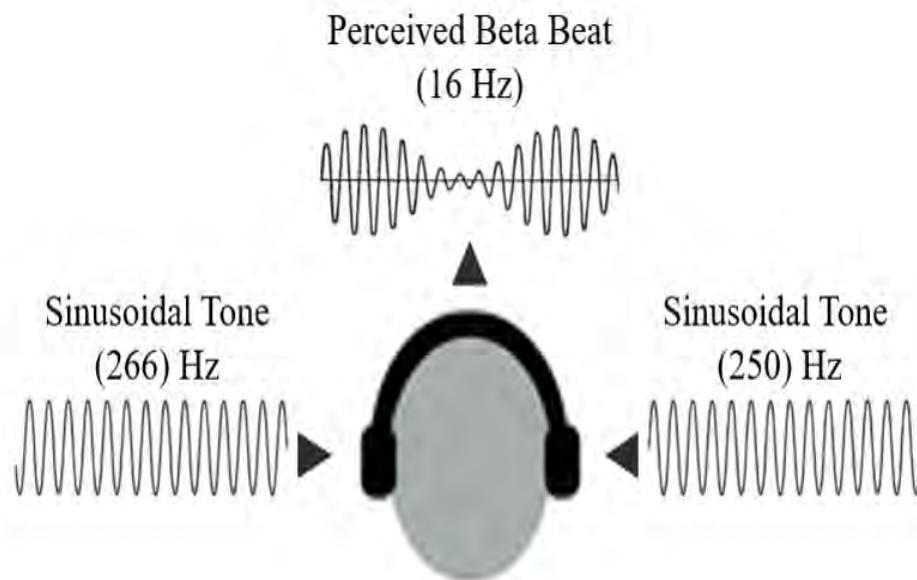
(b)

Figure 4: Presentation of the audio stimulus. (a) A 250 Hz pure sinusoidal tone and (b) 16 Hz beta binaural beats.

4.1.3. Vigilance task. The vigilance task considered in this study is the incongruent Stroop color-word task (I-SCWT). In a typical I-SCWT, a list of incongruent color words (ex: the word "red" written in yellow front color) is presented to the participants. In return, participants are asked to identify only the front colors instead of reading the words. As such, participants will experience an incongruent cognitive state when performing a less automated task (i.e. naming the front color) while inhibiting the interference arising from a more automated semantic task (reading the word) [150–153]. The degree to which participants' responses are affected by this inference has been used in many studies as a measure to assess executive or control [154–156], attentional control [157–159], processing speed [152, 160], and cognitive flexibility [161, 162]. Many researchers considered the Stroop effect as a case of automatic semantic vigilance in which response to the negative stimuli becomes more preferential with increasing time-on-task [163–166]. We believe that the I-SCWT is unique in comparison to traditional vigilance tasks since it does not fall neatly under the sensory vigilance classification. Based on nature and the design of the test, the I-SCWT can involve both sensory and cognitive processes and is thus more suitable to mimic real-life tasks.

In this study, a trial-based computerized and interactive I-SCWT was developed and presented via Matlab software (R2013a, Natick, MA, USA). Figure 5 shows the main views of the I-SCWT interface. As shown in Figure 5a a list of instructions in provided to the participants before starting the task. Following that, task trials are presented sequentially. For each trial, a single random color word, written in a random front color, was displayed on the screen. In return, participants were requested to click the button corresponding to the front color as fast and as accurate as they can. Subject responses were marked as either "correct", "incorrect", or "missed". After each trial, the reaction time was recorded, and a feedback message was displayed on the screen. To add an extra level of attentional challenge and to increases the rate of vigilance decrement, the background colors of the buttons were randomly set. In Addition, a mock user performance indicator that implied a poor performance by the participants in comparison with their peers was displayed with each trial. Only six response colors were considered - namely blue, green, red, magenta, cyan, and yellow.
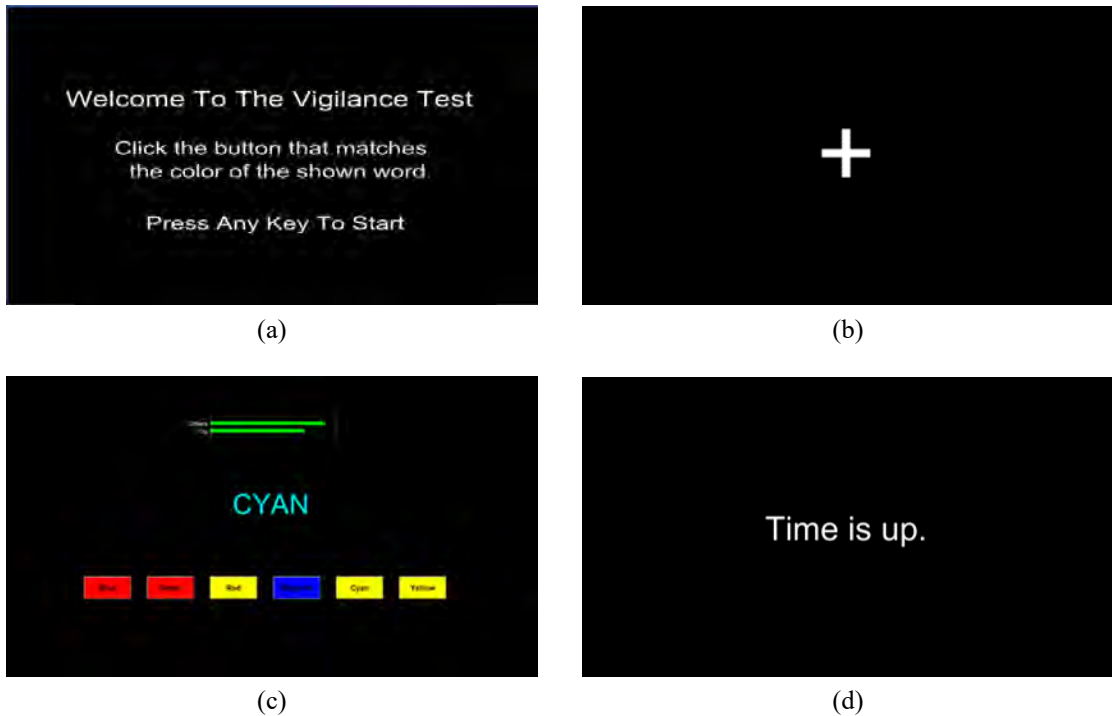
Figure 5: Different views of the I-SCWT interface. (a) Introductory instructions to participants, (b) pre- and post-task baseline, (c) an incongruent Stroop stimulus, and (d) post-trial feedback (no response example).

4.1.4. Experimental setup and EEG data acquisition. Figure 6 shows the experimental and data acquisition setup of this work. During the course of experimental sessions, surface brain activity was measured using the EEG ANT Neuro Waveguard system. The system consists of a set of 64 Ag/AgCl scalp electrodes configured in a wearable cap according to the standard 10-20 layout. Figures 7 shows the 10-20 scalp distribution of the EEG electrodes. The ASA Lab software was used to record the EEG signals and check electrode impedances (ASA Lab 4.9.2 acquisition software, ANT Neuro, Hengelo, Netherlands). Before recording, all electrode impedances were reduced to less than $10K\Omega$ by applying a conductive gel layer directly between the electrodes and the subject's head. The AFz electrode was set as the system ground, and all other electrode signals were referenced to the mastoid electrodes M1 and M2. The EEG signals were acquired at a sampling rate of 500 Hz. Using a parallel port interface between the stimulus PC and the EEG recording PC, the data was labeled using event triggers sent at the instants of stimulus representation and subject responses (i.e. correct, incorrect, or missed).

39
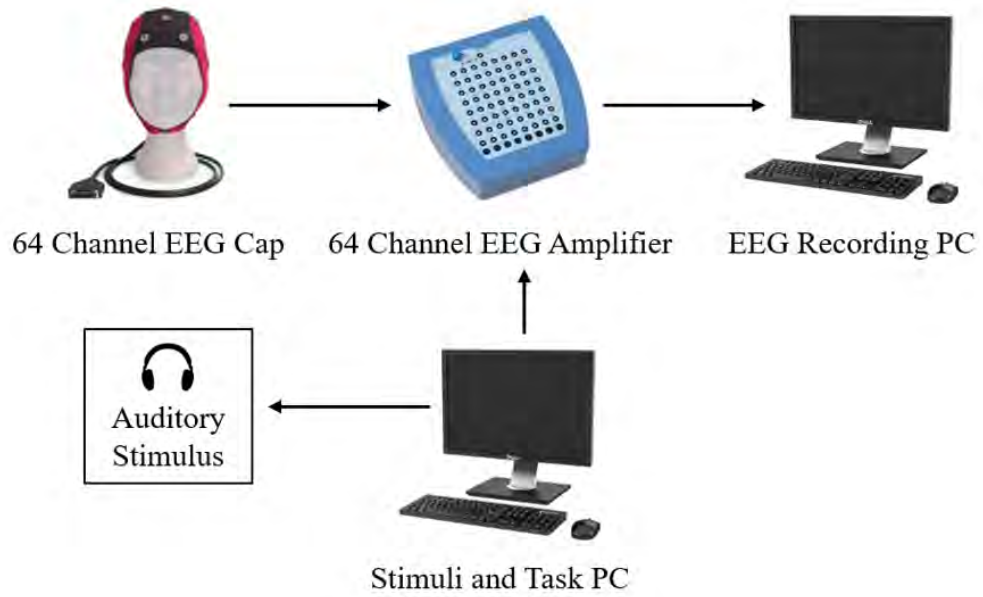
(a)
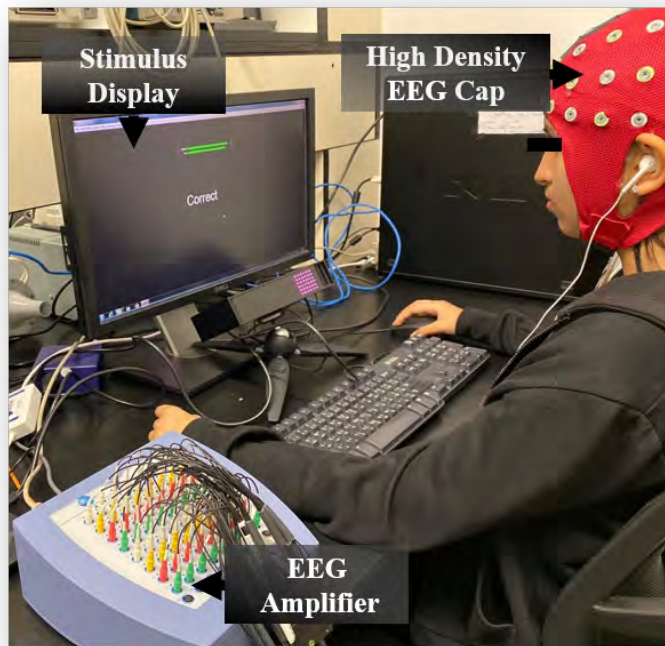
(b)

Figure 6: Experimental and data acquisition setup. (a) Schematic diagram of experimental setup and (b) actual laboratory setup.
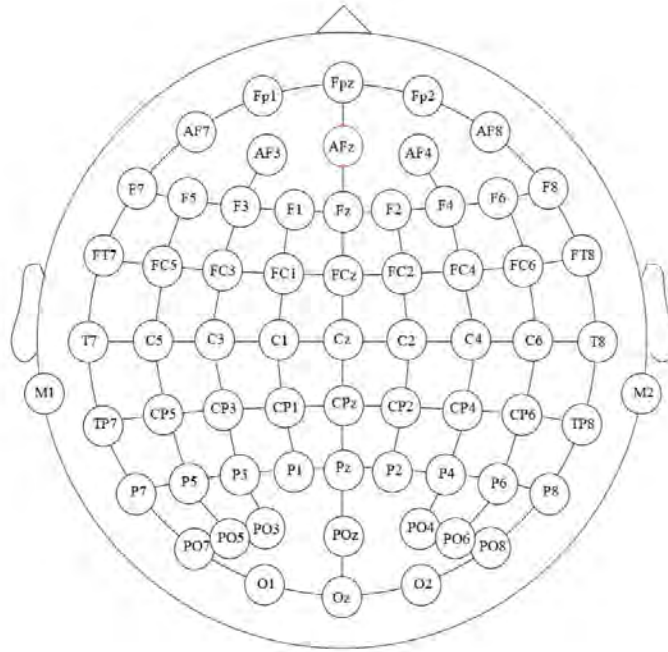
Figure 7: 10-20 layout of the EEG electrodes. The red channel (AFz) represents the system ground.

4.1.5. Procedure and task sequence. Figure 8 provides an overview of the experimental protocol and the I-SCWT sequence. The experiment consisted of two main scenarios based on three audio conditions: vigilance (no audio) and enhancement (pure sinusoidal tone or binaural beats). Each participant underwent a single experimental session, and each of the three conditions included nine randomly assigned participants. Complete sessions were scheduled on separate days and lasted around one hour, including subject preparation and task presentation. During a vigilance session, participants continuously performed a 30 min I-SCWT. Participants assigned to an enhancement condition performed the same task while listening to a pure sinusoidal tone or binaural beats. A two min baseline period preceded and followed all task periods (marked by the appearance of the plus sign (+) on the I-SCWT as shown in Figure 5b). Upon arrival, participants completed the informed consent procedure and filled demographic and health history forms. Following that, the experimenter introduced the vigilance task and performed a one min demonstration. While doing so, the experimenter provided clear instructions and answered all the participants' questions. Participants then underwent a five min training/warm-up phase, and performance feedback was provided

41

upon completion. The average reaction time scored during training was set as the maximum response time for each I-SCWT trial. Following the EEG setup, participants were comfortably seated in front of the stimulus PC and were instructed to avoid body movements to ensure the quality of the EEG data. When the experimenter was confident about the participants' understanding of all instructions, the actual I-SCWT task phase began. The experiment was carried out in the Biomedical Systems Laboratory at the American University of Sharjah. A quiet environment with controlled light and temperature levels was maintained during the experiment.
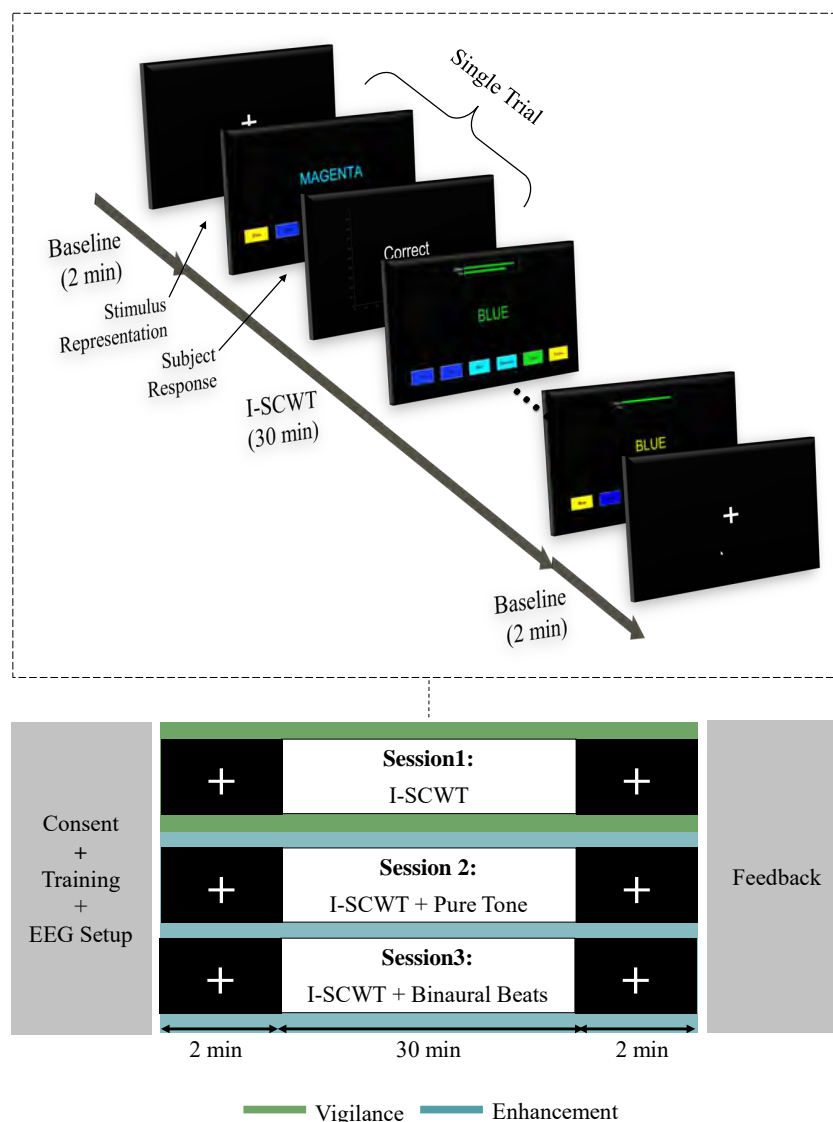
Figure 8: Overview of the experimental protocol and the I-SCWT sequence. Different sessions were scheduled on separate days, and a single session involved only one participant.

4.2.   Behavioral Data Processing and Analysis

Behavioral data such as trial reaction time to stimuli and detection accuracy were collected while solving the task. For a single trial, the reaction time was recorded as the time between stimulus representation and subject response. The detection accuracy was calculated based on the number of the color word correctly matched over the total number of the displayed color word targets. The behavioral data was used as an objective indication of vigilance decrement or enhancement.

4.3.   Functional Connectivity Analysis

4.3.1. EEG data preprocessing.   Before analysis, the raw signals were filtered to the 0.5 Hz-40 Hz band and re-referenced to the common average. The Independent Component Analysis was used to correct for eye movement and ECG artifacts. Components that appeared to contribute the most to the artifacts, typically two or three, were excluded, and the remaining ones were used to reconstruct the EEG signal. The EEG data were then epoched from 0.2s before the stimulus representation triggers to 1s after. The baseline of each epoch was removed using the 0.2s pre-stimulus data. Finally, artifactual epochs were identified and rejected by manual inspection. Further analysis was only restricted to two windows extracted from the first and last five min portions of the signal, each represented by 83 artifact-free epochs. The preprocessing steps were performed using Matlab custom scrips based on EEGLAB pop-up functions [167].

4.3.2. Phase locking value estimation.   Functional connectivity of within-band phase synchrony was estimated using the phase-locking value (PLV) statistic. The PLV quantifies bivariate interactions between time-series signals based on the consistency of their instantaneous relative phases. A popular estimate of the PLV in literature is based on the magnitude of the circular mean of unity relative phase vectors [168–170]. For two simultaneously recorded signals y(t) and x(t), such relation can be mathematically formulated as:

$$PLV = T^{-1} \left| \sum_{t=1}^{T} e^{i(\phi_x(t) - \phi_y(t))} \right|, \tag{7}$$

where T is the total number of sampled time points. $\phi_x(t)$ and $\phi_y(t)$ are the instantaneous phase values of *x* and *y* respectively at a time point t. The instantaneous relative phase values were obtained from the analytic representation of the EEG signals using the Hilbert transform [171]. Given a real signal y(t), its analytic representation z(t) can be in written in terms of Hilbert transform as:

$$z(t) = y(t) + j \, \widetilde{y}(t) = A(t)e^{\phi(t)}, \tag{8}$$

where $\widetilde{y}(t)$ is the Hilbert transform of y(t), computed as:

$$\widetilde{y}(t) \ = \ \frac{1}{\pi} \, PV \, \int_{-\infty}^{+\infty} \frac{y(\tau)}{t - \tau} d\tau, \tag{9}$$

where PV is the Cauchy principal value. The instantaneous relative phases can be obtained via the Hilbert transform as:

$$\phi_x(t) - \phi_y(t) = arctan \, \frac{\widetilde{x}(t)y(t) - x(t)\widetilde{y}(t)}{x(t)y(t) + \widetilde{x}(t)\widetilde{y}(t)} \tag{10}$$

The formulation of the PLV follows the hypothesis that connected cortical signals have instantaneous phases that evolve together [169]. In other words, highly connected signals are time-locked, and their relative phases are constant over time. Figure 9 illustrates concept of PLVs as estimated by equation 7. According to the mathematical definition, the PLV connectivity quantifies the speediness of the circular distribution of unity relative phases. The narrower the distribution, the greater the PLV. The PLV is thus an undirected estimate of functional connectivity with values bounded within the interval of [0 1] (the value of 1 reflects the case of absolute synchrony). In comparison to other functional connectivity estimators, the PLV does not require prior assumptions regarding the nature of the data and is thus better suited to the analysis of non-linear and non-stationary neurological signals [169, 172].

For each epoch, PLVs between electrode signals were estimated in the delta δ (0.1-4 Hz), theta θ (4- 8 Hz), alpha α (8-13 Hz), and beta β (13-30 Hz) frequency bands. As shown in Figure 10, the statistical significance of the estimated PLVs was determined by comparison to an empirical distribution of 100 surrogate PLV maps ($p <$

0.05). To destroy phase phase dependencies, the surrogate time series were derived from the original EEG time series with phase randomization in the Fourier domain. Other aspects of the signals were unchanged. To reduce volume conduction effects, PLVs corresponding to relative phase distributions with medians equivalent to 0 (mod π) were excluded [173]. Given that the estimated relative phases by equation 10 are within the interval $[-\pi/2, \pi/2]$, the distributions' medians were tested against the null median of 0. The test of median significance was conducted following the conventions of circular statistics with a significance level of 95% [174]. Each epoch was represented by four band-specific 62×62 adjacency matrices obtained by calculating the PLVs between all the possible pairs of EEG signals. The adjacency matrices signals were used in subsequent graph theory analysis.

(a)   (b)

(c)
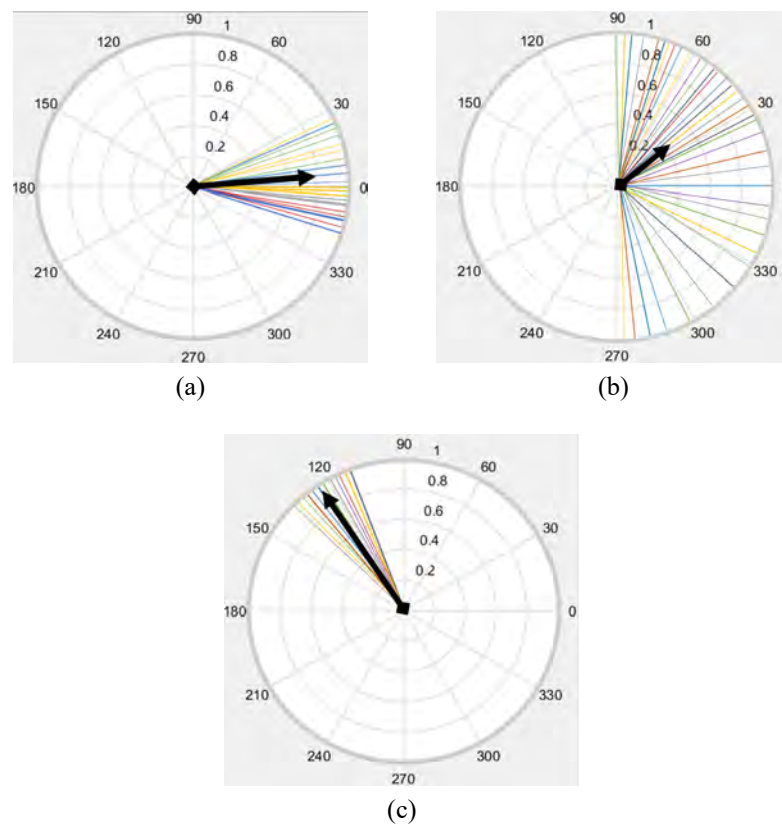
Figure 9: Graphical illustration of the phase-locking value estimate. (a) Possible volume conduction effect that can be corrected, (b) possible volume conduction effect that cannot be corrected, and (c) relative phase distribution corresponding to a high PLV. Colored arrows represent examples of unity relative phase vectors.
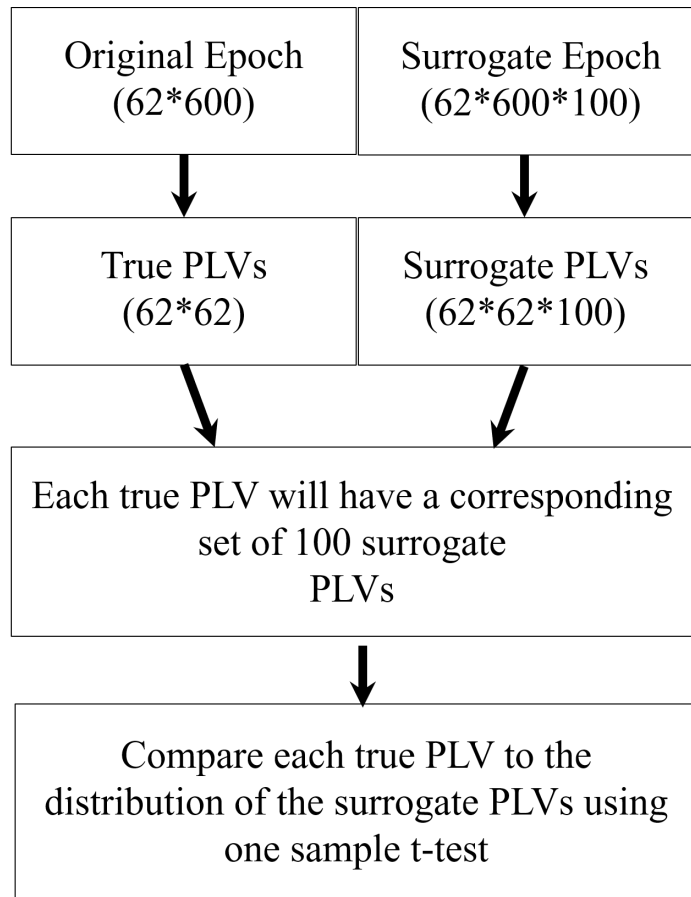
Figure 10: Schematic illustration for the analysis of phase-locking value statistical significance and generation of surrogate data.

4.3.3. Network construction and graph theory analysis. Network graph theoretical analysis was employed to examine and quantify the characteristics of cortical functional connectivity. The adjacency matrices were converted into full-scale networks consisting of nodes and weighted edges. Nodes corresponded to the 62 EEG electrode signals, and edges were represented by the estimated PLVs. In addition, sub-networks corresponding to the primary left and right frontal, central, temporal, parietal, and occipital cortical lobes were investigated. Shown in Figure 11 are the nodes constituent to each sub-network. Graph theory analysis (GTA) was carried out to characterize the global and local topology of the functional connectivity networks based on the concepts of node degree, node strength, clustering coefficient, and efficiency. Details about the definitions and the mathematical formulation of these metrics are provided below.
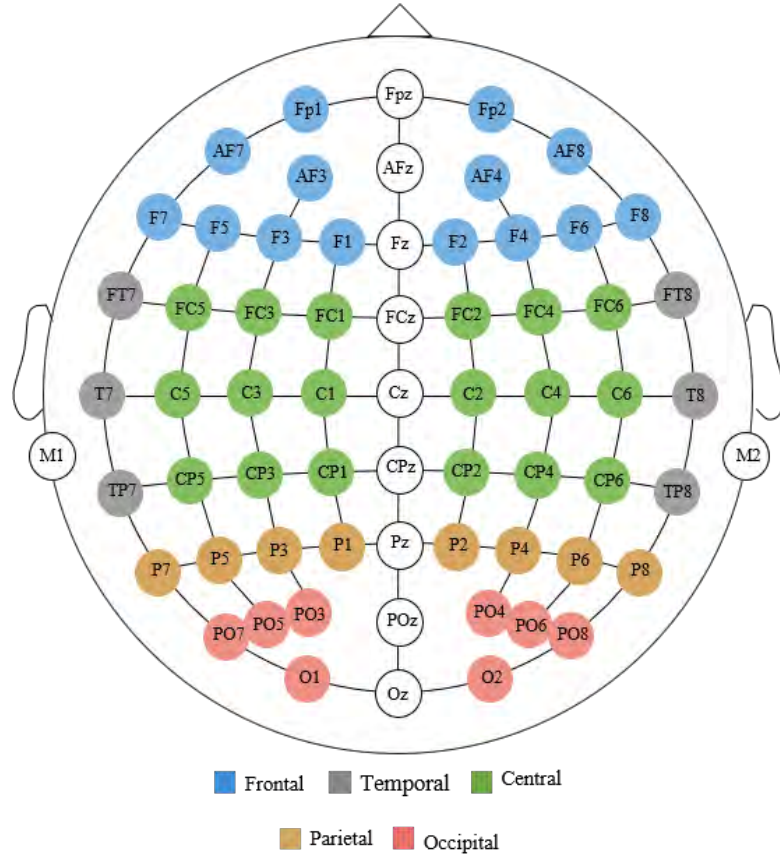
Figure 11: Arrangement of the 10-20 EEG electrodes in accordance to the primary left and right cortical lobes.

4.3.3.1. Node degree. A measure of centrality and that quantifies the importance of nodes within a network [175]. Mathematically, the local node degree d_i refers to the number of edges directly connected to a particular node (excluding self loops) normalized by the number of possible edges:

$$d_i = \frac{1}{N-1} \sum_{j \neq i \in N} a_{ij}, \tag{11}$$

where the elements a_{ij} refer to the edge status between node i and node j (i.e. $a_{ij} = 1$ if the edge weight $w_{ij} \neq 0$), and N is the total number of nodes within the network. The global node degree of a network (i.e. the arithmetic mean of all node degrees) reflects the overall density of connections and is usually used as a basis of comparing different networks.

4.3.3.2. Node strength. For a weighted network, the concept of node degree can be replaced by that of node strength considering edge weights instead of edge status [176]. Mathematically, the local node strength s_i is the weighted sum of edges connected to a node i:

$$s_i = \frac{1}{N-1} \sum_{j \neq i \in N} w_{ij} \tag{12}$$

In terms of brain activity, degree centrality (measured by node degree or node strength) reflects the involvement of cortical regions in information transmission and processing. Higher degree centralities correspond to densely connected nodes, or in other words, a higher localized brain activity [175]. Therefore, the degree centrality can quantitatively analyze the importance of the node in the brain functional network.

4.3.3.3. Network clustering coefficient. A measure network segregation that quantifies the tendency to which specialized processing occurs between densely inter-connected nodes [175]. The presence of such groups is quantified based on the concept of network modules or cliques. Higher presence of cliques within a network indicates higher segregation or specialized activity. For a node i, the local clustering coefficient C_i is calculated as the ratio between the sum of the geometric means of all existing 3-node weighted cliques and the number of all possible cliques. Within an undirected and weighted network, this can be mathematically expressed as [176]:

$$C_i = \frac{\sum_{j \neq i \in N} \sum_{h \neq (i,j) \in N} (w_{ij} w_{jh} w_{hi})^{1/3}}{s_i(s_i - 1)}, \tag{13}$$

4.3.3.4. Network efficiency. The local node efficiency is a measure of functional integration and it quantifies the degree to which specific nodes rabidly combine specialized information from other distributed nodes within the network [175]. Such property is characterized based the concept of a path between nodes. Shorter paths imply stronger potential for integration and thus a higher efficiency of information exchange. The local efficiency E_i is mathematically calculated average of the reciprocal

of the shortest paths to all other nodes within the network [177]:

$$E_i = \frac{1}{N(N-1)} \sum_{i \neq j \in N} \frac{1}{L_{ij}},$$
(14)

where Lij is the length of the shortest path between node i and j. The shortest bath between two nodes was found via the Dijkstra's algorithm, such that the sum of the lengths of its constituent edges is minimized [178–181]. The edge lengths are the reciprocal of edge weights. conventionally, paths between disconnected nodes are defined to have infinite lengths. Unlike other measures such as the characteristics path length, the efficiency can be thus meaningfully estimated for disconnected networks as zero, making it a superior metric of integration. The global versions of the node degree, node strength, clustering coefficient, and efficiency were obtained from the arithmetic means of their local versions over all nodes within the network.

Weak network connections estimated form neuroimaging data may be noisy or spurious. Thus, network thresholding is usually applied before GTA to eliminate weak edges and to highlight the effect of significant connections [182]. When studying different groups or conditions, it is necessary to compare networks having the same global density [183]. As such, the observed phenomena will not get biased due to the unbalanced number of network connections. Herein, sparsity thresholds were applied to preserve a specific proportion of the most significant edges [184–186]. For example, a 10% sparsity threshold applied to a network consisting of 62 nodes keeps only the highest 384 edge weights. No specific standard was applied to select a particular sparsity level before the GTA. Instead, a range from 0% to 100% with a step of 5% was explored. The complete connectivity analysis and GTA was performed via Matlab software (R2019a, Natick, MA, USA).

Chapter 5. Functional Connectivity Analysis under Cognitive Alertness and Vigilance Decrement States

This chapter provides an in-depth analysis to investigate TOT related changes in cortical functional connectivity. To recap, the phase-locking value statistic was employed to reconstruct the cortical connectivity networks under two mental states: cognitive alertness (0-5 min) and vigilance decrement (25-30 min). Different aspects of the connectivity networks were quantified and compared based on a GTA framework. Based on reported findings in literature, it was expected that alterations in functional connectivity due to vigilance decrement will result in a less optimal network topology. We further hypothesized that these alterations are region and band-specific.

5.1.   Changes in Functional Connectivity with Increased Time on Task

To provide an overview of differences in functional connectivity between the two mental states, Figures 12 to 15 show the plots of the connectivity networks. The edges represent the grand average PLV weights across subjects. For illustration purposes, the grand average network was thresholded at a 10% sparsity level. In all frequency bands, the network patterns showed decreases in connectivity weights under vigilance decrement. Also, distinct connections appeared between different nodes in the two states. Characterization of these changes using GTA is provided in the following sections.
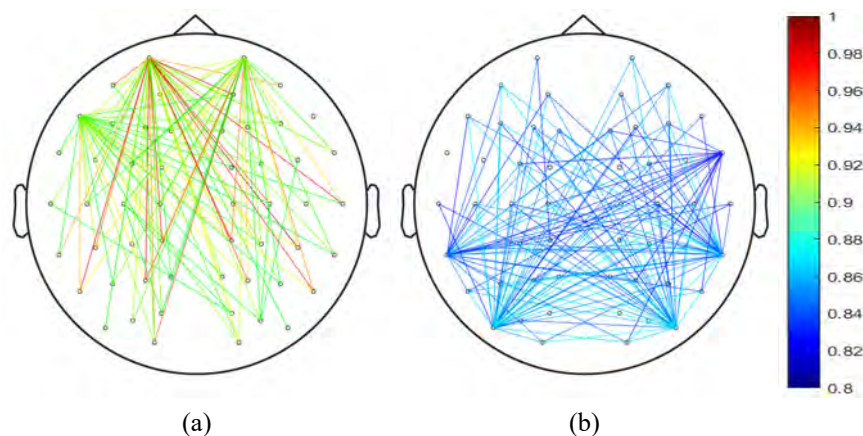
Figure 12: Grand averaged weighted connectivity networks in the delta frequency band under (a) cognitive alertness and (b) vigilance decrement states.
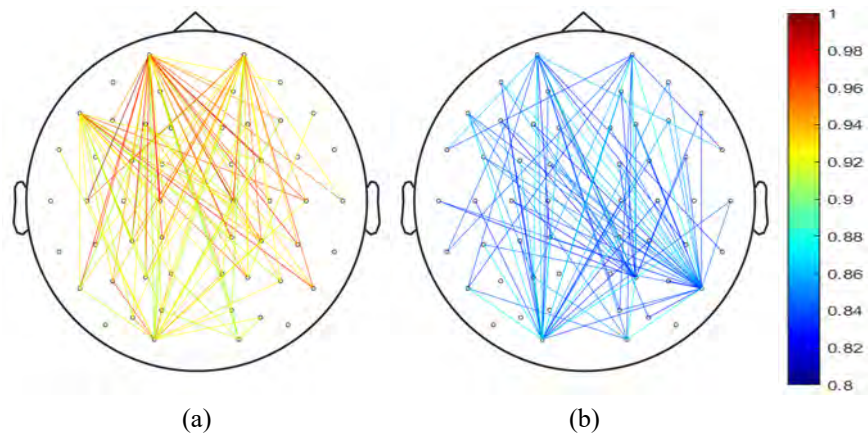
Figure 13: Grand averaged weighted connectivity networks in the theta frequency band under (a) cognitive alertness and (b) vigilance decrement states.
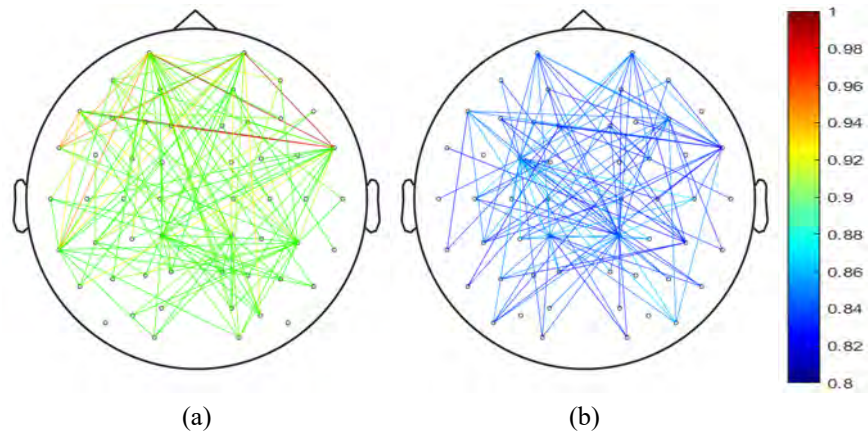
Figure 14: Grand averaged weighted connectivity networks in the alpha frequency band under (a) cognitive alertness and (b) vigilance decrement states.
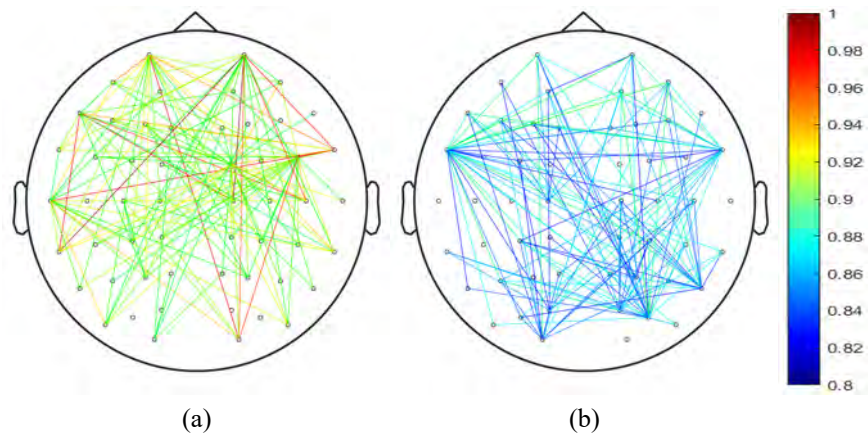
Figure 15: Grand averaged weighted connectivity networks in the beta frequency band under (a) cognitive alertness and (b) vigilance decrement states.

5.2. Full-Scale Global Network Topology Analysis

Figures 16 to 18 compare the full-scale functional networks under alertness and vigilance decrement states based on their global node strength (NS_g), clustering coefficient (CC_g), and efficiency (E_g), respectively. Plotted are the mean values with error bars indicating the standard error around the mean. To consider the effect of network sparsity level, the estimated metrics were plotted against a full sparsity range of 0% to 100% with a step of 5%. At each sparsity level, a paired sample t-test was employed to test the statistical significance of differences between the two cognitive states. The asterisks on the plots indicate a significant effect of cognitive state ($*: p < 0.05$, $**: p < 0.01$).

As shown in Figure 16, when the network sparsity increases, the NS_g also increases under both cognitive states and in all frequency bands. Such a pattern is expected since higher sparsity levels account for a higher number of edges, resulting in more dense networks. In addition, the effect of cognitive state was statistically significant over a wide sparsity range in all bands (i.e $> 20\%$). As shown in Figures 16c and 16d, the NS_g under alertness was significantly higher than that under vigilance decrement over a the full sparsity range in the alpha and beta bands ($p < 0.05$). In the delta (Figure 16a) and theta (Figure 16b) bands, statistical significance between the two cognitive states became more evident for sparsities higher than 40% ($p < 0.01$). As shown in Figures 17 and 18 , the CC_g and the E_g of the network followed a similar increasing pattern to that of the NS_g with the increase in sparsity level. However, differences in the CC_g between the two cognitive states were significant over a smaller sparsity range of 35% to 100%. As shown in Figures 17a, 17b,18a, and 18b, the effect of cognitive state in the delta and theta bands was more significant ($p < 0.01$) for higher sparsity levels (i.e.$> 40\%$). Subsequent results were obtained from the integral over a sparsity range of 50% to 95% to avoid potential biasing effects of selecting a particular threshold [187, 188]. This range was selected due to the following reasons: (1) differences between the two cognitive levels are significant for all GTA metrics, (2) for each mental state, the global GTA metrics are relatively constant, and (3) a sparsities down to 50% are enough to eliminate insignificant connections while preserving the structure of the underlying small world network [189].
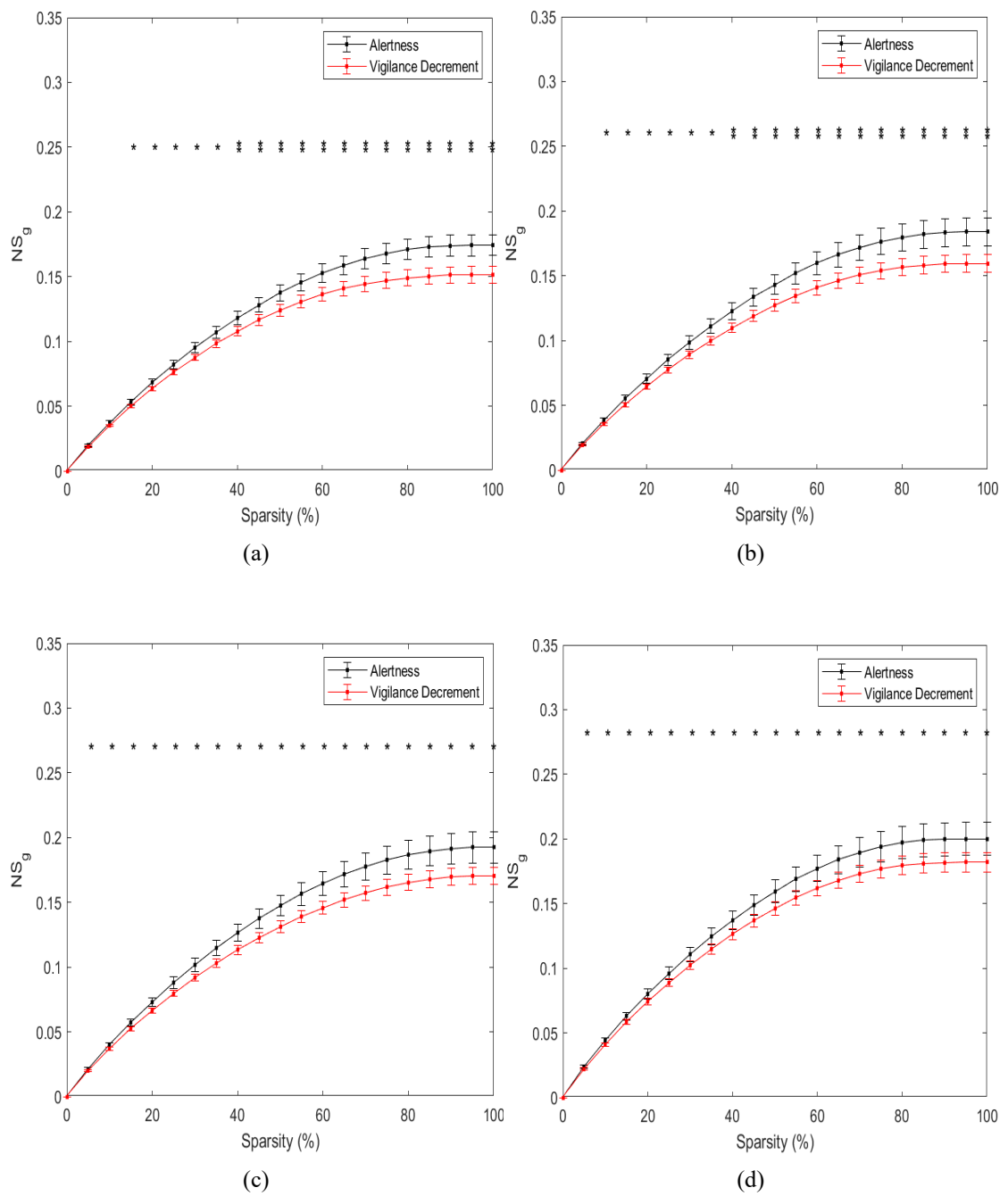
Figure 16: Comparison between the global node strength of the full-scale network under alertness and vigilance decrement states in the (a) delta, (b) theta, (c) alpha, and (d) beta bands. Plotted are the mean values across subjects with error bars indicating the standard error. The asterisks indicate a significant effect of cognitive state ($*: p < 0.05$, $**: p < 0.01$).
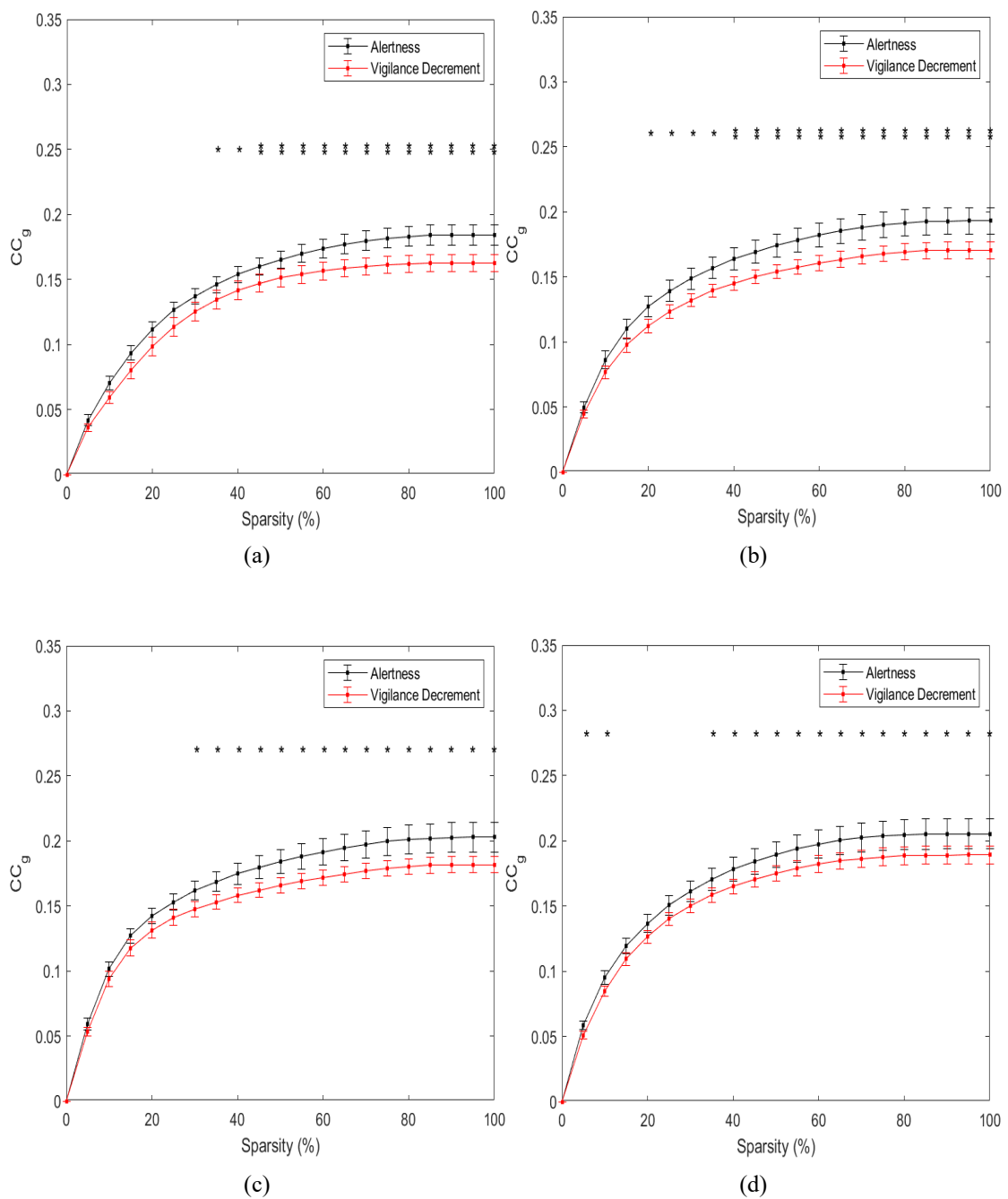
Figure 17: Comparison between the global clustering coefficient of the full-scale network under alertness and vigilance decrement states in the (a) delta, (b) theta, (c) alpha, and (d) beta bands. Plotted are the mean values across subjects with error bars indicating the standard error. The asterisks indicate a significant effect of cognitive state $(*: p < 0.05, **: p < 0.01)$.
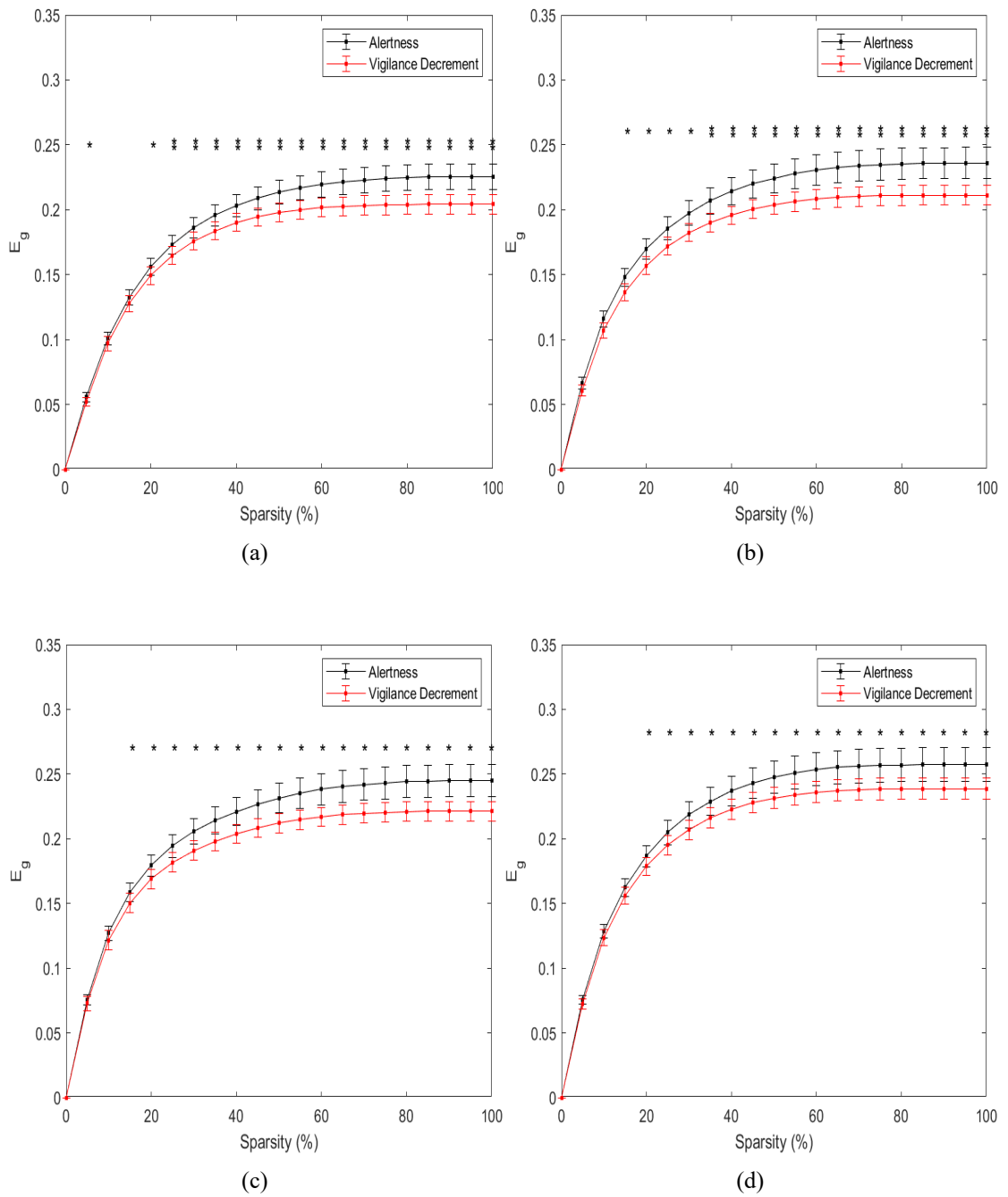
Figure 18: Comparison between the global efficiency of the full-scale network under alertness and vigilance decrement states in the (a) delta, (b) theta, (c) alpha, and (d) beta bands. Plotted are the mean values across subjects with error bars indicating the standard error. The asterisks indicate a significant effect of cognitive state ($*: p < 0.05$, $**: p < 0.01$).

5.3.   Full-Scale Local Network Topology Analysis

Figures 19 to 21 show the scalp maps of the full-scale local node strength, clustering coefficient, and efficiency. The mapped values represent the grand average across subjects. For each electrode (node), a paired sample t-test was employed to test the statistical significance of differences in local topology between alertness and vigilance decrement cognitive states. The asterisks (*) on the maps indicate a statistically significant difference ($p < 0.01$).

The results of the local nodal strength in Figure 19 show general full-scale decreases in connectivity under vigilance decrment in all frequency bands. In addition, high connectivity at the frontal electrodes (i.e. Fp1, Fpz, and Fp2) was observed under alertness and significantly decreased under vigilance decrement state. In the delta frequency band, local node strengths decreased at most of the electrodes under vigilance decrement. In the theta band, high local node strengths were observed at the occipital electrodes (i.e. POz, O1, Oz, and O2) under alertness state and slightly decreased with increasing TOT. All central and a few and temporal (i.e T7 and T8) node strengths significantly decreased under vigilance decrement. In the alpha band, high temporal and temporo-parietal node strengths were observed under alertness state (i.e. FT7, P5, P7, TP7, PO7, CP5, and C5 electrodes). The paired sample t-test at the electrode level showed significant decrements at the central (i.e. FC5, FC1, FC2, FC6) and occipital electrodes under vigilance decrement. The beta frequency band showed the highest connectivity at all electrodes under alertness state. Significant frontal and central decrements were observed under vigilance decrement (i.e. F1, Fz, F3, Fz, F4, F8, FC5, FC1,FC2, FC6, C3, CZ, and C4 electrodes). As shown in Figure 20, the full-scale local clustering coefficient generally decreased under vigilance decrement in all frequency bands. Interestingly, higher frequency networks (i.e alpha and beta) revealed increased functional segregation under the alertness state. Also, the lower frequency networks (i.e. delta and theta) showed significant decrements at all electrodes under vigilance decrement. Likewise, the local efficiency showed a frequency-specific decreasing connectivity pattern as shown in Figure 21.
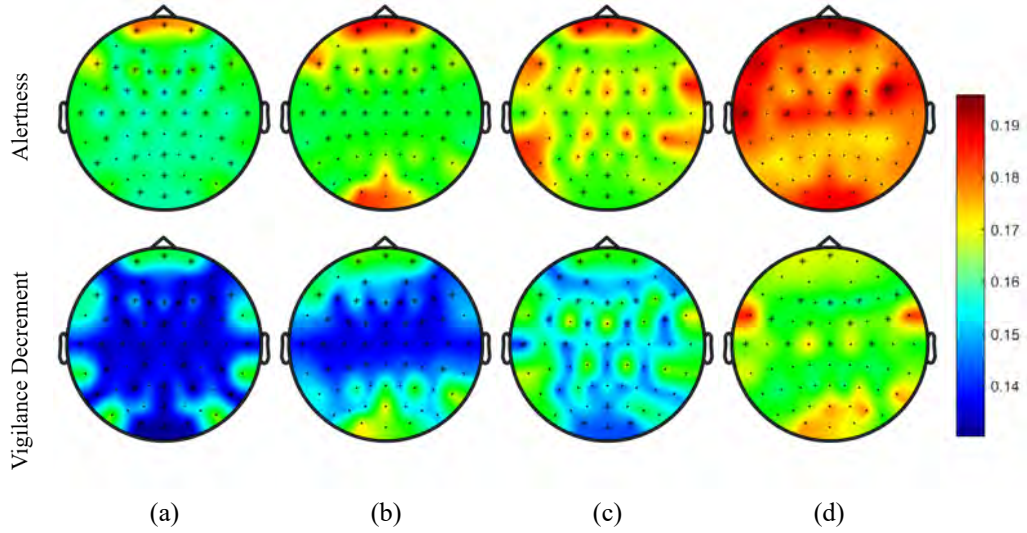
Figure 19: Scalp topographical maps of the local node strengths under alertness and vigilance decrement states in the (a) delta, (b) theta, (c) alpha, and (b) beta frequency bands. The mapped values represent the grand average across subjects. The asterisks (*) indicate a statistically significant local difference between the two cognitive states ($p < 0.01$).
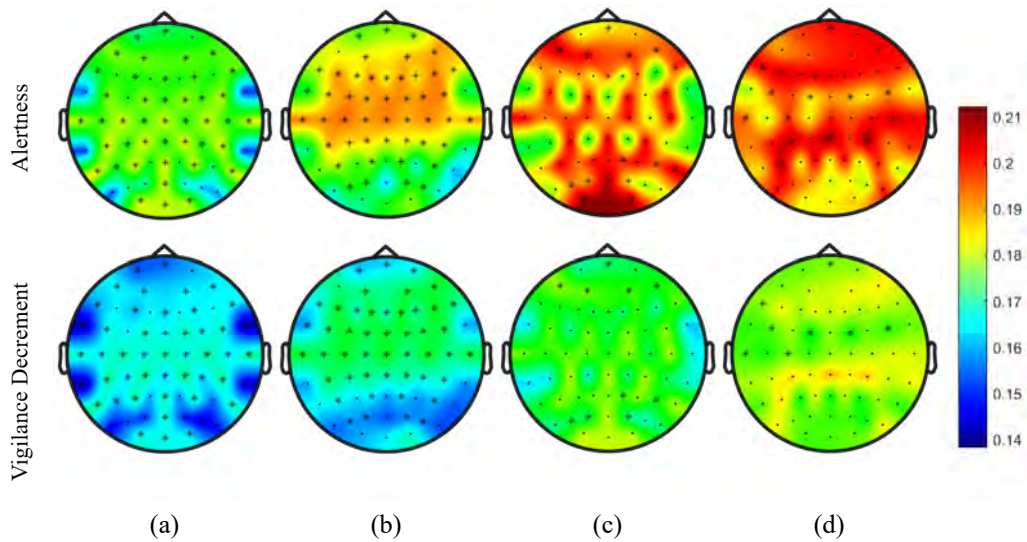
Figure 20: Scalp topographical maps of the local clustering coefficients under alertness and vigilance decrement states in the (a) delta, (b) theta, (c) alpha, and (b) beta frequency bands. The mapped values represent the grand average across subjects. The asterisks (*) indicate a statistically significant local difference between the two cognitive states ($p < 0.01$).
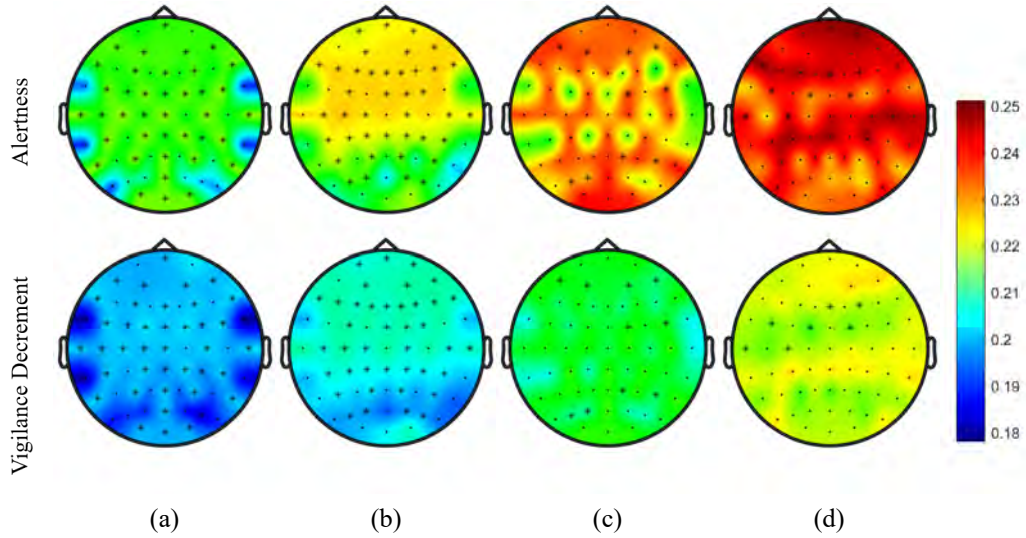
Figure 21: Scalp topographical maps of the local efficiency under alertness and vigilance decrement states in the (a) delta, (b) theta, (c) alpha, and (b) beta frequency bands. The mapped values represent the grand average across subjects. The asterisks (*) indicate a statistically significant local difference between the two cognitive states ($p < 0.01$).

5.4.   Analysis of Inta-Regional Connectivity Patterns

Based on the results discussed in the previous sections, we further hypothesized that TOT alterations in EEG functional connectivity are region and band-specific. In particular, we investigated whether vigilance decrement can be indicated by reduced functional connectivity in distinct brain regions and frequency bands. Regional connectivity was investigated for 10 cortical regions of interest (ROI). To reacap, each cortical ROI was represented by a sub-network consisting of its corresponding EEG electrodes and the PLV edges between them (see Figure 11). Regional sub-networks under alertness (0-5 min time window) and vigilance decrement (25-30 min time window) cognitive states were characterized by their ND_g, NS_g, CC_g, and E_g.

Following our hypothesis, a series of statistical tests were performed on the estimated GTA metrics for the regional sub-networks. For each GTA metric and frequency band, we performed a factorial repeated-measures ANOVA, with two within-subject factors: 1) *cognitive state* (alertness and vigilance decrement) and 2) *brain region* (left and right frontal, temporal, central, parietal, and occipital regions). Greenhouse Geisser correction was employed if the sphericity assumption was not met. As a follow up to the 2-way ANOVA test,a post-hoc pair-wise comparisons were performed to identify signif-

icant regional changes between alertness and vigilance decrement states. Fisher's LSD multiple comparison correction was employed. The significance level for all tests was set to 5%. The statistical analysis was based on the averaged values across all epochs for each subject. IBM SPSS Statistics software, version 25 (IBM Corp., Armonk, N.Y., USA) was used to perform the complete statistical analysis.

Figures 22 to 25 show the heat-maps for the regional ND_g, NS_g, CC_g, and E_g, respectively under alertness and vigilance decrement states. The mapped values represent the grand averages across subjects. The asterisks (*) indicate a statistically significant regional difference between the two cognitive states ($p < 0.01$). Table 1 summarizes the 2-way repeated ANOVA results. For each frequency band and each GTA metric, provided are the p-values for the effect of the cognitive state factor, the brain region factor, and their interaction. Discussed below are the statistical analysis results for each frequency band:

- In the **delta frequency band**, the analysis showed a significant main effect of the cognitive state factor for NS_g ($F_{1,8} = 14.12$, $p = 0.006$), CC_g ($F_{1,8} = 13.07$, $p = 0.007$), and E_g ($F_{1,8} = 16.32$, $p < 0.001$). Similarly, the main effect of brain regions was significant for NS_g ($F_{9,72} = 4.24$, $p = 0.026$), CC_g ($F_{9,72} = 32.08$, $p < 0.001$), and E_g ($F_{9,72} = 6.91$, $p = 0.005$). No significant interaction effects between the cognitive state factor and the brain region factor were observed. Pairwise multiple comparisons showed that all the GTA metrics significantly decreased under vigilance decrement for the left and right frontal and central networks. Moreover, the NS_g, CC_g, and E_g metrics showed decrements in the left and right parietal networks.

- In the **theta frequency band**, the main effect of cognitive state was significant for NS_g ($F_{1,8} = 16.89$, $p = 0.003$), CC_g ($F_{1,8} = 19.11$, $p = 0.002$), and E_g ($F_{1,8} = 14.53$, $p = 0.005$). Significant differences due to the brain region factor were only evident for CC_g ($F_{9,72} = 29.05$, $p < 0.001$) and E_g ($F_{9,72} = 5.28$, $p = 0.032$). Interaction effects were not significant for any of the GTA metrics. Pairwise comparisons showed that the NS_g, CC_g, and E_g metrics significantly

decreased under vigilance decrement for the left and right frontal and central networks. Regional decrements revealed by the ND_g metric were only significant for the left parietal network.

- In the **alpha frequency band**, the cognitive state factor had a significant main effect for NS_g ($F_{1,8} = 6.70$, $p = 0.032$), CC_g ($F_{1,8} = 6.57$, $p = 0.033$), and E_g ($F_{1,8} = 6.69$, $p = 0.032$). Similarly, the effect of the brain region factor was also significant for NS_g ($F_{9,72} = 5.82$, $p = 0.018$), CC_g ($F_{9,72} = 43.25$, $p < 0.001$), and E_g ($F_{9,72} = 11.96$, $p = 0.001$). Non of the interaction effects for any of the GTA metrics were significant. Pairwise multiple comparisons revealed significant decrements for the left frontal network for all GTA metrics. Moreover, the NS_g, CC_g, and E_g metrics significantly decreased under vigilance decrement for the left and right central and parietal networks. Moreover, the NS_g, CC_g, and E_g metrics showed decrements in the left and right parietal networks. Regional decrements revealed by the ND_g metric were also significant for the right central network.

- In the **beta frequency band**, the main effect of the cognitive state factor was significant for NS_g ($F_{1,8} = 5.50$, $p = 0.032$) and E_g ($F_{1,8} = 5.83$, $p = 0.042$). However, the effect of the brain region factor was statistically significant for all GTA metrics: ND_g ($F_{9,72} = 6.15$, $p = 0.001$), NS_g ($F_{9,72} = 9.71$, $p < 0.001$), CC_g ($F_{9,72} = 86.29$, $p < 0.001$), and E_g ($F_{9,72} = 18.42$, $p < 0.001$). Interestingly, significant interactions between the cognitive state and brain region factors were found for ND_g ($F_{9,72} = 3.41$, $p = 0.002$) and CC_g ($F_{9,72} = 3.42$, $p = 0.042$). Pairwise comparisons revealed significant decrements for the left parietal network for all GTA metrics. Moreover, the NS_g, CC_g, and E_g metrics significantly decreased under vigilance decrement for the left and right frontal and central networks. Regional decrements revealed by the NS_g and E_g metrics were also significant for the left temporal networks. The NS_g significantly decreased in the right frontal and central networks under vigilance decrement.

(a)   (b)
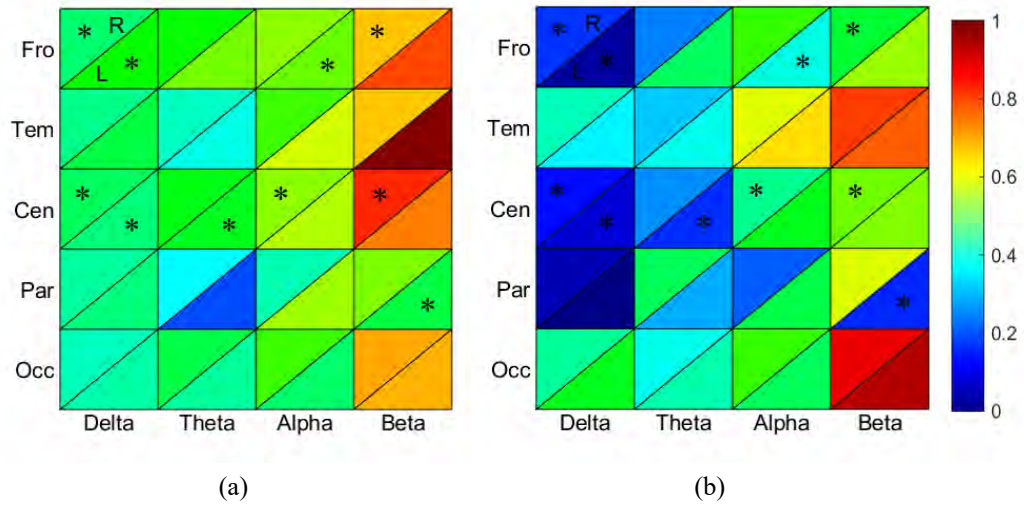
Figure 22: Heats maps for regional global node degree in different frequency bans un-
der alertness and vigilance decrement states. The mapped colors represent the grand
average across subjects. The asterisks (*) indicate a statistically significant difference
between the two cognitive states ($p < 0.05$). The L and R denote a left and right net-
work, respectively.

(a)   (b)
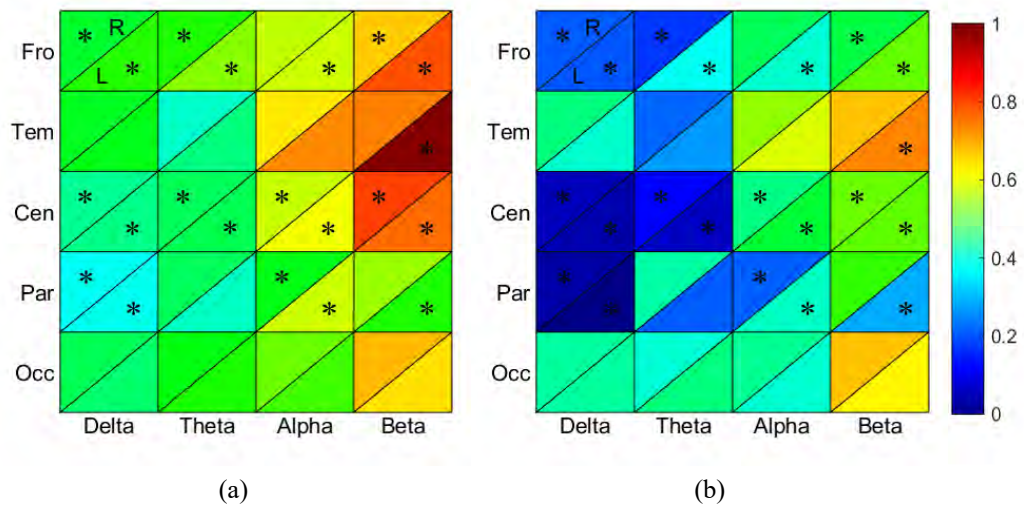
Figure 23: Heats maps for regional global node strength in different frequency bans
under alertness and vigilance decrement states. The mapped colors represent the grand
average across subjects. The asterisks (*) indicate a statistically significant difference
between the two cognitive states ($p < 0.05$). The L and R denote a left and right network,
respectively.

61
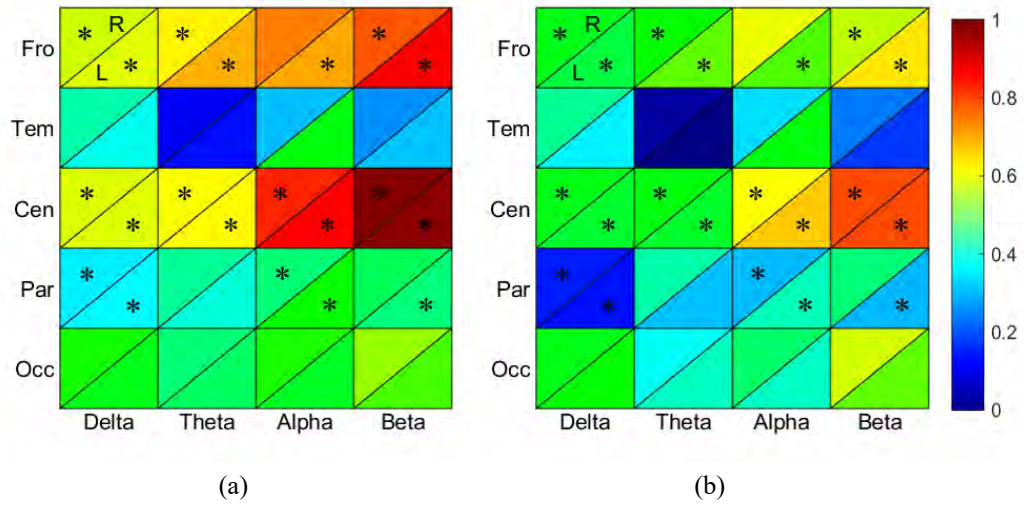
Figure 24: Heats maps for regional global clustering coefficient in different frequency bans under alertness and vigilance decrement states. The mapped colors represent the grand average across subjects. The asterisks (*) indicate a statistically significant difference between the two cognitive states ($p < 0.05$). The L and R denote a left and right network, respectively.
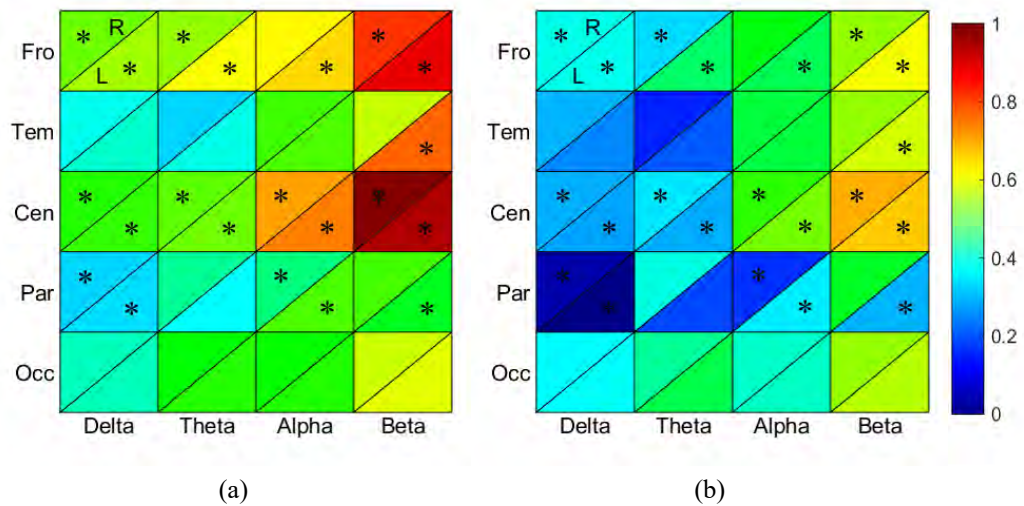
Figure 25: Heats maps for regional global efficiency in different frequency bans under alertness and vigilance decrement states. The mapped colors represent the grand average across subjects. The asterisks (*) indicate a statistically significant difference between the two cognitive states ($p < 0.05$). The L and R denote a left and right network, respectively.

Table 1: P-values for the ANOVA tests on the GTA metrics in different frequency bands.

Factor	Delta (δ)	Theta (θ)	Alpha (α)	Beta (β)
Global Node Degree (ND)				
Cognitive State	0.084	0.163	0.500	0.259
Brain Region	0.527	0.478	0.058	**0.001**
Cognitive State $\times$ Brain Region	0.129	0.423	0.589	**0.002**
Global Node Strength (NS)				
Cognitive State	**0.006**	**0.003**	**0.032**	**0.047**
Brain Region	**0.026**	0.194	**0.018**	**<0.001**
Cognitive State $\times$ Brain Region	0.134	0.171	0.345	0.059
Global Clustering Coefficient (CC)				
Cognitive State	**0.007**	**0.002**	**0.033**	0.053
Brain Region	**<0.001**	**<0.001**	**<0.001**	**<0.001**
Cognitive State $\times$ Brain Region	0.124	0.156	0.187	**0.024**
Global Efficiency (E)				
Cognitive State	**0.004**	**0.005**	**0.032**	**0.042**
Brain Region	**0.005**	**0.032**	**0.001**	**<0.001**
Cognitive State $\times$ Brain Region	0.129	0.093	0.227	0.080

Note: **Bolded** values indicate significant effects.

5.5. Hemispheric Asymmetry of Intra-Regional Networks

Many studies have revealed differences between the functional organization of the left and right cortical hemispheres. Most of these studies suggested functional hemispheric asymmetry as a meaningful biomarker underlying variation of cortical activity under different cognitive states. To assess TOT effects on the asymmetry of regional connectivity patterns, we propose a novel laterality index based on the intra-regional GTA metrics:

$$LI = \frac{R-L}{R+L},$$
(15)

where R and L correspond to the estimated global GTA metrics for the right and left sub-networks, respectively. Equation 15 yields a LI value within the interval $[-1, 1]$, with positive values indicating right regional dominance and vice versa. For each cortical sub-network, band-specific laterality indices were computed based on the ND_g, NS_g,

CC_g, and E_g metrics. As such, the proposed LI can quantify regional differences in connection density, information transfer, functional integration, and functional segregation across the left and right hemispheres. Significant leftward or rightward dominances were only considered for LI distributions with means statistically different form zero ($P < 0.05$). The computed laterality indices were also statistically compared between the two cognitive states using a paired sample t-test.

5.5.1. Connection density. Figure 26 compares the regional LIs of the global node degree under alertness and vigilance decrement states. Plotted are the mean LI values with error bars representing the standard error. The plus symbol (+) indicates a significant asymmetry or LI, and the asterisks symbol (*) indicates a statistically different LI between the two mental states. As shown in Figure 26a, no significant regional asymmetries were observed in the delta frequency band. In the theta frequency band, significant leftward and rightward asymmetry was observed under vigilance decrement for the frontal and central networks, respectively. In the alpha frequency band, the frontal network showed a statistically significant rightward density under both alertness and vigilance decrement states. The central network showed a minor left asymmetry under alertness that increased to be significant under vigilance decrement. In the beta frequency band, the frontal and temporal networks showed significant leftward asymmetry under vigilance decrement and alertness states, respectively. Connectivity density within the right parietal network was statistically significant under vigilance decrement.

5.5.2. Information transfer. Figure 27 compares the regional LIs of the global node strength under alertness and vigilance decrement states. Plotted are the mean LI values with error bars representing the standard error. The plus symbol (+) indicates a significant asymmetry or LI, and the asterisks symbol (*) indicates a statistically different LI between the two mental states. As shown in Figure 27a, no significant regional asymmetries were observed in the delta frequency band. In the theta frequency band, the frontal network showed a statistically significant leftward information transfer under both alertness and vigilance decrement. The parietal region maintained a right hemispheric dominance under the two mental states. The central network showed a minor

right asymmetry under alertness that increased to be significant under vigilance decrement. Asymmetries observed for the temporal and occipital regions under both mental states were statistically insignificant. In the alpha band, information transfer within the temporal network showed a significant rightward asymmetry under both alertness and vigilance decrement. On the other hand, the parietal region maintained left dominance between the two mental states. The central network showed an insignificant right asymmetry under alertness that increased to be significant under vigilance decrement. Differences between the left and right hemispheric activity in the frontal and occipital regions were not significant under both mental states. In the beta band, information transfer within the left frontal and temporal networks was statistically higher under alertness. For vigilance decrement, left dominance was observed for the frontal activation, and right dominance was observed for the parietal activation. The laterality indices for the central and occipital networks were statistically insignificant under the two mental states.

5.5.3. Functional segregation. Figure 28 compares the regional LI of the global clustering coefficient under alertness and vigilance decrement states. Plotted are the mean LI values with error bars representing the standard error. The plus symbol (+) indicates a significant asymmetry or LI, and the asterisks symbol (*) indicates a statistically different LI between the two mental states. In the delta frequency band, rightward asymmetric functional segregation was only evident in the temporal network under vigilance decrement state. Asymmetries observed for other regional networks under both mental states were statistically insignificant. In the theta frequency band, the frontal network showed a statistically significant leftward functional segregation under both alertness and vigilance decrement. The parietal network showed a minor right asymmetry under alertness that increased to be significant under vigilance decrement. Asymmetries observed for the temporal, central, and occipital regions statistically insignificant for both mental states. In the alpha frequency band, functional segregation within the frontal network showed a slight rightward asymmetry under alertness that increased to be significant under vigilance decrement. In addition, the central network showed a slight leftward asymmetry under alertness that increased to be significant un-

der vigilance decrement. Both the temporal and parietal networks maintained left dominance under both mental states. The occipital network showed a significant left dominance under alertness state only. In the beta frequency band, functional segregating of the frontal networks showed leftward dominance under both mental states. The slight rightward asymmetry of the parietal network under alertness state increased with TOT to become statistically significant under vigilance decrement state. The temporal, central and occipital networks did not show significant differences between left and right functional segregation.

5.5.4. Functional integration. Figure 29 compares the regional LI of the global efficiency under alertness and vigilance decrement states in the delta, theta, alpha, and beta frequency bands. Plotted are the mean LI values with error bars representing the standard error. The plus symbol (+) indicates a significant asymmetry or LI, and the asterisks symbol (*) indicates a statistically different LI between the two mental states. As shown in Figure 29a, no significant asymmetries of regional functional integration were observed in the delta frequency band. In the theta frequency band, the frontal network showed a statistically significant leftward functional integration under alertness and vigilance decrement. The parietal region maintained a right hemispheric dominance under the two mental states. The central network showed a minor right asymmetry under alertness that significantly increased under vigilance decrement. Asymmetries observed for the temporal and occipital regions under both mental states were statistically insignificant. In the alpha band, functional integration within the temporal network showed a significant rightward asymmetry under both alertness and vigilance decrement. The central network showed an insignificant leftward asymmetry under alertness that increased to be significant under vigilance decrement. On the other hand, leftward asymmetry of the parietal network was only significant under alertness states. Differences between the left and right hemispheric activity in the frontal and occipital regions were statistically insignificant under both mental states. In the beta band, functional integration within the left temporal networks was statistically higher under alertness state only. For vigilance decrement, right dominance was observed for the parietal network only. The lateral-

ity indices for the frontal, central, and occipital networks were statistically insignificant under the two mental states.
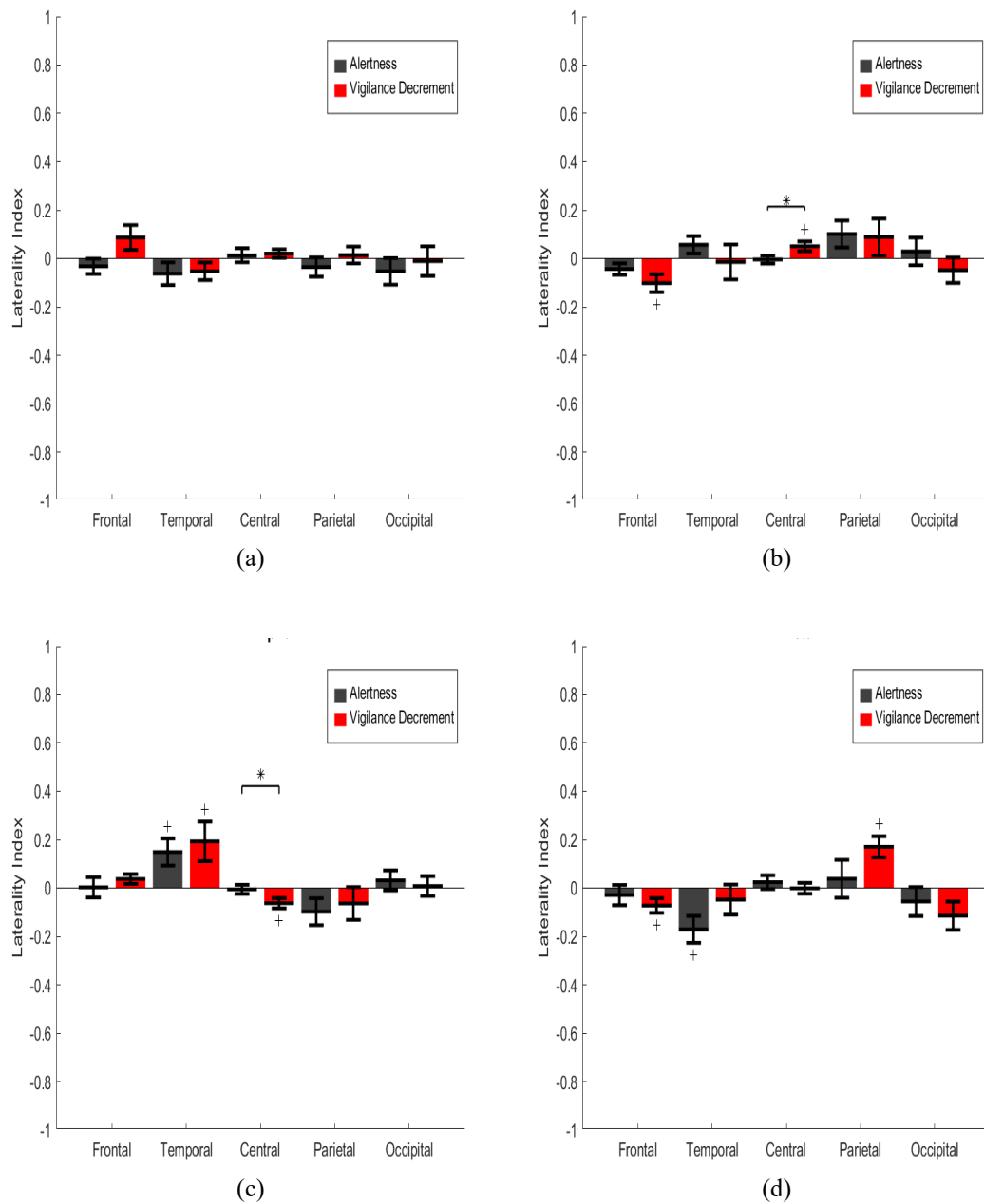
Figure 26: Comparison between the node strength laterality indices under alertness and vigilance decrement states in the (a) delta, (b) theta, (c) alpha, and (d) beta frequency bands. Plotted are the mean values across subjects with error bars indicating the standard error. The plus symbol (+) indicates a significant asymmetry or LI, and the asterisks symbol (*) indicates a statistically different LI between the two mental states.
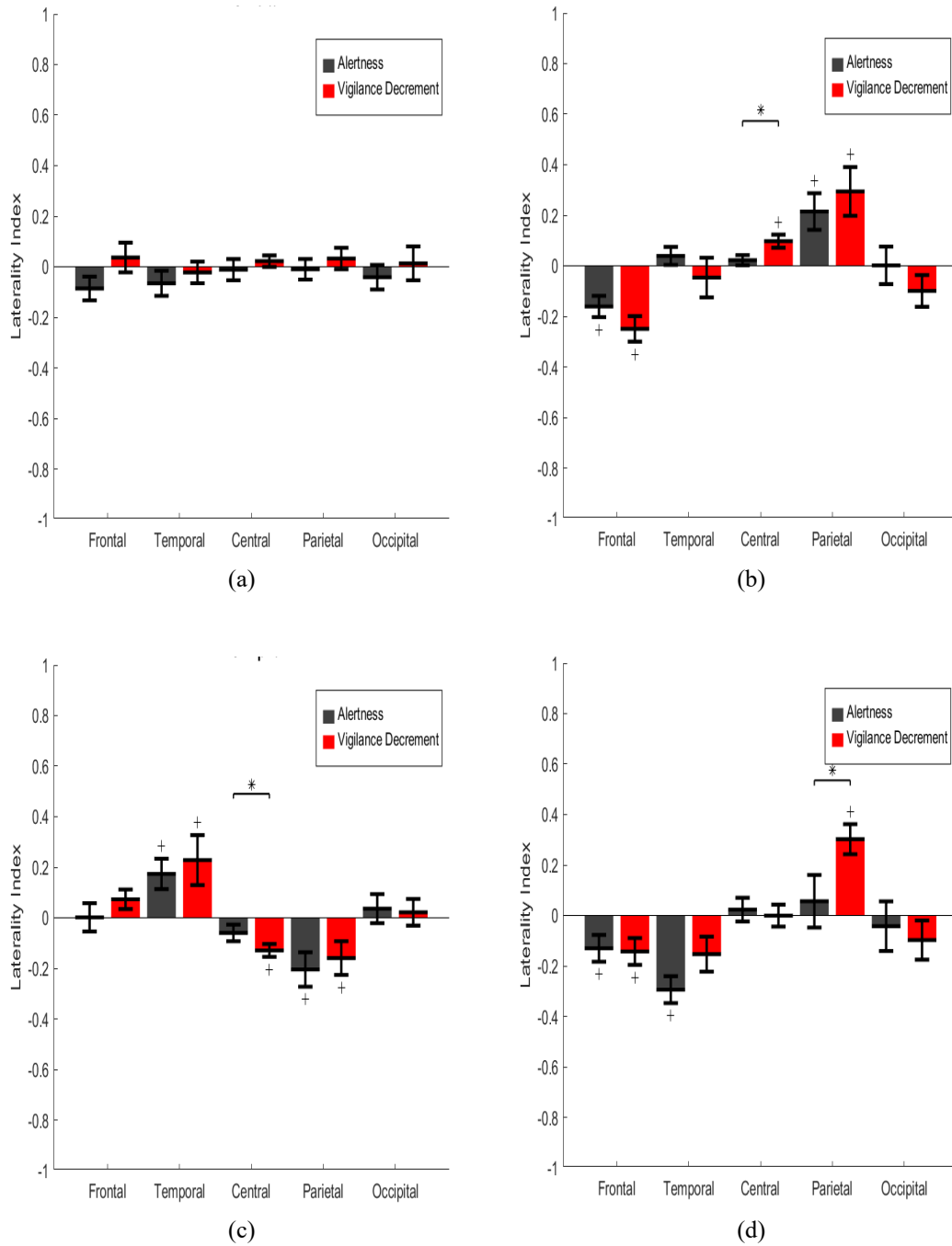
Figure 27: Comparison between the node strength laterality indices under alertness and vigilance decrement states in the (a) delta, (b) theta, (c) alpha, and (d) beta frequency bands. Plotted are the mean values across subjects with error bars indicating the standard error. The plus symbol (+) indicates a significant asymmetry or LI, and the asterisks symbol (*) indicates a statistically different LI between the two mental states.
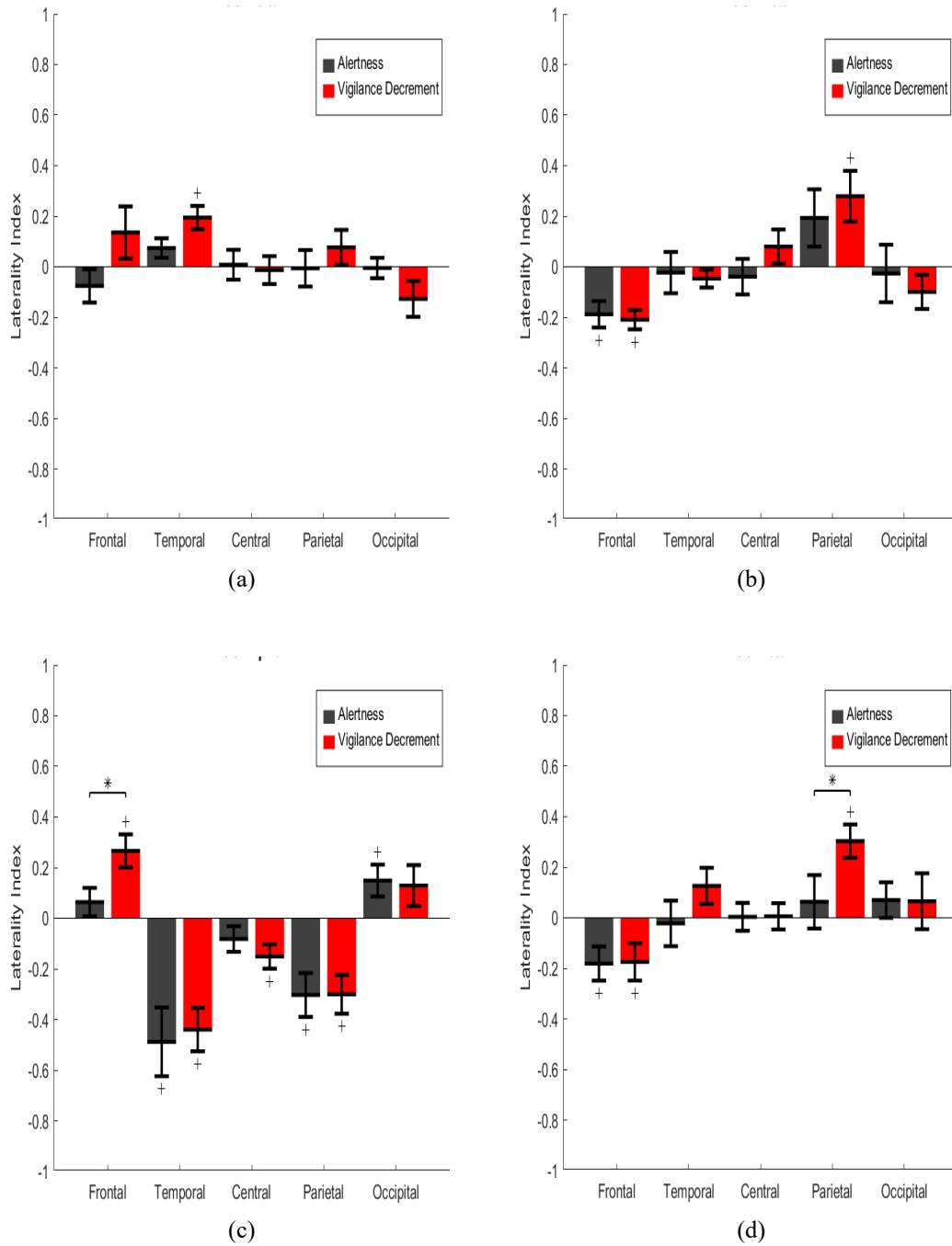
Figure 28: Comparison between the clustering coefficient laterality indices under alertness and vigilance decrement states in the (a) delta, (b) theta, (c) alpha, and (d) beta frequency bands. Plotted are the mean values across subjects with error bars indicating the standard error. The plus symbol (+) indicates a significant asymmetry or LI, and the asterisks symbol (*) indicates a statistically different LI between the two mental states.
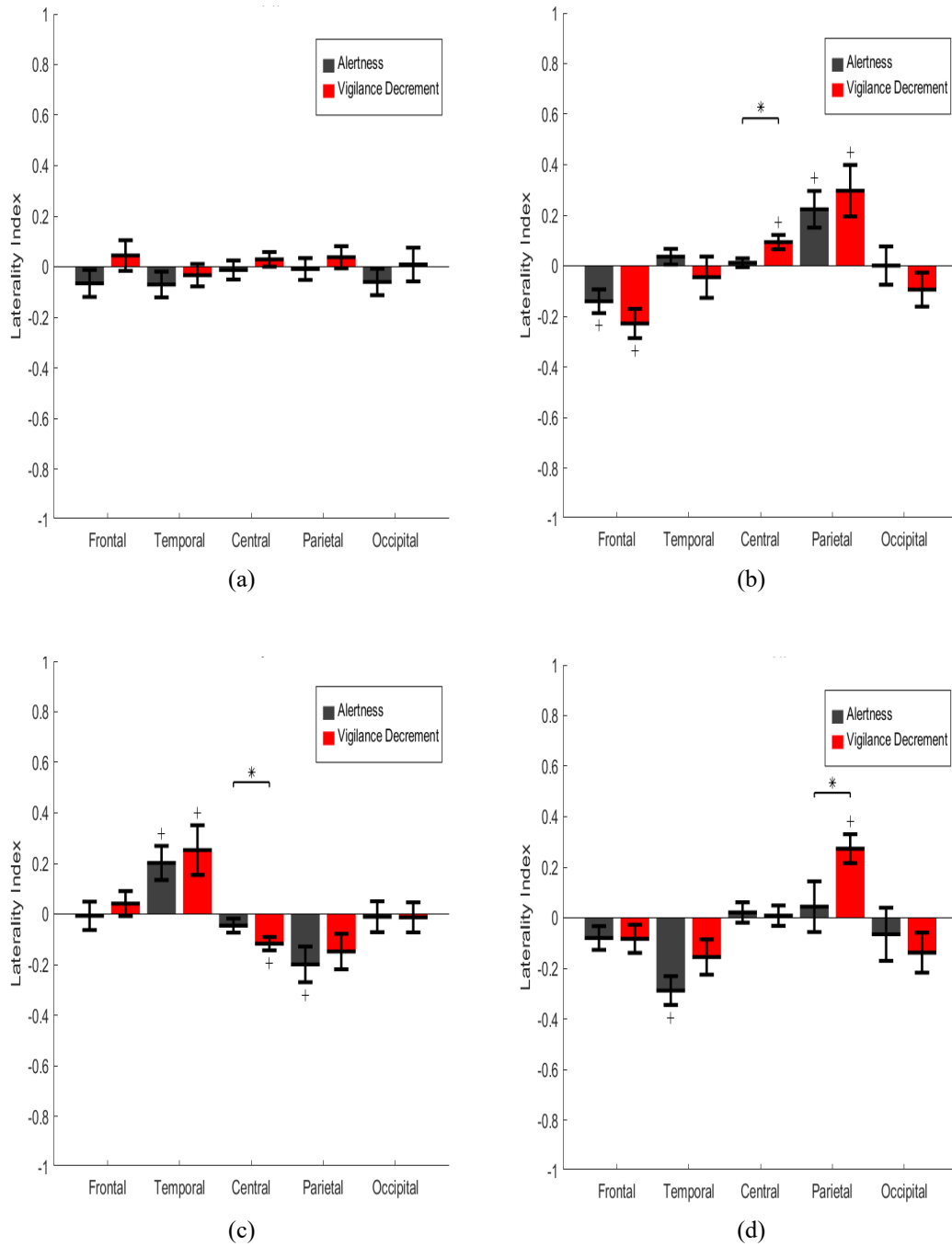
Figure 29: Comparison between the efficiency laterality indices under alertness and vigilance decrement states in the (a) delta, (b) theta, (c) alpha, and (d) beta frequency bands. Plotted are the mean values across subjects with error bars indicating the standard error. The plus symbol (+) indicates a significant asymmetry or LI, and the asterisks symbol (*) indicates a statistically different LI between the two mental states.

5.6.   Classification Analysis for Detection of Vigilance Decrement

Machine learning classification analysis was employed to evaluate the effectiveness of detecting vigilance decrement based on regional connectivity patterns. Our primary focus was to discover which brain regions provide the highest detection accuracy. Five different feature sets were investigated for each regional sub-network based on the estimated GTA metrics. Each of the node degree(*ND*), node strength (*NS*), clustering coefficient (*CC*), and efficiency (*EFF*) features were obtained by concatenating the corresponding band-specific GTA metrics, resulting in a 1×4 feature set for each epoch. Moreover, the *All* feature was obtained by concatenating the previous features resulting in a 1×16 set. To further emphasize potential asymmetry patterns, the same feature sets were extracted for two additional sub-networks corresponding to all left and all right electrodes. A support vector machine (SVM) model with a Gaussian kernel was employed to classify two mental states: alertness and vigilance decrement. The model's performance, especially its robustness against subject differences, was evaluated based on a leave-one-subject-out (LOSO) cross-validation scheme. In analogy to the typical K-fold cross-validation, the testing set in each iteration consisted of the 166 epochs of a single participant (83 epochs for each class). As such, observations from the same participant were never mixed between training and testing sets, thus eliminating potential bias toward high fake accuracies. In each validation iteration, tuning of the kernels space and regularization strength parameters was done via Bayesian optimization. Optimization was based on minimizing the cross-validation loss.The remaining hyperparameters parameters were set to the default values in Matlab. Finally, the quantification of classification performance was based on detection accuracy, sensitivity, and specificity, with vigilance decrement considered as the positive class. The complete classification analysis was performed via Matlab software (R2019a, Natick, MA, USA). The obtained results using different feature sets are discussed below in details.

Tables 2 to 4 show the overall classification results for different cortical sub-networks and using different GTA feature sets. The values presented in the tables represent the average $\pm$ the standard deviations of the classification accuracy, sensitivity, and specificity across folds. The results show that the right cortical sub-networks generally provided better classification performance in comparison to the left sub-networks,

71

regardless of the used feature set. In specific, the right central sub-network gave the best classification result (accuracy = 84.27%, sensitivity= 87.42%, and specificity = 81.12%) using the CC feature set. On the other hand, the left frontal sub-network showed the worst performance for all feature sets. Specifically, using the ND feature set, the left frontal network gave the smallest classification accuracy of 39.36%. These observations indicate that the right hemisphere is generally more sensitive to vigilance decrement. Also, the accuracy for the all right sub-network was higher than the all left sub-network, further confirming the superior sensitivity of the whole right hemisphere to vigilance decrement. It is worth mentioning that concatenating the four GTA feature sets for each cortical region did not improve the classification performance, and the results were comparable to those obtained from single feature sets. This might be due to the high correlation betwwen the feature sets.

Table 2: Classification accuracy (%) for different cortical sub-networks using different GTA feature sets

	ND (mean ± std)	NS (mean ± std)	CC (mean ± std)	EFF (mean ± std)	All GTA (mean ± std)
Left Frontal	39.36 ± 6.96	37.39 ± 5.19	47.72 ± 5.91	44.38 ± 13.37	43.17 ± 17.77
Right Frontal	72.36 ± 10.15	81.19 ± 8.88	78.71± 6.72	74.30 ± 9.01	79.59 ± 14.41
Left Temporal	49.26 ± 6.29	47.52 ± 9.88	48.33 ± 6.61	51.47 ± 7.34	46.72 ± 8.64
Right Temporal	67.94 ± 8.95	80.05 ± 10.77	62.91 ± 9.63	72.56 ± 12.47	77.31 ± 11.53
Left Central	56.02 ± 13.03	54.15 ± 6.81	46.32 ± 10.44	53.88 ± 6.46	55.89 ± 5.71
Right Central	70.88 ± 10.65	79.45 ± 10.91	84.27 ± 9.15	76.97 ± 12.20	78.98 ± 11.28
Left Parietal	52.81 ± 8.37	55.29 ± 9.44	55.62 ± 10.91	57.56 ± 10.59	54.82 ± 7.87
Right Parietal	67.74 ± 11.09	71.35 ± 9.35	62.72 ± 13.03	66.27 ± 12.49	61.58 ± 10.66
Left Occipital	47.32 ± 5.74	47.52 ± 13.59	49.73 ± 12.31	49.87 ± 10.26	52.14 ± 9.69
Right Occipital	72.16 ± 2.77	68.54 ± 11.92	59.84 ± 13.85	71.49 ± 13.36	68.61 ± 9.67
All Left	66.13 ± 13.39	63.99 ± 13.59	52.61 ± 8.60	61.18 ± 15.62	67.00 ± 16.86
All Right	70.75 ± 13.30	72.96 ± 18.79	76.17 ± 8.56	72.16 ± 24.11	73.23 ± 18.42

Table 3: Classification sensitivity (%) for different cortical sub-networks using different GTA feature sets

	ND (mean ± std)	NS (mean ± std)	CC (mean ± std)	EFF (mean ± std)	All GTA (mean ± std)
Left Frontal	34.54 ±13.75	44.85 ±12.52	49.4 ±18.78	42.17 ±12.11	42.17 ±17.1
Right Frontal	82.33 ±15.28	89.29 ±10.6	86.35 ±11.01	81.26 ±10.3	91.57 ±11.19
Left Temporal	44.18 ±11.96	52.07 ±22.39	58.63 ±21.83	56.09 ±16.11	51.14 ±14.32
Right Temporal	77.11 ±10.89	83.8 ±13.91	90.5 ±6.53	77.91 ±10.83	79.92 ±16.4
Left Central	59.17 ±23.95	54.75 ±11.29	52.61 ±22.62	49.4 ±19.76	61.58 ±20.07
Right Central	78.31 ±11.67	82.2 ±19.28	87.42 ±9	79.79 ±21.81	80.32 ±19.94
Left Parietal	56.89 ±14.02	59.17 ±21.04	74.83 ±19.3	62.65 ±18.31	59.17 ±16.27
Right Parietal	77.51 ±12.91	86.21 ±11.26	82.73 ±14.98	81.93 ±21.98	69.21 ±17.76
Left Occipital	42.84 ±20.9	48.86 ±16.44	51.27 ±22.75	60.64 ±16.34	56.89 ±17.22
Right Occipital	82.73 ±17.97	79.79 ±23.55	64.26 ±24.83	80.46 ±17.3	78.85 ±17.7
All Left	70.15 ±12.25	69.08 ±14.36	52.61 ±16.4	67.07 ±17.36	73.36 ±18.22
All Right	78.85 ±19.97	76.31 ±22.46	78.58 ±13.83	76.44 ±24.68	78.98 ±20.55

Table 4: Classification specificity (%) for different cortical sub-networks using different GTA feature sets

	ND (mean ± std)	NS (mean ± std)	CC (mean ± std)	EFF (mean ± std)	All GTA (mean ± std)
Left Frontal	44.18 ±15.88	49.93 ±13.03	46.05 ±17.54	46.59 ±16.02	44.18 ±30.11
Right Frontal	62.38 ±20.91	73.09 ±15.36	71.08 ±17.03	67.34 ±12.48	67.6 ±29.44
Left Temporal	54.35 ±8.86	42.97 ±16.81	38.02 ±18.76	46.85 ±16.48	42.3 ±15.93
Right Temporal	58.77 ± 14.6	76.31 ±15.89	35.34 ±17.41	67.2 ±21.25	74.7 ±15.52
Left Central	52.88 ± 25.57	53.55 ±18.59	40.03 ±15.68	58.37 ±16.31	50.2 ±22.26
Right Central	63.45 ±21.44	76.71 ±12.75	81.12 ±13.86	74.16 ±12.3	77.64 ±11.88
Left Parietal	48.73 ±22.01	51.41 ±16.11	36.41 ±18.12	52.48 ±18.61	50.47 ± 16.96
Right Parietal	57.97 ±19.43	56.49 ±16.23	42.7 ±20.22	50.6 ±20.46	53.95 ±19.52
Left Occipital	51.81 ±16.23	46.18 ±19.45	48.19 ±26.71	39.09 ±14.79	47.39 ±22.31
Right Occipital	61.58 ±14.09	57.3 ±24.41	55.42 ±27.58	62.52 ±23.87	58.37 ±24.31
All Left	62.12 ±19.83	58.9 ±25.48	52.61 ±24.74	55.29 ±28.26	60.64 ±30.3
All Right	62.65 ±18.13	69.61 ±27.27	73.76 ±15.53	67.87 ±31.27	67.47 ±27.25

Chapter 6. Vigilance Enhancement Using Auditory Stimulation

This chapter investigates the effect of auditory stimulation on the participants' behavioral performance and cortical functional connectivity while performing the I-SCWT. We hypothesized that stimulation through a 250Hz pure sinusoidal tone (PSTS) or 16Hz binaural beats (BBS) could enhance cortical connectivity and vigilance performance. Under different auditory conditions, band-specific full-scale PLV networks were constructed for two vigilance levels: level 1 corresponded to the task time between 0-5 min, and level 2 corresponded to the time between 25-30 min. For each auditory stimulus condition (PSTS or BBS), GTA was employed at different sparsity thresholds to characterize the effect of TOT on the global topology of the constructed networks. The global topologies of the networks was quantified based on their global node strengths, clustering coefficients, and efficiencies. Moreover, statistical analysis was employed on the estimated GTA metrics to determine whether auditory stimulation induced significant improvements in cortical functional connectivity. Indications of vigilance enhancement were further explored by the analysis of behavioral data with increased TOT. As mentioned earlier in the methodology chapter, each audio condition included nine randomly assigned participants, with no significant age or gender differences.

6.1.   Full-Scale Global Network Analysis at Different Sparsity Thresholds

   6.1.1. Pure sinusoidal tone condition.   Figures 30 to 32 compare the full-scale networks reconstructed for the two vigilance levels under the PSTS condition based on their NS_g, CC_g, and E_g, respectively. For each time window, the mean of the GTA metrics over all participants and the standard error was plotted as a function of the network sparsity level. A full sparsity range of 0% to 100% with a step of 5% was considered. At each sparsity level, a paired sample t-test was employed to test the statistical significance of differences between the two cognitive states. The results show that the estimated global metrics generally increase when increasing the network sparsity in all frequency bands. Such a pattern is expected since higher sparsity levels account for a higher number of edges, resulting in more dense networks. In addition, this increasing

pattern was also observed for the full-scale results under the no audio condition (see Figures 16 to 18 in chapter 5). Generally, the paired sample t-tests showed no significant differences between the two vigilance levels over the full sparsity range in all frequency bands. Also, the range of the GTA metrics under this condition (i.e. [0,0.6]) is bigger than that under the no audio condition (i.e. [0, 0.3]). These observations indicate an enhanced full-scale cortical connectivity as a result of PSTS. To be consistent with the approach followed in chapter 5, subsequent PSTS results were obtained from the integral over a sparsity range of 50% to 95%. This range is enough to eliminate insignificant connections while preserving the structure of the underlying small world network [189].

6.1.2. Binaural beats condition.   Figures 33 to 35 compare the full-scale networks reconstructed for the two vigilance levels under the BBS condition based on their NS_g, CC_g, and E_g, respectively. For each time window, the mean of the GTA metrics over all participants and the standard error was plotted as a function of the network sparsity level (0% to 100% with a step of 5%). At each sparsity level, a paired sample t-test was employed to test the statistical significance of differences between the two cognitive states. The results show that the estimated global metrics generally increase when increasing the network sparsity in all frequency bands. This pattern is in accordance with the results obtained for the no audio and PSTS conditions. In all frequency bands and for all GTA metrics, paired sample t-tests showed no significant differences between the two vigilance levels over the full sparsity ranges. Also, the range of the GTA metrics under this condition (i.e. [0,0.6]) is similar to that under PSTS but is bigger than that under the no audio condition (i.e. [0, 0.3]). This indicates an enhanced full-scale cortical connectivity as a result of BBS in comparison to the no audio condition. However, the results show similar global characteristics under both PSTS and BBS conditions. This suggests that BBT stimulation did not induce further cortical entrainment effects nor enhanced the global full-scale connectivity. To be consistent with the approach followed in chapter 5, subsequent BBS results were obtained from the integral over the sparsity range of 50% to 95%. This range is enough to eliminate insignificant connections while preserving the structure of the underlying small world network [189].

Figure 30: Comparison between the global node strengths of the full-scales networks under the two vigilance levels of the pure tone condition and in the (a) delta, (b) theta, (c) alpha, and (d) beta bands. Plotted are the mean values across subjects with error bars indicating the standard error.
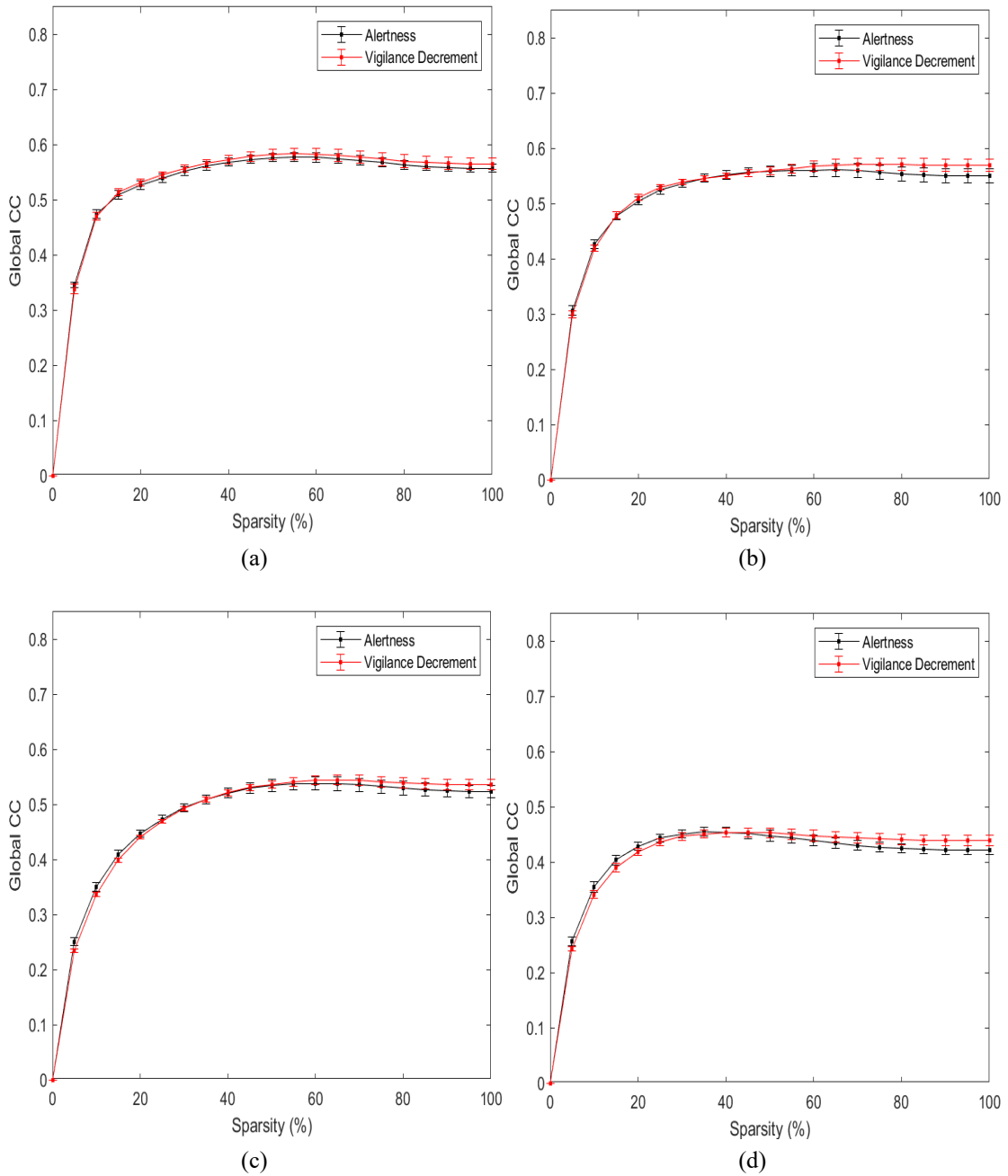
Figure 31: Comparison between the global clustering coefficients of the full-scales networks under the two vigilance levels of the pure tone condition in the (a) delta, (b) theta, (c) alpha, and (d) beta bands. Plotted are the mean values across subjects with error bars indicating the standard error.
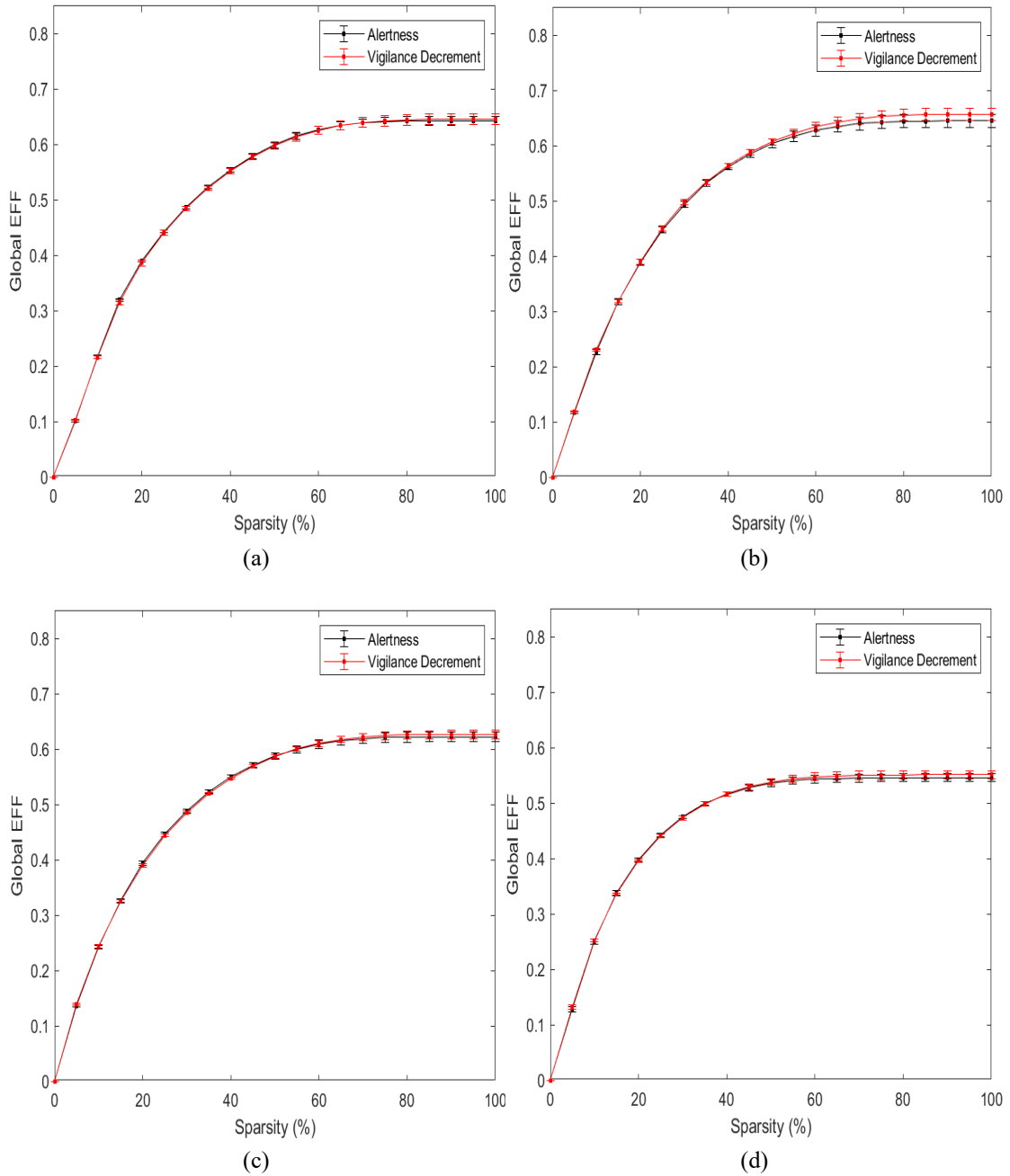
Figure 32: Comparison between the global efficiencies of the full-scales networks under the two vigilance levels of the pure tone condition in the (a) delta, (b) theta, (c) alpha, and (d) beta bands. Plotted are the mean values across subjects with error bars indicating the standard error.
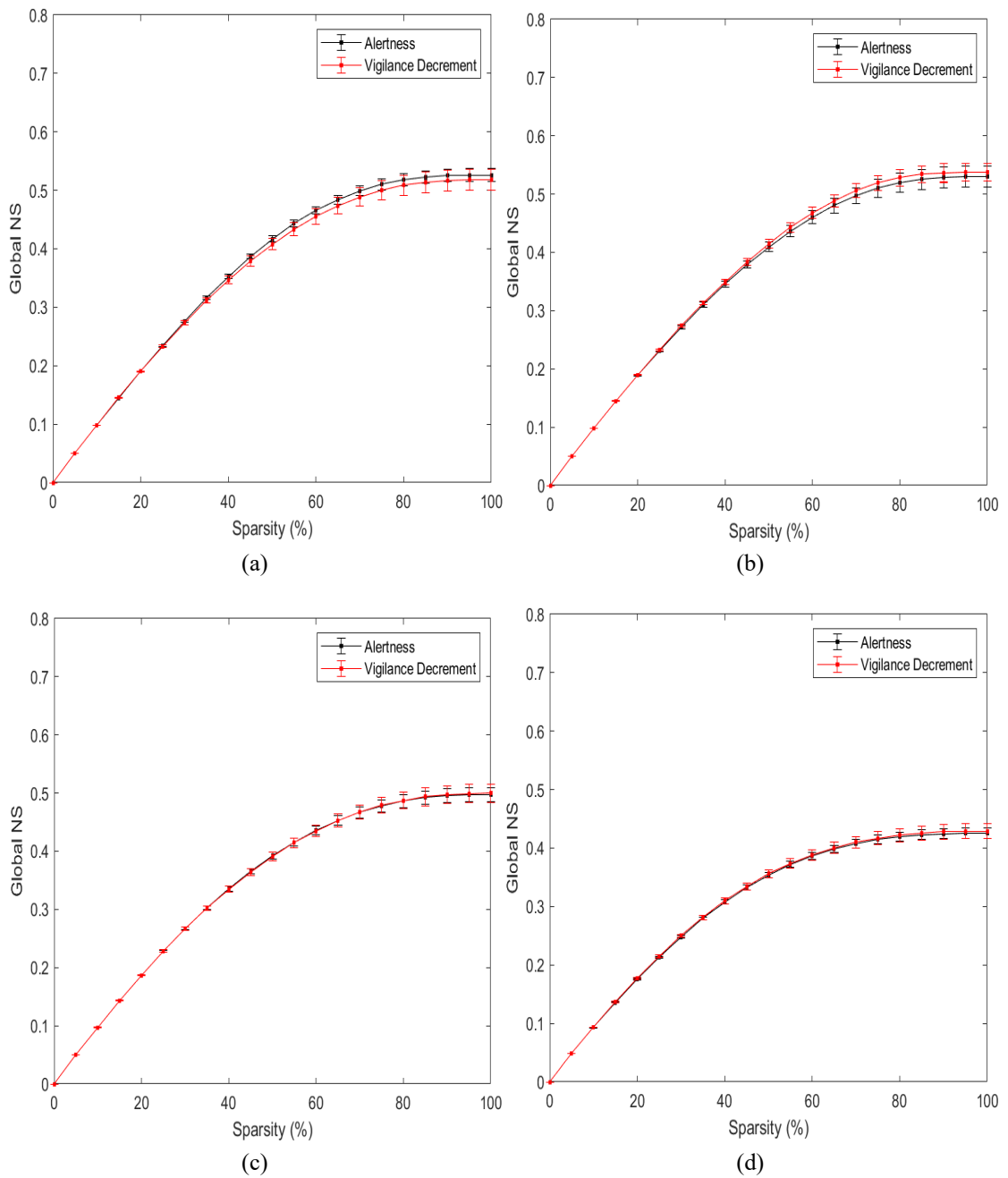
Figure 33: Comparison between the global node strengths of the full-scales networks under the two vigilance levels of the binaural beats condition in the (a) delta, (b) theta, (c) alpha, and (d) beta bands. Plotted are the mean values across subjects with error bars indicating the standard error.
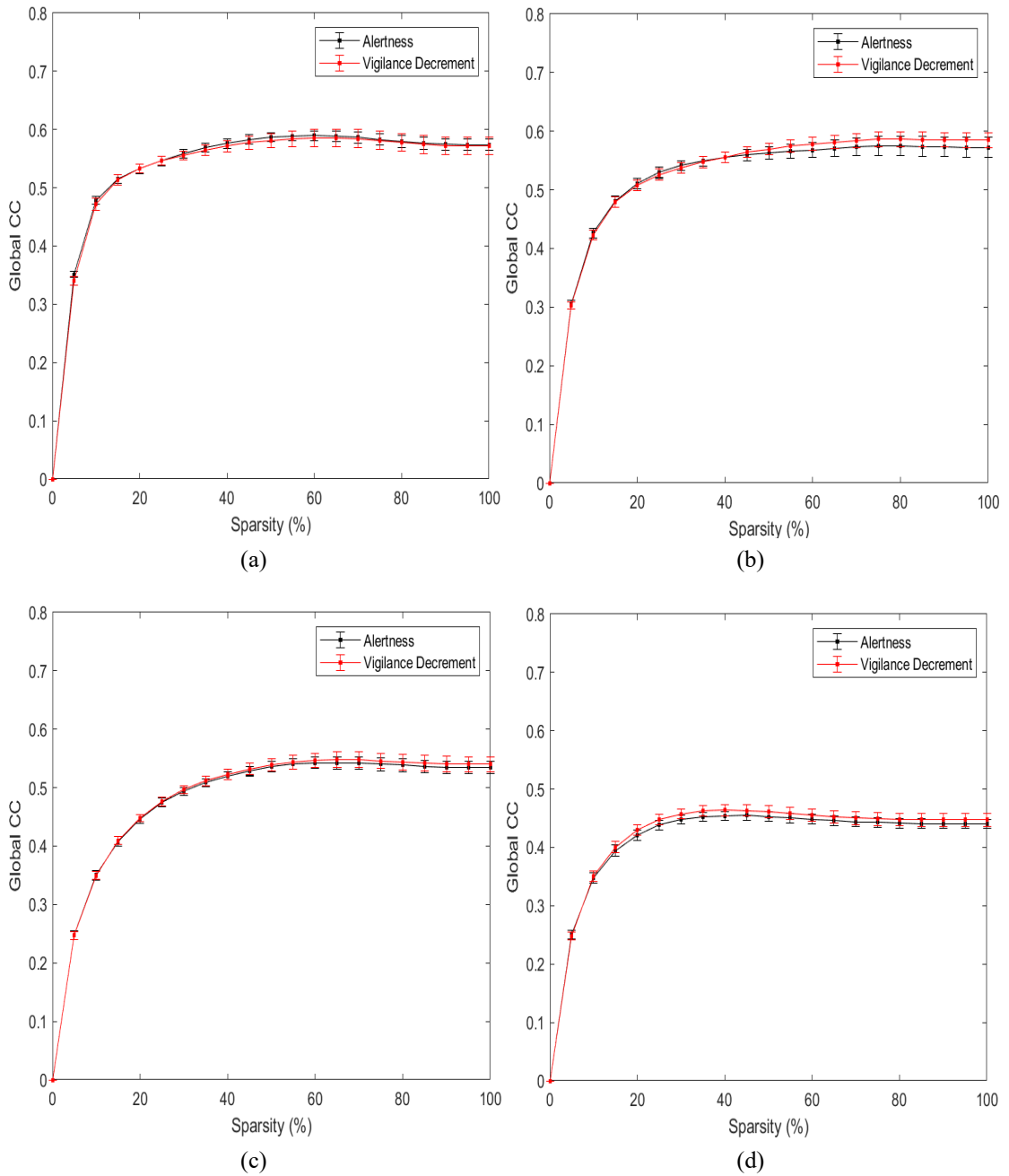
Figure 34: Comparison between the global clustering coefficients of the full-scales networks under the two vigilance levels of the binaural beats condition in the (a) delta, (b) theta, (c) alpha, and (d) beta bands. Plotted are the mean values across subjects with error bars indicating the standard error.
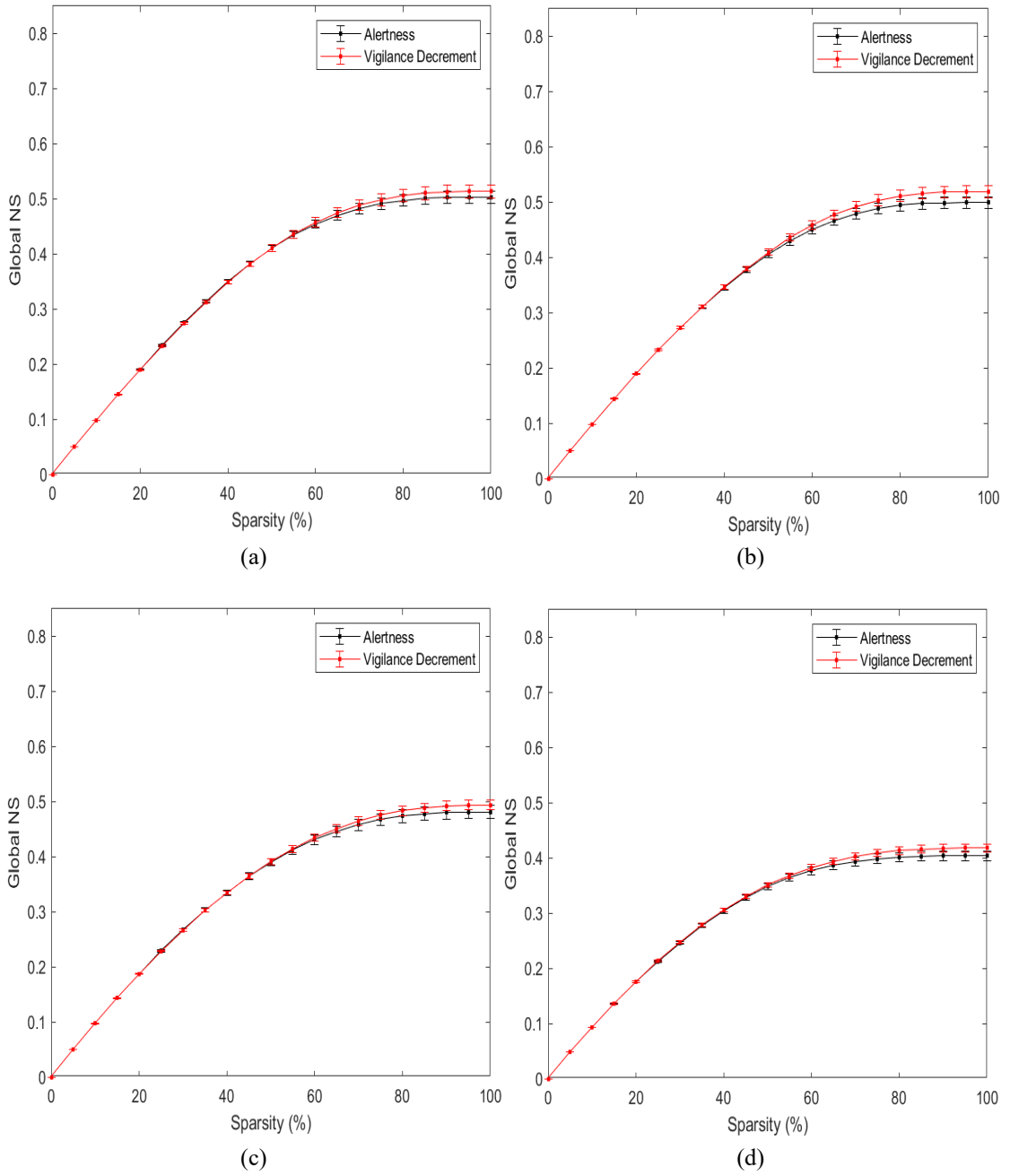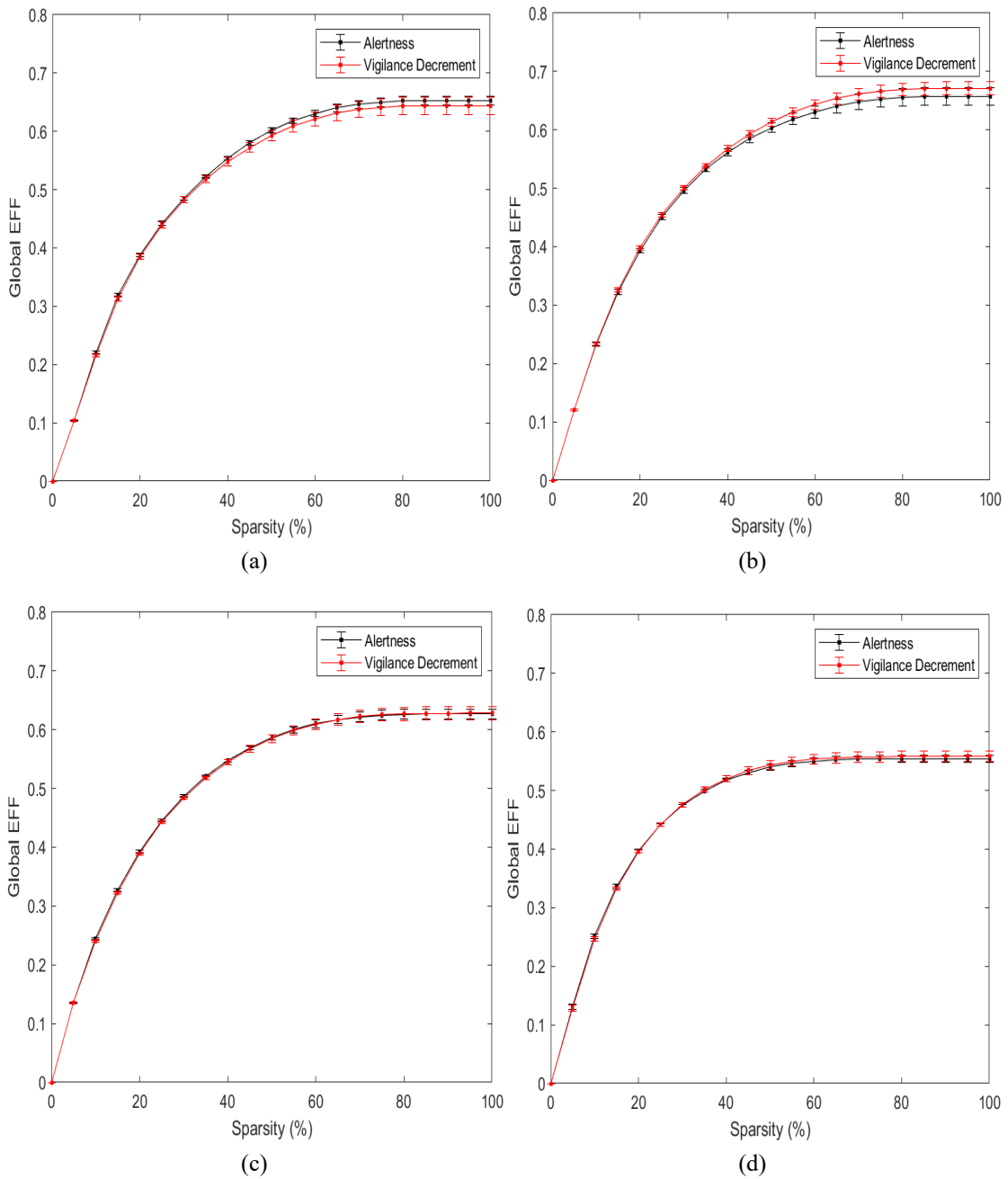
Figure 35: Comparison between the global efficiencies of the full-scales networks under the two vigilance levels of the binaural beats condition in the (a) delta, (b) theta, (c) alpha, and (d) beta bands. Plotted are the mean values across subjects with error bars indicating the standard error.

6.2. Comparison Between Different Auditory Conditions

6.2.1. Behavioral analysis. The behavioral performance under the three audio conditions was evaluated based on changes in the participants' response reaction time and detection accuracy. The behavioral data collected during the 30 min I-SCWT task was divided into six non-overlapping blocks, each of 5 min duration. Average reaction times and detection accuracies were compared over time and between conditions.

6.2.1.1. Reaction time. Recall that maximum response time for experimental I-SCWT trials was set independently for each participant. Accordingly, each reaction time was normalized by its corresponding maximum response time before analysis. As such, the effect of individual differences on the results was minimized. Also, the analysis of reaction time data excluded reaction times corresponding to incorrect and missed responses (less than 5%). Figure 36 compares time-related changes in the reaction times between different auditory conditions. For each time window, plotted is the mean with the error bars representing the standard error. The p-values on the plot were obtained by statistically comparing the first and last blocks of each auditory condition using a paired sample t-test (font colors are mapped to conditions). The results show that the average reaction time decreased with increasing TOT in all conditions. Statistical analysis between the first and last time blocks showed significant decrements over time in all conditions ($p < 0.05$). Also, differences between reaction times scored under the three conditions were notable, especially for the 0-25 min duration. The no audio condition had the highest average reaction times in all-time blocks in comparison to the other auditory conditions. PSTS significantly reduced the reaction times over the whole task duration, and BBT further reduced it. On average, enhancement via PSTS resulted in a 2.45% and a 5.08% improvement in the participants' reaction times during the first and last time blocks, respectively. Similarly, enhancement via BBS resulted in a 7% and a 5.55% improvement in the first and last time blocks respectively.

6.2.1.2. Detection accuracy. Figure 37 compares changes in detection accuracy between different auditory conditions over time. For each time window, plotted is

82

the mean across subjects with the error bars representing the standard error. The results show that the average detection accuracy generally increased with increasing TOT in all conditions. Pairwise t-test comparison between the first and last time blocks showed no change in performance under the no audio condition (p= 0.119). In contrast, statistical analysis between the first and last time blocks showed significant increments with time under the PSTS and BBS conditions ($p < 0.05$). Also, differences between the accuracies scored under the three conditions were notable during the total 30 min task duration. The no audio condition had the lowest average accuracy in all-time blocks in comparison to the other auditory conditions. On average, enhancement via PSTS showed a 12.68% and a 25.84% improvement in the participants' accuracy during the first and last time blocks, respectively. Similarly, enhancement via BBS showed a 20.69% and a 26.01% improvement in the first and last time blocks respectively.
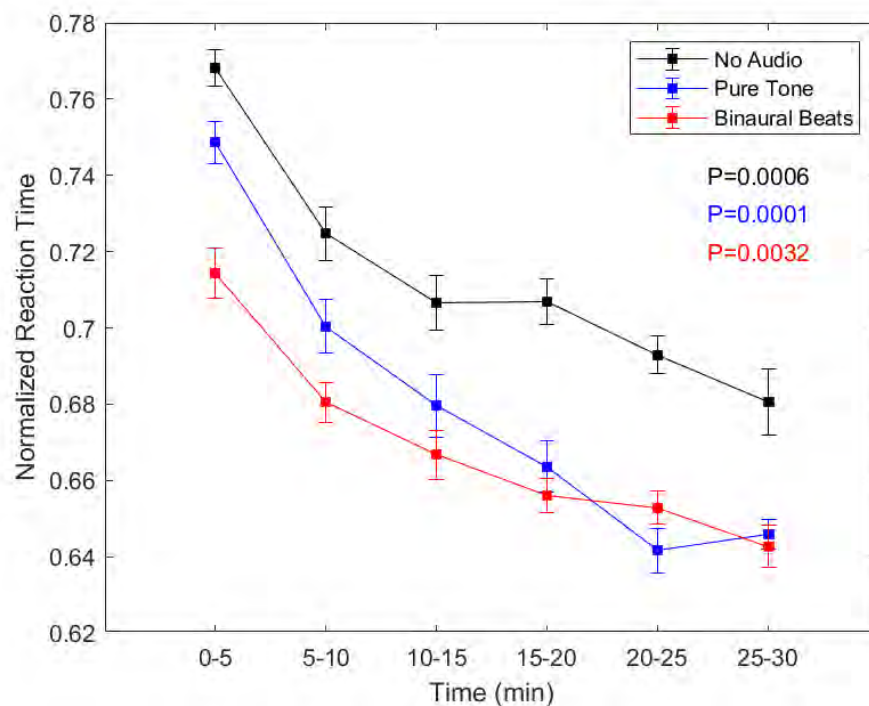
Figure 36: Evaluation of response reaction time with time-on-task under different auditory conditions. Plotted are the mean with the error bars representing the standard error. The p-values were obtained by statistically comparing the first and last blocks of each auditory condition (font colors are mapped to conditions).
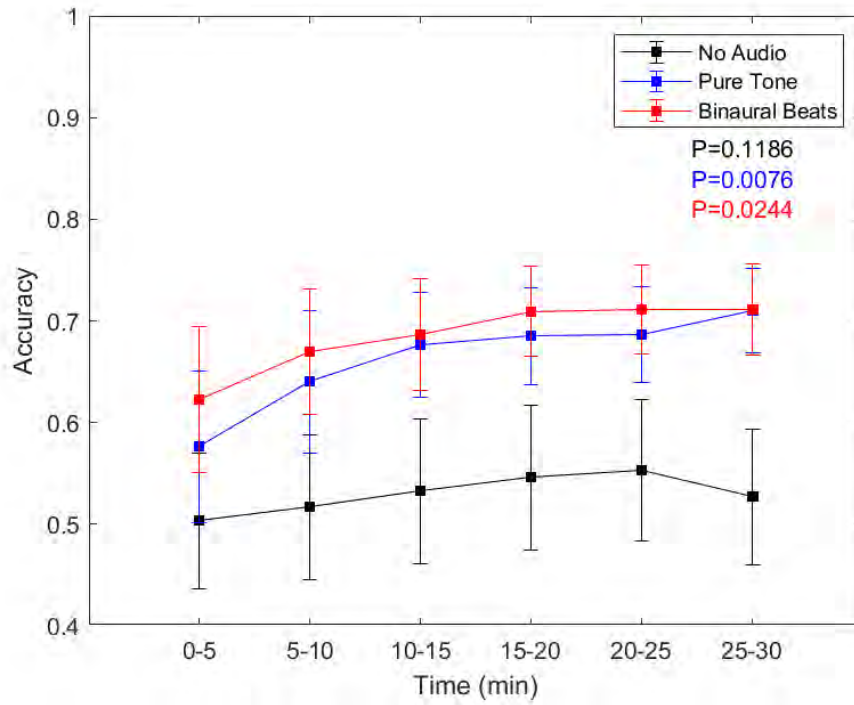
Figure 37: Evaluation of detection accuracy with time-on-task under different auditory conditions. Plotted are the mean with the error bars representing the standard error. The p-values were obtained by statistically comparing the first and last blocks of each auditory condition (font colors are mapped to conditions).

6.2.2. Full-scale global graph theory analysis. Figures 38 to 40 compare TOT changes in the NS_g, CC_g, and E_g under different auditory conditions. Plotted are the mean values across subjects with error bars denoting the standard error around the mean. For each condition, a paired sample t-test was employed to evaluate the significance of differences between the two vigilance levels. Also, each vigilance level was statistically compared between conditions. The asterisks on the plots indicate significant differences ($*: p < 0.05$, $**: p < 0.01$, $***: p < 0.001$). As shown in Figure 38, the NS_g significantly decreased with increasing TOT under the no-audio condition ($p < 0.01$ for delta and theta bands and $p < 0.05$ for alpha and beta bands). In all frequency bands, the NS_g observed under the PSTS and BBS conditions was significantly higher in comparison to that under the no-audio condition ($p < 0.001$). Moreover, the NS_g remained high with increased TOT under PSTS and BBS. No differences were observed between the PSTS and BBS conditions for the two vigilance levels. Likewise, the CC_g and the E_g significantly dropped under the no audio condition and remained

84

high under both PSTS and BBS conditions with increased TOT. These results indicate that audio stimulation significantly enhanced the efficiency of information processing and transfer regardless of the levels of TOT.
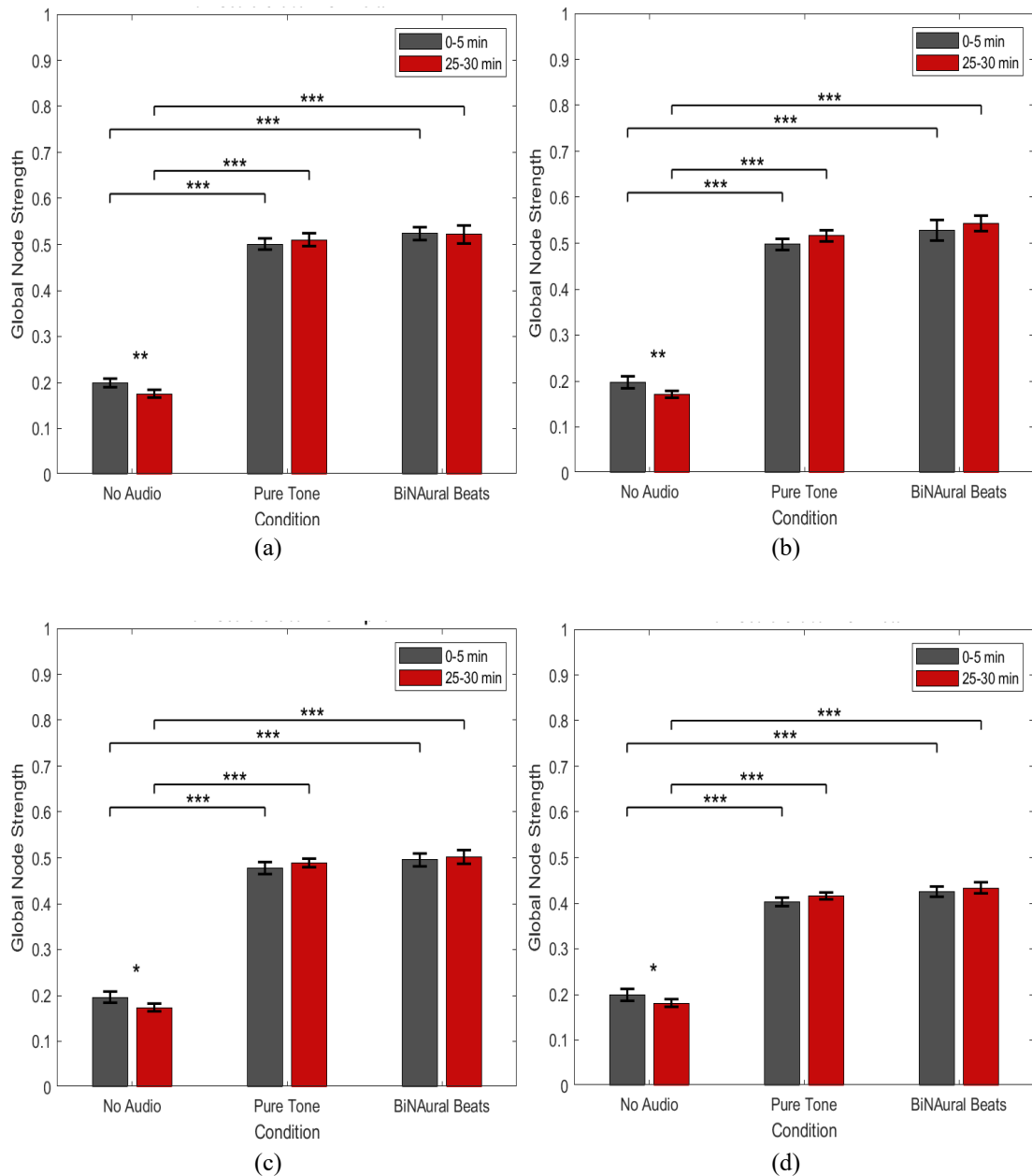
Figure 38: Comparison between the global node strengths under different vigilance levels and audio conditions. Comparison is specific to the (a) delta, (b) theta, (c) alpha, and (d) beta bands. Plotted are the mean values across subjects with error bars denoting the standard error. The asterisks indicate significant differences between vigilance levels ($*: p < 0.05, **: p < 0.01, ***: p < 0.001$).
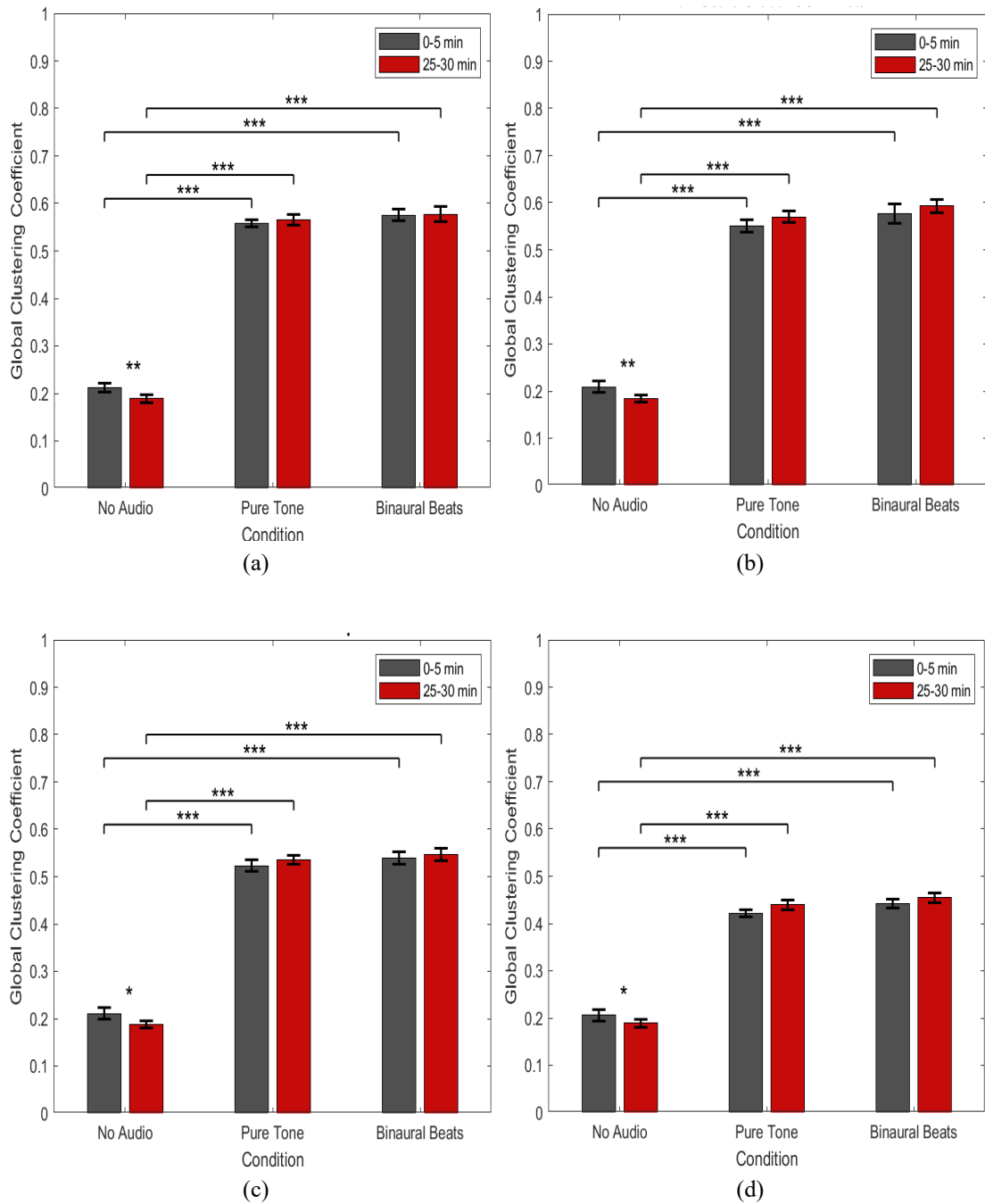
Figure 39: Comparison between the global clustering coefficient under different vigilance levels and audio conditions. Comparison is specific to the (a) delta, (b) theta, (c) alpha, and (d) beta bands. Plotted are the mean values across subjects with error bars denoting the standard error. The asterisks indicate significant differences between vigilance levels ($*: p < 0.05$, $**: p < 0.01$, $***: p < 0.001$).
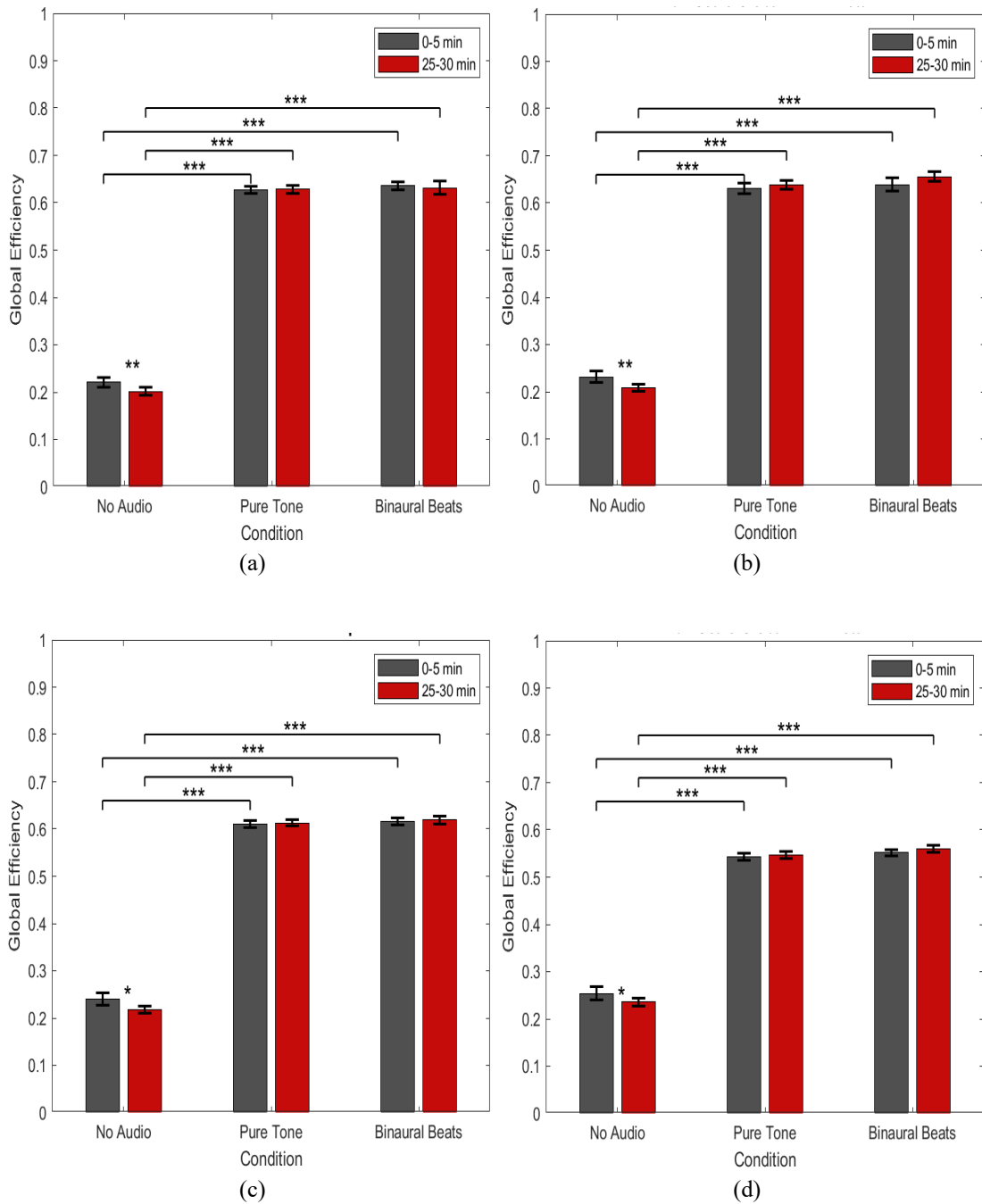
Figure 40: Comparison between the global efficiency under different vigilance levels and audio conditions. Comparison is specific to the (a) delta, (b) theta, (c) alpha, and (d) beta bands. Plotted are the mean values across subjects with error bars denoting the standard error. The asterisks indicate significant differences between vigilance levels ($*: p < 0.05$, $**: p < 0.01$, $***: p < 0.001$).

Chapter 7. Conclusion

This thesis addressed two main vigilance-related problems with prominent relevance in a variety of operational and industrial settings. Firstly, a quantitative vigilance assessment approach based on graph theory analysis of EEG functional connectivity was proposed. Secondly, the effectiveness of using auditory stimulation to enhance cortical connectivity and vigilance performance was investigated. The EEG data was collected through a novel protocol based on a computerized version of the incongruent Stroop color-word task (I-SCWT). The proposed experimental protocol included two main scenarios, based on three audio conditions: vigilance (no audio) and enhancement (pure sinusoidal tone or binaural beats). The vigilance states were induced by performing a 30 min I-SCWT. Meanwhile, the enhanced mental states were provoked by integrating a 250Hz pure sinusoidal tone or beta (16 Hz) binaural beats with the vigilance task. The phase-locking value statistic was used to model cortical connectivity under alertness, vigilance decrement, and enhanced mental states. Extensive graph theory analysis was then employed to quantify and compare different topological aspects of the connectivity networks.

7.1. Major Findings

The experimental results showed that the 30 min I-SCWT effectively elicited alteration in cortical connectivity. The PLV statistic was sensitive to vigilance decrement, and the overall phase synchronization between brain regions decreased, resulting in a less optimal network structure. Investigation of intra-regional PLV networks suggested that changes in functional connectivity under vigilance decrement are specific to cortical areas and EEG frequency bands. Subject independent classification analysis, using GTA features corresponding to a single cortical region and frequency band, showed an accuracy of 84.27% to detect vigilance decrement. Under the audio-enhanced mental states, cortical connectivity remained high until the end of the total task duration. Also, significant improvements in the participants' performance were observed in comparison to the no-audio condition. On average, pure tone stimulation showed a 25.84% improvement in the participants' detection accuracy towards the end of the task. Similarly, enhancement via binairal beats showed a 26.01% improvement. The results confirm that

the proposed framework is reliable to quantify different aspects of cortical functional connectivity under different vigilance levels. Moreover, the topology of intra-regional connectivity patterns can be quantified as simple and dimensionality-reduced indices to detect vigilance decrement with reliable accuracy. Finally, the results provide evidence for the enhancement of cognitive processing and behavioral performance through auditory stimulation.

7.2. Recommendations and Future Research Directions

It is worthy to note that the main limitation of this study is the small sample size, and the number of participants involved was too small to overrule biases due to individual differences. The larger sample size is needed to ensure sufficient statistical power and further support our findings. Provided below are several future research recommendations build upon this work:

- The PLV is one of the most predictive functional connectivity estimators and is proven to be efficient in mental state discrimination contexts. Even though the PLV demonstrated sensitivity to vigilance decrement as induced by the I-SCWT, other functional connectivity estimators are worth the investigation.

- In this work, cortical connectivity was estimated between electrode signals at the sensor space to ensure a simple vigilance assessment approach. Performing the analysis in the source space rather than the sensor space increases the complexity but provides a more reliable mapping of regional cortical connectivity. Moreover, the comparison between sensor space and source space approaches is necessary to determine if the increased complexity is of value.

- The connectivity analysis in this work was restricted to two-time windows, selected at the beginning and end of the task. For each subject, GTA was then employed, assuming stationarity of epochs under each time window, and results were interpreted based on grand average values. However, studies have shown that brain activity is spontaneous and varies temporally for the same subject [190,191]. It is thus worthy to employ dynamic functional connectivity and GTA framework to characterize and quantify the time-profile of cortical connectivity. Also, it is ex-

pected that this approach will capture the difference between the effects of PSTS and BBS on cortical connectivity.

- In this work, vigilance assessment was mainly based on the analysis of EEG data. EEG is the most used neuroimaging modality in vigilance, mental fatigue, and emotion studies. However, other physiological and neuroimaging modalities such as near-infrared spectroscopy, magnetoencephalography, and eye-tracking could provide complementary information regarding the neural and physiological mechanisms underlying vigilance. Thus, studying vigilance using a multi-modal neuroimaging approach would be an advantage, If so, employing feature fusion methods is expected to improve the accuracy of detecting vigilance decrement.

- In this work, each type of audio stimulus was based on a single frequency. Future studies could consider investigating and comparing the effect of different sinusoidal and binaural beat frequencies. Also, a continuous and prolonged audio stimulus for more than 30 min is worth the investigation. Finally, the effects of after stimulation on performance and cortical connectivity are yet to be explored.

References

[1] N. H. Mackworth, "The breakdown of vigilance during prolonged visual search," *Quarterly Journal of Experimental Psychology*, vol. 1, no. 1, pp. 6–21, 1948.

[2] W. S. Helton and J. S. War, "Signal salience and the mindlessness theory of vigilance," *Acta Psychologica*, vol. 129, no. 1, pp. 18 – 25, 2008.

[3] D. R. Thomson, D. Besner, and D. Smilek, "A resource-control account of sustained attention: Evidence from mind-wandering and vigilance paradigms," *Perspectives on Psychological Science*, vol. 10, no. 1, pp. 82–96, 2015.

[4] R. Kurzban, A. Duckworth, J. W. Kable, and J. Myers, "An opportunity cost model of subjective effort and task performance," *Behavioral and Brain Sciences*, vol. 36, no. 6, p. 661–679, 2013.

[5] G. Borragain, H. Slama, M. Bartolomei, and P. Peigneux, "Cognitive fatigue: A time-based resource-sharing account," *Cortex*, vol. 89, pp. 71 – 84, 2017.

[6] D. Gartenberg, B. Z. Veksler, G. Gunzelmann, and J. G. Trafton, "An act-r process model of the signal duration phenomenon of vigilance," *Proceedings of the Human Factors and Ergonomics Society Annual Meeting*, vol. 58, no. 1, pp. 909–913, 2014.

[7] D. Gartenberg, G. Gunzelmann, S. Hassanzadeh-Behbaha, and J. G. Trafton, "Examining the role of task requirements in the magnitude of the vigilance decrement," *Frontiers in Psychology*, vol. 9, p. 1504, 2018.

[8] W. H. Teichner, "The detection of a simple visual signal as a function of time of watch," *Human Factors*, vol. 16, no. 4, pp. 339–352, 1974.

[9] R. F. I. Meuter and P. F. Lacherez, "When and why threats go undetected: Impacts of event rate and shift length on threat detection accuracy during airport baggage screening," *Human Factors*, vol. 58, no. 2, pp. 218–228, 2016.

[10] M. KÃrber, A. Cingel, M. Zimmermann, and K. Bengler, "Vigilance decrement and passive fatigue caused by monotony in automated driving," *Procedia Manufacturing*, vol. 3, pp. 2403 – 2409, 2015.

[11] E. Nasholm, S. Rohlfing, and J. D. Sauer, "Pirate stealth or inattentional blindness? the effects of target relevance and sustained attention on security monitoring for experienced and naÃ¯ve operators," *PLOS ONE*, vol. 9, no. 1, pp. 1–8, 01 2014.

[12] B. D. Sawyer, V. S. Finomore, G. J. Funke, V. F. Mancuso, M. E. Funke, G. Matthews, and J. S. Warm, "Cyber vigilance: Effects of signal probability and event rate," *Proceedings of the Human Factors and Ergonomics Society Annual Meeting*, vol. 58, no. 1, pp. 1771–1775, 2014.

[13] A. J. Small, M. W. Wiggins, and T. Loveday, "Cue-based processing capacity, cognitive load and the completion of simulated short-duration vigilance tasks in power transmission control," *Applied Cognitive Psychology*, vol. 28, no. 4, pp. 481–487, 2014.

[14] L.-W. Ko, O. Komarov, W. D. Hairston, T.-P. Jung, and C.-T. Lin, "Sustained attention in real classroom settings: An eeg study," *Frontiers in Human Neuroscience*, vol. 11, p. 388, 2017.

[15] J. C. Ballard, "Computerized assessment of sustained attention: Interactive effects of task demand, noise, and anxiety," *Journal of Clinical and Experimental Neuropsychology*, vol. 18, no. 6, pp. 864–882, 1996.

[16] P. Nathalie, N. Xavier, H. David, and S. Eric, "Psychophysiological investigation of vigilance decrement: Boredom or cognitive fatigue?" *Physiology and Behavior*, vol. 93, no. 1, pp. 369 – 378, 2008.

[17] M. Hirshkowitz, L. Cueva, and J. Herman, "The multiple vigilance test," *Behavior Research Methods, Instruments, and Computers*, vol. 25, no. 2, pp. 272–275, 06 1993.

[18] R. Jaques, K. Kamal, Y. K. Maxim, L. Jianbo, and R. Sridhar, "Pc-pvt 2.0: An updated platform for psychomotor vigilance task testing, analysis, prediction, and visualization," *Journal of Neuroscience Methods*, vol. 304, pp. 39 – 45, 2018.

[19] J. C. Ballard, "Computerized assessment of sustained attention: A review of factors affecting vigilance performance," *Journal of Clinical and Experimental Neuropsychology*, vol. 18, no. 6, pp. 843–863, 1996.

[20] B. Dalton, D. Behm, and A. Kibele, "Effects of sound types and volumes on simulated driving, vigilance tasks and heart rate," *Occupational Ergonomics*, vol. 7, no. 3, pp. 153–168, 01 2007.

[21] E. Greenlee, P. DeLucia, and D. Newton, "Driver vigilance in automated vehicles: Hazard detection failures are a matter of time," *Human Factors: The Journal of the Human Factors and Ergonomics Society*, vol. 60, no. 4, pp. 465–476, 3 2018.

[22] M. Jackson, R. Croft, G. Kennedy, K. Owens, and M. Howard, "Cognitive components of simulated driving performance: Sleep loss effects and predictors," *Accident Analysis and Prevention*, vol. 50, pp. 438 – 444, 2013.

[23] W. Kirchner, "Age differences in short-term retention of rapidly changing information," *Journal of experimental psychology*, vol. 55, no. 4, pp. 352–358, April 1958.

[24] E. Kathrin, K. S. Nora, M. Gunther, T. Marion, K. Peter, J. Carole, R. Nathalie, K. Pascal, and H. Martin, "Sex specific relationships between infants mental rotation ability and amiotic sex hormones," *Neuroscience Letters*, vol. 707, pp. 134–298, 2019.

[25] R. Sladky, I. Stepniczka, E. Boland, M. Tik, C. Lamm, A. Hoffmann, J. Buch, D. Niedermeier, J. Field, and C. Windischberger, "Neurobiological differences in mental rotation and instrument interpretation in airline pilots," *Sci Rep*, vol. 6, no. 28104, p. 28104, 06 2016.

[26] G. Hirschfeld, M. Thielsch, and B. Zernikow, "Reliabilities of mental rotation tasks - limits to the assessment of individual differences," *Journal of Biomedicine and Biotechnology*, vol. 2017, pp. 1–7, 1 2014.

[27] K. O. Wioletta, Z. Dariusz, W. Piotr, A. Paweł, and P. Robert, "Acoustic neuro-feedback increases beta erd during mental rotation task," *Applied Psychophysiology and Biofeedback*, vol. 44, no. 2, pp. 103–115, 2018.

[28] R. Brandt, D. Herrero, T. Massetti, T. B. Crocetta, R. Guarnieri, C. B. de Mello Monteiro, M. da Silveira Viana, G. G. Bevilacqua, L. C. de Abreu, and A. Andrade, "The brunel mood scale rating in mental health for physically active and apparently healthy populations," *Health*, vol. 08, pp. 125–132, 2016.

[29] M. R. Smith, R. Chai, H. T. Nguyen, S. M. Marcora, and A. J. Coutts, "Comparing the effects of three cognitive tasks on indicators of mental fatigue," *The Journal of Psychology*, vol. 153, no. 8, pp. 759–783, 2019, pMID: 31188721.

[30] S. Shacham, "A shortened version of the profile of mood states." *Journal of personality assessment*, vol. 47 3, pp. 305–6, 1983.

[31] J. D. Lane, S. J. Kasian, J. E. Owens, and G. R. Marsh, "Binaural auditory beats affect vigilance performance and mood," *Physiology and Behavior*, vol. 63, no. 2, pp. 249 – 252, 1998.

[32] W. S. Helton, "Validation of a short stress state questionnaire," *Proceedings of the Human Factors and Ergonomics Society Annual Meeting*, vol. 48, no. 11, pp. 1238–1242, 2004.

[33] G. N. Dimitrakopoulos, I. Kakkos, Z. Dai, H. Wang, K. Sgarbas, N. Thakor, A. Bezerianos, and Y. Sun, "Functional connectivity analysis of mental fatigue reveals different network topological alterations between driving and vigilance tasks," *IEEE Transactions on Neural Systems and Rehabilitation Engineering*, vol. 26, no. 4, pp. 740–749, 2018.

[34] J. Victor S. Finomore, T. H. Shaw, J. S. Warm, G. Matthews, and D. B. Boles, "Viewing the workload of vigilance through the lenses of the nasa-tlx and the mrq," *Human Factors*, vol. 55, no. 6, pp. 1044–1063, 2013, pMID: 24745198.

[35] Y. Groen, A. B. M. Fuermaier, L. I. Tucha, M. Weisbrod, S. Aschenbrenner, and O. Tucha, "A situation-specific approach to measure attention in adults with adhd: The everyday life attention scale (elas)." *Applied neuropsychology. Adult*, pp. 1–30, 2018.

[36] B. Oken, M. Salinsky, and S. Elsas, "Vigilance, alertness, or sustained attention: physiological basis and measurement," *Clinical Neurophysiology*, vol. 117, no. 9, pp. 1885 – 1901, 2006.

[37] F. D. David and W. P. John, "Microcomputer analyses of performance on a portable, simple visual rt task during sustained operations," *Behavior Research Methods, Instruments, and Computers*, vol. 17, no. 6, pp. 652–655, 1985.

[38] H. R. Ian, M. Tom, A. Jackie, T. B. Bart, and Y. Jenny, "Oops: Performance correlates of everyday attentional failures in traumatic brain injured and normal subjects," *Neuropsychologia*, vol. 35, no. 6, pp. 747 – 758, 1997.

[39] M. Esterman, S. K. Noonan, M. Rosenberg, and J. DeGutis, "In the Zone or Zoning Out? Tracking Behavioral and Neural Fluctuations During Sustained Attention," *Cerebral Cortex*, vol. 23, no. 11, pp. 2712–2723, 08 2012.

[40] s. Van, R. D. THIJS, R. FRONCZEK, H. A. M. MIDDELKOOP, G. J. LAMMERS, and J. G. VAN DIJK, "Sustained attention to response task (sart) shows impaired vigilance in a spectrum of disorders of excessive daytime sleepiness," *Journal of Sleep Research*, vol. 21, no. 4, pp. 390–395, 2012.

[41] J. Ballard, "Assessing attention: comparison of response-inhibition and traditional continuous performance tests," *Journal of clinical and experimental neuropsychology*, vol. 23, no. 3, pp. 331–350, June 2001.

[42] N. D. Joux], P. N. Russell, and W. S. Helton, "A functional near-infrared spectroscopy study of sustained attention to local and global target features," *Brain and Cognition*, vol. 81, no. 3, pp. 370 – 375, 2013.

[43] W. S. Helton, T. D. Hollander, J. S. Warm, L. D. Tripp, K. S. Parsons, G. Matthews, W. N. Dember, R. Parasuraman, and P. A. Hancock, "The abbreviated vigilance task and cerebral hemodynamics," *Journal of Clinical and Experimental Neuropsychology*, vol. 29, pp. 545 – 552, 2007.

[44] W. S. Helton, U. Ossowski, and S. Malinen, "Post-disaster depression and vigilance: a functional near-infrared spectroscopy study," *Experimental Brain Research*, vol. 226, pp. 357–362, 2013.

[45] M. E. Funke, J. S. Warm, G. Matthews, M. Riley, J. Victor Finomore, J. Gregory J. Funke, J. Benjamin Knott, and J. Michael A. Vidulich, "A comparison of cerebral hemovelocity and blood oxygen saturation levels during vigilance performance," *Proceedings of the Human Factors and Ergonomics Society Annual Meeting*, vol. 54, no. 18, pp. 1345–1349, 2010.

[46] W. S. Helton, J. S. Warm, L. D. Tripp, G. Matthews, R. Parasuraman, and P. A. Hancock, "Cerebral lateralization of vigilance: A function of task difficulty," *Neuropsychologia*, vol. 48, no. 6, pp. 1683 – 1688, 2010.

[47] M. Zhao, T. M. Gersch, B. S. Schnitzer, B. A. Dosher, and E. Kowler, "Eye movements and attention: The role of pre-saccadic shifts of attention in perception, memory and the control of saccades," *Vision Research*, vol. 74, pp. 40 – 60, 2012, visual Attention 2012 Volume I.

[48] J. Hoffman and B. Subramaniam, "The role of visual attention in saccadic eye movements," *Perception and psychophysics*, vol. 57, pp. 787–95, 09 1995.

[49] I. P. Bodala, N. I. Abbasi, Y. Sun, A. Bezerianos, H. Al-Nashash, and N. V. Thakor, "Measuring vigilance decrement using computer vision assisted eye tracking in dynamic naturalistic environments," in *2017 39th Annual International Conference of the IEEE Engineering in Medicine and Biology Society (EMBC)*, 2017, pp. 2478–2481.

[50] I. P. Bodala, S. Kukreja, J. Li, N. V. Thakor, and H. Al-Nashash, "Eye tracking and eeg synchronization to analyze microsaccades during a workload task," in *2015 37th Annual International Conference of the IEEE Engineering in Medicine and Biology Society (EMBC)*, 2015, pp. 7994–7997.

[51] I. P. Bodala, Y. Ke, H. Mir, N. V. Thakor, and H. Al-Nashash, "Cognitive workload estimation due to vague visual stimuli using saccadic eye movements," in *2014 36th Annual International Conference of the IEEE Engineering in Medicine and Biology Society*, 2014, pp. 2993–2996.

[52] L. S. Colzato, H. A. Slagter, M. M. SpapÃ©, and B. Hommel, "Blinks of the eye predict blinks of the mind," *Neuropsychologia*, vol. 46, no. 13, pp. 3179 – 3183, 2008.

[53] K. Fukuda, J. A. Stern, T. B. Brown, and M. B. Russo, "Cognition, blinks, eye-movements, and pupillary movements during performance of a running memory task." *Aviation, space, and environmental medicine*, vol. 76 7 Suppl, pp. C75–85, 2005.

[54] W. Qing, S. BingXi, X. Bin, and Z. Junjie, "A perclos-based driver fatigue recognition application for smart vehicle space," in *2010 Third International Symposium on Information Processing*, 2010, pp. 437–441.

[55] R. Zangróniz, A. Martínez-Rodrigo, J. Pastor, M. López, and A. Fernández-Caballero, "Electrodermal activity sensor for classification of calm/distress condition," *Sensors*, vol. 17, no. 10, p. 2324, Oct 2017.

[56] C. Lim, R. Barry, E. Gordon, A. Sawant, C. Rennie, and C. Yiannikas, "The relationship between quantified eeg and skin conductance level," *International Journal of Psychophysiology*, vol. 21, no. 2, pp. 151 – 162, 1996.

[57] M. Frederikson and B. T. Engel, "ardiovascular and electrodermal adjustments during a vigilance task in patients with borderline and established hypertension," *Journal of Psychosomatic Research*, vol. 29, no. 3, pp. 235–246, 1985.

[58] A. Luque-Casado, M. Zabala, E. Morales, M. Mateo-March, and D. Sanabria, "Cognitive performance and heart rate variability: The influence of fitness level," *PLOS ONE*, vol. 8, no. 2, pp. 1–9, 02 2013.

[59] A. Henelius, M. Sallinen, M. Huotilainen, K. Müller, J. Virkkala, and K. Puolamäki, "Heart Rate Variability for Evaluating Vigilant Attention in Partial Chronic Sleep Restriction," *Sleep*, vol. 37, no. 7, pp. 1257–1267, 07 2014.

[60] I. G. Damousis, D. Tzovaras, and M. G. Strintzis, "A fuzzy expert system for the early warning of accidents due to driver hypo-vigilance," in *Artificial Intelligence Applications and Innovations*, I. Maglogiannis, K. Karpouzis, and M. Bramer, Eds. Boston, MA: Springer US, 2006, pp. 345–352.

[61] M. H. Sigari, "Driver hypo-vigilance detection based on eyelid behavior," in *2009 Seventh International Conference on Advances in Pattern Recognition*, Feb 2009, pp. 426–429.

[62] M. A. Boksem, T. F. Meijman, and M. M. Lorist, "Effects of mental fatigue on attention: An erp study," *Cognitive Brain Research*, vol. 25, no. 1, pp. 107 – 116, 2005.

[63] A. Haubert, M. Walsh, R. Boyd, M. Morris, M. Wiedbusch, M. Krusmark, and G. Gunzelmann, "Relationship of event-related potentials to the vigilance decrement," *Frontiers in Psychology*, vol. 9, p. 237, 2018.

[64] J. F. Hopstaken, D. van der Linden, A. B. Bakker, and M. A. J. Kompier, "A multifaceted investigation of the link between mental fatigue and task disengagement," *Psychophysiology*, vol. 52, no. 3, pp. 305–315, 2015.

[65] N. I. Abbasi, I. P. Bodala, A. Bezerianos, Y. Sun, H. Al-Nashash, and N. V. Thakor, "Role of multisensory stimuli in vigilance enhancement- a single trial event related potential study," *2017 39th Annual International Conference of the IEEE Engineering in Medicine and Biology Society (EMBC)*, pp. 2446–2449, July 2017.

[66] S. Waninger, C. Berka, A. Meghdadi, M. S. Karic, K. Stevens, C. Aguero, T. Sitnikova, D. H. Salat, and A. Verma, "Event-related potentials during sustained attention and memory tasks: Utility as biomarkers for mild cognitive impairment," *Alzheimer's and Dementia: Diagnosis, Assessment and Disease Monitoring*, vol. 10, pp. 452 – 460, 2018.

[67] M. Matousek and I. Petersan, "A method for assessing alertness fluctuations from eeg spectra," *Electroencephalography and Clinical Neurophysiology*, vol. 55, no. 1, pp. 108 – 113, 1983.

[68] A. S. Gevins, M. E. Smith, L. K. McEvoy, and D. Yu, "High-resolution eeg mapping of cortical activation related to working memory: effects of task difficulty, type of processing, and practice." *Cerebral cortex*, vol. 7 4, pp. 374–85, 1997.

[69] C.-H. Chuang, L.-W. Ko, T.-P. Jung, and C.-J. Lin, "Kinesthesia in a sustained-attention driving task," *NeuroImage*, vol. 91, pp. 187–202, 2014.

[70] S. K. Lal and A. Craig, "A critical review of the psychophysiology of driver fatigue," *Biological Psychology*, vol. 55, no. 3, pp. 173 – 194, 2001.

[71] E. Wascher, B. Rasch, J. Sanger, S. Hoffmann, D. Schneider, G. Rinkenauer, H. Heuer, and I. Gutberlet, "Frontal theta activity reflects distinct aspects of mental fatigue," *Biological Psychology*, vol. 96, pp. 57 – 65, 2014.

[72] S. Makeig and T.-P. Jung, "Tonic, phasic, and transient eeg correlates of auditory awareness in drowsiness," *Cognitive Brain Research*, vol. 4, no. 1, pp. 15 – 25, 1996.

[73] E. C.-P. Chua, S.-C. Yeo, I. T.-G. Lee, L.-C. Tan, P. Lau, S. Cai, X. Zhang, K. Puvanendran, and J. J. Gooley, "Sustained attention performance during sleep deprivation associates with instability in behavior and physiologic measures at baseline," *Sleep*, vol. 37, no. 1, pp. 27–39, January 2014.

[74] A. T. Kamzanova, A. M. Kustubayeva, and G. Matthews, "Use of eeg workload indices for diagnostic monitoring of vigilance decrement," *Human Factors*, vol. 56, no. 6, pp. 1136–1149, 2014, pMID: 25277022.

[75] A. Martel, S. Dahne, and B. Blankertz, "Eeg predictors of covert vigilant attention," *Journal of Neural Engineering*, vol. 11, no. 3, p. 035009, may 2014.

[76] M. Li, J. Fu, and B. Lu, "Estimating vigilance in driving simulation using probabilistic pca," in *2008 30th Annual International Conference of the IEEE Engineering in Medicine and Biology Society*, Aug 2008, pp. 5000–5003.

[77] Lei Cao, Jie Li, Yaoru Sun, Huaping Zhu, and Chungang Yan, "Eeg-based vigilance analysis by using fisher score and pca algorithm," in *2010 IEEE International Conference on Progress in Informatics and Computing*, vol. 1, Dec 2010, pp. 175–179.

[78] L. Shi, Y. Jiao, and B. Lu, "Differential entropy feature for eeg-based vigilance estimation," in *2013 35th Annual International Conference of the IEEE Engineering in Medicine and Biology Society (EMBC)*, July 2013, pp. 6627–6630.

[79] F. G. Freeman, P. J. Mikulka, M. W. Scerbo, and L. Scott, "An evaluation of an adaptive automation system using a cognitive vigilance task," *Biological Psychology*, vol. 67, no. 3, pp. 283 – 297, 2004.

[80] C. Berka, D. J. Levendowski, M. N. Lumicao, A. H. L. Yau, G. Davis, V. T. Zivkovic, R. Olmstead, P. D. Tremoulet, and P. L. Craven, "Eeg correlates of task engagement and mental workload in vigilance, learning, and memory tasks." *Aviation, space, and environmental medicine*, vol. 78 5 Suppl, pp. B231–44, 2007.

[81] A. Marchetti, F. Baglio, I. Costantini, O. Dipasquale, F. Savazzi, R. Nemni, F. Sangiuliano Intra, S. Tagliabue, A. Valle, D. Massaro, and I. Castelli, "Theory of mind and the whole brain functional connectivity: Behavioral and neural evidences with the amsterdam resting state questionnaire," *Frontiers in Psychology*, vol. 6, p. 1855, 2015.

[82] K. J. Blinowska, "Review of the methods of determination of directed connectivity from multichannel data," *Medical and Biological Engineering and Computing*, vol. 49, no. 5, pp. 521–529, May 2011.

[83] B. Ed and S. Olaf, "Complex brain networks: graph theoretical analysis of structural and functional systems," *Nature Reviews Neuroscience*, vol. 10, p. 186–198, 2009.

[84] M. X. Cohen, *Analyzing Neural Time Series Data.* One Rogers Street, Cambridge: MIT Press, 1979, pp. 429–447.

[85] J. D. Bonita, L. C. C. Ambolode, B. M. Rosenberg, C. J. Cellucci, T. A. A. Watanabe, P. E. Rapp, and A. M. Albano, "Time domain measures of inter-channel eeg correlations: a comparison of linear, nonparametric and nonlinear measures," *Cognitive Neurodynamics*, vol. 8, no. 1, pp. 1–15, Feb 2014.

[86] A. M. Bastos and J.-M. Schoffelen, "A tutorial review of functional connectivity analysis methods and their interpretational pitfalls," *Frontiers in Systems Neuroscience*, vol. 9, p. 175, 2016.

[87] V. Sakkalis, "Review of advanced techniques for the estimation of brain connectivity measured with eeg/meg," *Computers in Biology and Medicine*, vol. 41, no. 12, pp. 1110 – 1117, 2011, special Issue on Techniques for Measuring Brain Connectivity.

[88] A. Ide, M. Chiappalone, L. Berdondini, V. Sanguineti, and S. Martinoia, "Cross-correlation based methods for estimating the functional connectivity in cortical networks," *BMC Neuroscience*, vol. 8, no. 2, p. P63, Jul 2007.

[89] L. A. Baccala and K. Sameshima, "Partial directed coherence: a new concept in neural structure determination," *Biological Cybernetics*, vol. 84, no. 6, pp. 463–474, May 2001.

[90] L. Faes and G. Nollo, "Multivariate frequency domain analysis of causal interactions in physiological time series," in *Biomedical Engineering, Trends in Electronics*, A. N. Laskovski, Ed. Rijeka: IntechOpen, 2011, ch. 21.

[91] B. T. Schmidt, A. S. Ghuman, and T. J. Huppert, "Whole brain functional connectivity using phase locking measures of resting state magnetoencephalography," *Frontiers in Neuroscience*, vol. 8, p. 141, 2014.

[92] G. Tononi, O. Sporns, and G. M. Edelman, "A measure for brain complexity: relating functional segregation and integration in the nervous system," *Neurobiology*, vol. 91, no. 11, pp. 5033–5037, 1994.

[93] G. Marrelec, P. Bellec, A. Krainik, H. Duffau, M. Palagrini-Issac, S. Leharicy, H. Benali, and J. Doyon, "Regions, systems, and the brain: Hierarchical measures of functional integration in fmri," *Medical Image Analysis*, vol. 12, no. 4, pp. 484 – 496, 2008.

[94] O. Sporns, "Network attributes for segregation and integration in the human brain," *Current Opinion in Neurobiology*, vol. 23, no. 2, pp. 162 – 171, 2013, macrocircuits.

[95] Y. Sun, J. Lim, K. Kwok, and A. Bezerianos, "Functional cortical connectivity analysis of mental fatigue unmasks hemispheric asymmetry and changes in small-world networks," *Brain and Cognition*, vol. 85, pp. 220 – 230, 2014.

[96] Y. Sun, J. Lim, Z. Dai, K. Wong, F. Taya, Y. Chen, J. Li, N. Thakor, and A. Bezerianos, "The effects of a mid-task break on the brain connectome in healthy participants: A resting-state functional mri study," *NeuroImage*, vol. 152, pp. 19 – 30, 2017.

[97] C. Gießing, C. M. Thiel, A. F. Alexander-Bloch, A. X. Patel, and E. T. Bullmore, "Human brain functional network changes associated with enhanced and impaired attentional task performance," *Journal of Neuroscience*, vol. 33, no. 14, pp. 5903–5914, 2013.

[98] M. Alavash, P. Doebler, H. Holling, C. M. Thiel, and C. Gieaying, "Is functional integration of resting state brain networks an unspecific biomarker for working memory performance?" *NeuroImage*, vol. 108, pp. 182 – 193, 2015.

[99] V. Dubljevia, C. Venero, and S. Knafo, "Chapter 1 - what is cognitive enhancement?" in *Cognitive Enhancement*, S. Knafo and C. Venero, Eds.   San Diego: Academic Press, 2015, pp. 1–9.

[100] K. A. MacLean, E. Ferrer, S. R. Aichele, D. A. Bridwell, A. P. Zanesco, T. L. Jacobs, B. G. King, E. L. Rosenberg, B. K. Sahdra, P. R. Shaver, B. A. Wallace, G. R. Mangun, and C. D. Saron, "Intensive meditation training improves perceptual discrimination and sustained attention," *Psychological Science*, vol. 21, no. 6, pp. 829–839, 2010, pMID: 20483826.

[101] K. Lambourne and P. Tomporowski, "The effect of exercise-induced arousal on cognitive task performance: A meta-regression analysis," *Brain Research*, vol. 1341, pp. 12 – 24, 2010, exercise and the Brain.

[102] R. Ballester, F. Huertas, E. Molina, and D. Sanabria, "Sport participation and vigilance in children: Influence of different sport expertise," *Journal of Sport and Health Science*, vol. 7, no. 4, pp. 497 – 504, 2018.

[103] Sheela, H. Nagendra, and S. Tikhe, "Efficacy of yoga for sustained attention in university students," *Ayu*, vol. 34, pp. 270–2, 07 2013.

[104] S. Telles, R. K. Gupta, S. Verma, N. Kala, and A. Balkrishna, "Changes in vigilance, self rated sleep and state anxiety in military personnel in india following yoga," *BMC Research Notes*, vol. 11, 2018.

[105] H. R. Lieberman, C. M. Falco, and S. S. Slade, "Carbohydrate administration during a day of sustained aerobic activity improves vigilance, as assessed by a novel ambulatory monitoring device, and mood," *The American Journal of Clinical Nutrition*, vol. 76, no. 1, pp. 120–127, 07 2002.

[106] T. M. McLellan, G. H. Kamimori, D. M. Voss, D. G. Bell, K. G. Cole, and D. E. Johnson, "Caffeine maintains vigilance and improves run times during night operations for special forces." *Aviation, space, and environmental medicine*, vol. 76 7, pp. 647–54, 2005.

[107] Y. Hirano and M. Onozuka, "Chewing and attention: A positive effect on sustained attention," *BioMed Research International*, vol. 2015, pp. 1–6, 05 2015.

[108] A. J. Johnson, "Cognitive facilitation following intentional odor exposure," *Sensors*, vol. 11, no. 5, p. 5469–5488, May 2011.

[109] E. Matsubara, M. Fukagawa, T. Okamoto, A. Fukuda, C. Hayashi, K. Ohnuki, K. Shimizu, and R. Kondo, "Volatiles emitted from the leaves of <i>laurus nobilis</i> l. improve vigilance performance in visual discrimination task," *Biomedical Research*, vol. 32, no. 1, pp. 19–28, 2011.

[110] S. A. McBride, R. F. Johnson, D. J. Merullo, and J. Ronald E. Bartow, "Effects of the periodic administration of odor or vibration on a 3-hr. vigilance task," *Perceptual and Motor Skills*, vol. 98, no. 1, pp. 307–318, 2004, pMID: 15058891.

[111] S. Zhang, D. Wang, N. Afzal, Y. Zhang, and R. Wu, "Rhythmic haptic stimuli improve short-term attention," *IEEE Transactions on Haptics*, vol. 9, no. 3, pp. 437–442, 2016.

[112] G. R. Arrabito, G. Ho, B. Aghaei, C. Burns, and M. Hou, "Sustained attention in auditory and visual monitoring tasks: Evaluation of the administration of a rest break or exogenous vibrotactile signals," *Human Factors*, vol. 57, no. 8, pp. 1403–1416, 2015, pMID: 26276365.

[113] I. P. Bodala, J. Li, N. V. Thakor, and H. Al-Nashash, "Eeg and eye tracking demonstrate vigilance enhancement with challenge integration," *Frontiers in Human Neuroscience*, vol. 10, p. 273, 2016.

[114] D. E. Wolfe and L. K. Noguchi, "The Use of Music with Young Children to Improve Sustained Attention during a Vigilance Task in the Presence of Auditory Distractions," *Journal of Music Therapy*, vol. 46, no. 1, pp. 69–82, 03 2009.

[115] A. Gupta, B. Bhushan, and L. Behera, "Short-term enhancement of cognitive functions and music: A three-channel model," *Scientific Reports*, vol. 8, no. 15528, 2018.

[116] B. S. Löffler, H. I. Stecher, S. Fudickar, D. de Sordi, F. Otto-Sobotka, A. Hein, and C. S. Herrmann, "Counteracting the slowdown of reaction times in a vigilance experiment with 40-hz transcranial alternating current stimulation," *IEEE Transactions on Neural Systems and Rehabilitation Engineering*, vol. 26, no. 10, pp. 2053–2061, 2018.

[117] L. Annarumma, A. D'Atri, V. Alfonsi, and L. De Gennaro, "The efficacy of transcranial current stimulation techniques to modulate resting-state eeg, to affect vigilance and to promote sleepiness," *Brain Sciences*, vol. 8, no. 7, p. 137, Jul 2018.

[118] J. T. Nelson, R. A. McKinley, E. J. Golob, J. S. Warm, and R. Parasuraman, "Enhancing vigilance in operators with prefrontal cortex transcranial direct current stimulation (tdcs)," *NeuroImage*, vol. 85, pp. 909 – 917, 2014, neuro-enhancement.

[119] C. E. Giurgea, "The nootropic concept and its prospective implications," *Drug Development Research*, vol. 2, no. 5, pp. 441–446, 1982.

[120] J. L. Szalma, T. N. Daly, G. W. L. Teo, G. M. Hancock, and P. A. Hancock, "Training for vigilance on the move: a video game-based paradigm for sustained attention," *Ergonomics*, vol. 61, no. 4, pp. 482–505, 2018, pMID: 29125389.

[121] J. Szalma, T. Schmidt, G. Teo, and P. Hancock, "Vigilance on the move: video game-based measurement of sustained attention," *Ergonomics*, vol. 57, no. 9, pp. 1315–1336, 2014, pMID: 25001010.

[122] F. Al-Shargie, U. Tariq, H. Mir, H. Alawar, F. Babiloni, and H. Al-Nashash, "Vigilance decrement and enhancement techniques: A review," *Brain Sciences*, vol. 9, no. 8, 2019.

[123] D. Gong, H. He, D. Liu, W. Ma, L. Dong, C. Luo, and D. Yao, "Enhanced functional connectivity and increased gray matter volume of insula related to action video game playing," *Scientific Reports*, vol. 5, no. 9763, pp. 1–7, 2015.

[124] L. Steenbergen, R. Sellaro, A.-K. Stock, C. Beste, and L. S. Colzato, "Action video gaming and cognitive control: Playing first person shooter games is associated with improved action cascading but not inhibition," *PLOS ONE*, vol. 10, no. 12, pp. 1–15, 12 2015.

[125] J. Feng, I. Spence, and J. Pratt, "Playing an action video game reduces gender differences in spatial cognition," *Psychological Science*, vol. 18, no. 10, pp. 850–855, 2007, pMID: 17894600.

[126] R. Li, U. Polat, W. Makous, and D. Bavelier, "Enhancing the contrast sensitivity function through action video game training," *Nature Neuroscience*, vol. 12, pp. 549–551, 2009.

[127] C. S. Green], M. A. Sugarman, K. Medford, E. Klobusicky, and D. Bavelier, "The effect of action video game experience on task-switching," *Computers in Human Behavior*, vol. 28, no. 3, pp. 984 – 994, 2012.

[128] A. Miyake, N. P. Friedman, M. J. Emerson, A. H. Witzki, A. Howerter, and T. D. Wager, "The unity and diversity of executive functions and their contributions to complex frontal lobe tasks: A latent variable analysis," *Cognitive Psychology*, vol. 41, no. 1, pp. 49 – 100, 2000.

[129] R. Battleday and A.-K. Brem, "Modafinil for cognitive neuroenhancement in healthy non-sleep-deprived subjects: A systematic review," *European Neuropsychopharmacology*, vol. 25, no. 11, pp. 1865 – 1881, 2015.

[130] R. Draganova, B. Ross, A. Wollbrink, and C. Pantev, "Cortical Steady-State Responses to Central and Peripheral Auditory Beats," *Cerebral Cortex*, vol. 18, no. 5, pp. 1193–1200, 09 2007.

[131] O. etrovich, *The Effects of Binaural Beats on Emotion and Cognition- Master's Thesis*.   University of South Florida, 2018, pp. 1–49.

[132] B. Tanasic, "Binaural arousal - sound that synchronizes the brain," *Open Access Journal of Biomedical Engineering and Biosciences*, vol. 1, 03 2018.

[133] R. Le Scouarnec, R. Poirier, J. Owens, J. Gauthier, A. G. Taylor, and P. Rodeheaver, "Use of binaural beat tapes for treatment of anxiety: A pilot study of tape preference and outcomes," *Alternative therapies in health and medicine*, vol. 7, pp. 58–63, 02 2001.

[134] B. Isik, A. Esen, B. Bayakerkmen, A. Kilinas, and D. Menziletoglu, "Effectiveness of binaural beats in reducing preoperative dental anxiety," *British Journal of Oral and Maxillofacial Surgery*, vol. 55, no. 6, pp. 571 – 574, 2017.

[135] G. F. Oster, "Auditory beats in the brain." *Scientific American*, vol. 229 4, pp. 94–102, 1973.

[136] L. Joseph, W. Jonathan, and H. J.M, "On the frequency limits of binaural beats," *Journal of the Acoustical Society of America*, vol. 22, pp. 468–473, 1950.

[137] X. Gao, H. Cao, D. Ming, H. Qi, X. Wang, X. Wang, R. Chen, and P. Zhou, "Analysis of eeg activity in response to binaural beats with different frequencies," *International Journal of Psychophysiology*, vol. 94, no. 3, pp. 399 – 406, 2014.

[138] D. Foster, "Eeg and subjective correlates of alpha frequency binaural beats stimulation combined with alpha biofeedback," PhD dissertation, Memphis State University, 1999.

[139] H. Pratt, A. Starr, H. J. Michalewski, A. Dimitrijevic, N. Bleich, and N. Mittelman, "A comparison of auditory evoked potentials to acoustic beats and to binaural beats," *Hearing Research*, vol. 262, no. 1, pp. 34 – 44, 2010.

[140] T. S. Ala, M. A. Ahmadi-Pajouh, and A. M. Nasrabadi, "Cumulative effects of theta binaural beats on brain power and functional connectivity," *Biomedical Signal Processing and Control*, vol. 42, pp. 242 – 252, 2018.

[141] B. Isik, A. Esen, B. Büyükerkmen, A. Kilinç, and D. Menziletoglu, "Effectiveness of binaural beats in reducing preoperative dental anxiety," *British Journal of Oral and Maxillofacial Surgery*, vol. 55, no. 6, pp. 571 – 574, 2017.

[142] C. Beauchene, N. Abaid, R. Moran, R. A. Diana, and A. Leonessa, "The effect of binaural beats on verbal working memory and cortical connectivity," *Journal of Neural Engineering*, vol. 14, no. 2, p. 026014, feb 2017.

[143] S. A. Reedijk, A. Bolders, L. S. Colzato, and B. Hommel, "Eliminating the attentional blink through binaural beats: A case for tailored cognitive enhancement," *Frontiers in Psychiatry*, vol. 6, p. 82, 2015.

[144] F. Lopez-Caballero and C. Escera, "Binaural beat: A failure to enhance eeg power and emotional arousal," *Frontiers in Human Neuroscience*, vol. 11, p. 557, 2017.

[145] B. Hommel, R. Sellaro, R. Fischer, S. Borg, and L. S. Colzato, "High-frequency binaural beats increase cognitive flexibility: Evidence from dual-task crosstalk," *Frontiers in Psychology*, vol. 7, 2016.

[146] L. S. Colzato, H. Barone, R. Sellaro, and B. Hommel, "More attentional focusing through binaural beats: evidence from the global–local task," *Psychological Research*, vol. 81, no. 1, pp. 271–277, Jan 2017.

[147] D. Navon, "Forest before trees: The precedence of global features in visual perception," *Cognitive Psychology*, vol. 9, no. 3, pp. 353 – 383, 1977.

[148] P. Goodin, J. Ciorciari, K. Baker, A.-M. Carrey, M. Harper, and J. Kaufman, "A high-density eeg investigation into steady state binaural beat stimulation," *PLOS ONE*, vol. 7, no. 4, pp. 1–8, 04 2012.

[149] V. Pablo, R. Candelaria, G. Aída, J. Talamantes, A. Pablo, and B. Jorge, "Circadian rhythms in components of attention," *Biological Rhythm Research*, vol. 36, no. 2, pp. 57–65, 2005.

[150] J. R. Stroop, "Studies of interference in serial verbal reactions," *Journal of Experimental Psychology*, vol. 18, no. 6, p. 643–662, 1935.

[151] F. Scarpina and S. Tagini, "The stroop color and word test," *Frontiers in Psychology*, vol. 8, p. 557, 2017.

[152] D. A. Washburn, "The stroop effect at 80: The competition between stimulus control and cognitive control," *Journal of the Experimental Analysis of Behavior*, vol. 105, no. 1, pp. 3–13, 2016.

[153] P. A. Starreveld and W. L. Heij, "Picture-word interference is a stroop effect: A theoretical analysis and new empirical findings," *Psychonomic Bulletin and Review*, vol. 24, no. 3, p. 721–733, 2017.

[154] N. S. Wecker, J. H. Kramer, A. Wisniewski, and D. C. Delis, "Age effects on executive ability," *Neuropsychology*, vol. 14, no. 3, p. 409–414, 2000.

[155] W. V. der Elst, M. P. J. V. Boxtel, G. J. P. V. Breukelen, and J. Jolles, "The stroop color-word test: Influence of age, sex, and education; and normative data for a large sample across the adult age range," *Assessment*, vol. 13, no. 1, pp. 62–79, 2006.

[156] M. E. Meier and M. J. Kane, "Working memory capacity and stroop interference: global versus local indices of executive control." *Journal of experimental psychology. Learning, memory, and cognition*, vol. 39 3, pp. 748–759, 2013.

[157] E. Vakil, H. Weisz, L. Jedwab, Z. Groswasser, and S. Aberbuch, "Stroop color-word task as a measure of selective attention: Efficiency in closed-head-injured patients," *Journal of Clinical and Experimental Neuropsychology*, vol. 17, no. 3, pp. 335–342, 1995.

[158] F. Gutiérrez-Martínez, M. Ramos-Ortega, and J. Vila-Chaves, "Executive effectiveness on stroop type interference tasks. a validation study of a numerical and manual version (canum)," *Annals of Psychology*, vol. 34, no. 1, pp. 184–196, Dec. 2017.

[159] M. J. Kane and R. W. Engle, "Working-memory capacity and the control of attention: the contributions of goal neglect, response competition, and task set to stroop interference." *Journal of experimental psychology. General*, vol. 132 1, pp. 47–70, 2003.

[160] J. Jankovic, M. P. McDermott, J. Carter, S. Gauthier, Christopher, L. I. Golbe, S. Huber, W. Koller, C. W. Olanow, and I. Shoulson, "Variable expression of parkinson's disease: a base-line analysis of the datatop cohort. the parkinson study group." *Neurology*, vol. 40 10, pp. 1529–34, 1990.

[161] C. M. Macleod, "Half a century of research on the stroop effect: an integrative review." *Psychological bulletin*, vol. 109 2, pp. 163–203, 1991.

[162] A. R. Jensen and W. D. Rohwer, "The stroop color-word test: A review," *Acta Psychologica*, vol. 25, pp. 36 – 93, 1966.

[163] E. Verstraeten, R. Cluydts, D. Pevernagie, and G. Hoffmann, "Executive function in sleep apnea: Controlling for attentional capacity in assessing executive attention," *Sleep*, vol. 27, no. 4, pp. 685–693, 2004.

[164] W. Killgore, N. Grugle, R. Reichardt, D. Killgore, and T. Balkin, "Executive functions and the ability to sustain vigilance during sleep loss," *Aviation Space and Environmental Medicine*, vol. 80, no. 2, pp. 81–87, 2009.

[165] N. Peach, D. M. Jovev, A. Foster, and H. Jackson, "Testing the stroop effect in a nonclinical sample: Hypervigilance or difficulty to disengage?" *Journal of Experimental Psychopathology*, vol. 3, no. 3, pp. 496–510, 2012.

[166] S. Galer, R. Schmitz, X. De Tiage, P. Van Bogaert, and P. Peigneux, "Response-stimulus interval duration modulates interference in the stroop task both in children and adults," *Human Neuroscience Archive*, vol. 54, no. 1, pp. 97–110, 2014.

[167] C. Brunner, A. Delorme, and S. Makeig, "Eeglab – an open source matlab toolbox for electrophysiological research," *Biomedizinische Technik. Biomedical engineering*, vol. 134, pp. 9–21, 9 2013.

[168] S. Aydore, D. Pantazis, and R. M. Leahya, "A note on the phase locking value and its properties," *NeuroImage*, vol. 74, pp. 231 – 244, 2013.

[169] J.-P. Lachaux, E. Rodriguez, J. Martinerie, and F. J. Varela, "Measuring phase synchrony in brain signals," *Human Brain Mapping*, vol. 8, no. 4, pp. 194–208, 1999.

[170] M. Florian, L. Klaus, D. Peter, and E. E. Christian, "Mean phase coherence as a measure for phase synchronization and its application to the eeg of epilepsy patients," *Physica D: Nonlinear Phenomena*, vol. 144, no. 3, pp. 358 – 369, 2000.

[171] M. Rosenblum and J. Kurths, "Analysing synchronization phenomena from bi-variate data by means of the hilbert transform," in *Nonlinear Analysis of Physio-logical Data*, H. Kantz, J. Kurths, and G. Mayer-Kress, Eds. Berlin, Heidelberg: Springer, 1998, pp. 91–99.

[172] M. L. V. Quyen], J. Foucher, J.-P. Lachaux, E. Rodriguez, A. Lutz, J. Martinerie, and F. J. Varela, "Comparison of hilbert transform and wavelet methods for the analysis of neuronal synchrony," *Journal of Neuroscience Methods*, vol. 111, no. 2, pp. 83 – 98, 2001.

[173] C. J. Stam, G. Nolte, and A. Daffertshofer, "Phase lag index: Assessment of functional connectivity from multi channel eeg and meg with diminished bias from common sources," *Human Brain Mapping*, vol. 28, no. 11, pp. 1178–1193, 2007.

[174] K. MARDIA, "Tests for samples from von mises populations," in *Statistics of Di-rectional Data*, ser. Probability and Mathematical Statistics: A Series of Mono-graphs and Textbooks, K. Mardia, Ed. Academic Press, 1972, pp. 131 – 170.

[175] M. Rubinov and O. Sporns, "Complex network measures of brain connectivity: Uses and interpretations," *NeuroImage*, vol. 52, no. 3, pp. 1059 – 1069, 2010, computational Models of the Brain.

[176] G. Fagiolo, "Clustering in complex directed networks," *Physical review. E, Sta-tistical, nonlinear, and soft matter physics*, vol. 76, pp. 26–107, 09 2007.

[177] V. Latora and M. Marchiori, "Efficient behavior of small-world networks," *Phys Rev Lett*, vol. 67, no. 19, 01 2001.

[178] M. Sniedovich, "Dijkstra's algorithm revisited: the dynamic programming con-nexion," *Control and Cybernetics*, vol. 35, no. 3, pp. 599–620, 2006.

[179] W. Shu-Xi, "The improved dijkstra's shortest path algorithm and its application," *Procedia Engineering*, vol. 29, pp. 1186 – 1190, 2012, 2012 International Work-shop on Information and Electronics Engineering.

[180] A. Javaid, "Understanding dijkstra algorithm," *SSRN Electronic Journal*, vol. 29, no. 3, pp. 1–7, 1 2013.

[181] T. H. Cormen, C. E. Leiserson, R. L. Rivest, and C. Stein, "Dijkstra's algorithm," in *Introduction to Algorithms (Second ed.)*. MIT Press and McGraw–Hill, 2001, p. 595–601.

[182] C. R. Buchanan, M. E. Bastin, S. J. Ritchie, D. C. Liewald, J. W. Madole, E. M. Tucker-Drob, I. J. Deary, and S. R. Cox, "The effect of network thresholding and weighting on structural brain networks in the uk biobank," *NeuroImage*, vol. 211, p. 116443, 2020.

[183] N. Langer, A. Pedroni, and L. Jancke, "The problem of thresholding in small-world network analysis," *PLOS ONE*, vol. 8, no. 1, pp. 1–9, 01 2013.

[184] S. Achard and E. Bullmore, "Efficiency and cost of economical brain functional networks," *PLOS Computational Biology*, vol. 3, no. 2, pp. 1–10, 02 2007.

[185] M. Jalili and M. Knyazeva, "Constructing brain functional networks from eeg: Partial and unpartial correlations," *Journal of integrative neuroscience*, vol. 10, pp. 213–32, 6 2011.

[186] F. De Vico Fallani, L. Astolfi, F. Cincotti, D. Mattia, D. la Rocca, E. Maksuti, S. Salinari, F. Babiloni, B. Vegso, G. Kozmann, and Z. Nagy, "Evaluation of the brain network organization from eeg signals: A preliminary evidence in stroke patient," *The Anatomical Record*, vol. 292, no. 12, pp. 2023–2031, 2009.

[187] M. Kamiński, M. Ding, W. Truccolo, and S. Bressler, "Evaluating causal relations in neural systems: Granger causality, directed transfer function and statistical assessment of significance," *Biological cybernetics*, vol. 85, pp. 145–57, 09 2001.

[188] S.-Y. Tsai, "Reproducibility of structural brain connectivity and network metrics using probabilistic diffusion tractography," *Nature Scientific Reports*, vol. 8, no. 11562, 2018.

[189] K. A. Garrison, D. Scheinost, E. S. Finn, X. Shen, and R. T. Constable, "The (in)stability of functional brain network measures across thresholds," *NeuroImage*, vol. 118, pp. 651 – 661, 2015.

[190] D. S. Bassett, N. F. Wymbs, M. A. Porter, P. J. Mucha, J. M. Carlson, and S. T. Grafton, "Dynamic reconfiguration of human brain networks during learning," *Proceedings of the National Academy of Sciences*, vol. 108, no. 18, pp. 7641–7646, 2011.

[191] C. Catie and H. G. Gary, "Time frequency dynamics of resting-state brain connectivity measured with fmri," *NeuroImage*, vol. 50, no. 1, pp. 81 – 98, 2010.

Vita

Omnia Hassanin was born in 1996, in Abu Dhabi, United Arab Emirates. She received her primary and secondary education in Abu Dhabi, United Arab Emirates. In 2014, Omnia graduated high school as a class valedictorian and was ranked the ninth among high school graduates in Abu Dhabi. In the same year, she was awarded the H.H Sheikha Fatima bint Mubarak Undergraduate Scholarship to Abu Dhabi University. Four years later, she graduated Summa Cum Laude with a B.S. in Electrical Engineering and a Minor in Computer Engineering. In September 2018, Omnia received a graduate teaching and research assistantship to join the Biomedical Engineering Graduate Program at the American University of Sharjah. Up until the course of her M.S. studies, Omnia authored and co-authored five scientific papers in fields related to biomedical signal and image processing.